Control of Physical Human-Robot Interaction:

Mimicking Human Assistance

BY

EHSAN NOOHI BEZANJANI
B.Sc., University of Tehran, 1999
M.Sc., KNT University of Technology, 2002
Ph.D., University of Tehran, 2010

THESIS

Submitted as partial fulfillment of the requirements
for the degree of Doctor of Philosophy in Electrical and Computer Engineering
in the Graduate College of the
University of Illinois at Chicago, 2017

Chicago, Illinois

Defense Committee:

Miloš Žefran, Chair and Advisor
Brian Ziebart, Computer Science
James L. Patton, Bioengineering
Max Berniker, Mechanical and Industrial Engineering
Brenna D. Argall, Northwestern University

to Narges

ACKNOWLEDGMENTS

I'm indebted to many people for their continuing support leading to this dissertation. First, I would like to thank my adviser, Miloš Žefran, for his support and trust. His supportive guidance helped me navigate through the problems and his trust gave me enough freedom to enjoy exploring the field. I would also like to thank Jim Patton for inviting me to join his lab and supporting my research. I enjoyed being exposed to his insights and benefited from our discussions. I would also like to thank Brian Ziebart for supporting my research and sharing his lab's equipment with me. His knowledge in different aspects of robotics and statistics was exceptionally helpful when dealing with corner-cases in my research. I also thank Max Berniker for his valuable feedback on my proposal and my research. Many thanks to Brenna Argall for serving on my thesis committee and providing her valuable insights on my research.

I am also indebted to Majid Nili Ahmadabadi and Hamid D Taghirad, my previous advisers at University of Tehran and KNT University of Technology, for introducing me to the field of Robotics and Control. I owe them much gratitude and great respect for their guidance.

Many thanks go to the Sensory Motor Performance Program (SMPP) at the Rehabilitation Institute of Chicago (RIC) for including me in their research, especially the Motor Learning and Biorobotics (MLB) meetings. Furthermore, I would like to thank people in Robotics lab at the RIC for sharing their resources with my project, in particular, Eyad Hajissa and Yazan Abdel Majeed.

Being a member of Robotics lab at the University of Illinois at Chicago (UIC) was a great experience for me. The collaborations and discussions over the years helped me grow, personally and intellectually. I thank my co-authors, Sina Parastegari and Bahareh Abbasi, for their contributions in the projects.

ACKNOWLEDGMENTS (Continued)

Many of the ideas in our work emerged from our discussions and teamwork. Also many thanks go to my labmates and officemates: Maria Javaid, Wen Jiang, Yao Feng, Andrey Yavolovsky and Sima Behpour.

To my parents: my life, my education, my prosper, I owe all to you. I thank you and my sisters, Sudeh and Fatemeh, for your continuing support. To my wife, Narges: your unconditional love made this whole journey possible. I thank you for making me the luckiest person that I know.

EN

PREFACE

This dissertation is an original intellectual product of the author, E. Noohi. All of the work presented here was conducted in the Robotics Lab at the University of Illinois at Chicago. The human studies reported in this thesis followed a protocol (#2011-0579) that was reviewed and approved by the Institutional Review Board (IRB). At the University of Illinois at Chicago, reviewing the protocols is administrated by the Office for Protection of Research Subjects (OPRS). The proposed protocol is presented in Appendix A and its approval notice along with the approved consent document and recruitment material can be found in Appendix B-E.

The umbrella project for this work is on the topic of physical Human-Robot Interaction (pHRI), the ways that human and robot can communicate physically, and how a robot can collaborate with a human in performing activities such as object manipulation and hand-over. The main project has been partially supported by National Science Foundation (NSF) under Grants CNS-0910988, IIS-0905593 and CNS-1035914. The results of these works have previously appeared as a book chapter (Noohi and Žefran, 2017), an article in IEEE Transactions on Robotics (Noohi et al., 2016), and several workshop and conference publications: RO-MAN'16 (Noohi and Žefran, 2016; Abbasi et al., 2016), ICRA'16 (Parastegari et al., 2016), WHC'15 (Noohi et al., 2015), Humanoids'14 (Noohi and Žefran, 2014), IROS'14 (Noohi et al., 2014). The copyright permissions for reusing the published materials have been presented in Appendix F.

Ehsan Noohi
February 8, 2017

CONTRIBUTION OF AUTHORS

A version of Chapter 5 has been published in World Haptic Conference (Noohi et al., 2015). Miloš Žefran, my adviser, was the lead investigator in this project. I was responsible for building and developing the majority of the ideas, conducting the human study, collecting and analyzing the data and finally, composing the manuscript. Sina Parastegari was involved in the early stages of concept formation (regarding the correlation similarity metric) and contributed to manuscript edits.

A version of Chapters 6, 7, 9 and 10 has been published in IEEE Transactions on Robotics (Noohi et al., 2016). Miloš Žefran, my adviser, was the lead investigator in this project. I was responsible for building and developing the majority of the ideas, conducting the human study, collecting and analyzing the data and finally, composing the manuscript. James L. Patton was a supervisory author and was involved in concept formation and manuscript composition.

TABLE OF CONTENTS

TABLE OF CONTENTS (Continued)

CHAPTER **PAGE**

TABLE OF CONTENTS (Continued)

LIST OF TABLES

LIST OF FIGURES

FIGURE **PAGE**

FIGURE **PAGE**

LIST OF FIGURES (Continued)

FIGURE **PAGE**

LIST OF ABBREVIATIONS

ADL	Activity of Daily Living
ANN	Artificial Neural Network
ANOVA	Analysis of Variations
HHI	Human-Human Interaction
HMM	Hidden Markov Model
IRB	Institutional Review Board
L/F	Leader / Follower scenario
MTC	Minimum Torque Change
NSF	National Science Foundation
OPRS	Office for Protection of Research Subjects
pHHI	Physical Human-Human Interaction
pHRI	Physical Human-Robot Interaction
RIC	Rehabilitation Institute of Chicago
RMSE	Root-Mean-Square Error
SPB	Single-Person-Bimanual scenario
Sync	Synchronized scenario
UIC	University of Illinois at Chicago

SUMMARY

Engineering an assistive robot, capable of serving human needs and performing daily chores, has been a long-sought-for goal for the Robotics field as a whole. One of the main challenges facing researchers is on how to build the robot to be accepted by humans. There are many factors involved in having a robot and a human effectively collaborating, including technological limitations, anthropomorphic elements, ethical concerns, social factors, etc. One of the less explored aspects of this problem is physical interaction between a human and a robot.

Envision a robotic assistant that is helping a human, moving a piece of furniture. Since the human and the robot are haptically coupled, every small movement/force of the robot is perceived by the human and can be interpreted as a clue for the next action. At the same time, the human expects the robot to understand the cues he/she is giving. In other words, the human expects the interaction to be fluid and natural, as it is with a human partner. Note that in a physical interaction between two humans, the kinesthetic cues serve as a communication channel that guarantees the success of the collaboration, even in cases when the verbal communication is missing.

In this thesis, we focus on the physical interaction between a human and a robot. We first study the characteristics of a natural human-human physical interaction and explore different features of cooperation between two humans. In particular, we propose an abstract model for the quality of cooperation, a mathematical model for the motion trajectory during the interaction and a novel approach in modeling the interaction force between two humans. Based on these models that we construct for a natural human-

human interaction, we propose a set of control policies that replicates the same interaction features and mimics human's behavior during a physical interaction between a human and a robot.

CHAPTER 1

INTRODUCTION

A broad range of robotic applications require robots to physically interact with humans. A few examples are rehabilitation and robotic assistance for disabled and elderly people, robotic surgery, education and entertainment. One of the main challenges in physical Human-Robot Interaction (pHRI) is how to define the cooperation. On the one hand, in the context of assistive robotics, a good cooperation happens when the robot carries the majority of the workload and the human only provides guidance. This scenario is usually referred to as leader/follower scenario. On the other hand, in the context of elderly care, a good cooperation involves demanding the elder person to engage in the task as much as he/she can. It helps the elder person to slow down muscle deterioration (atrophy) and prevent hospitalization. Another complication in defining a successful cooperation is human's excellent capability for adaptation. Usually, it is the human who adjusts his/her actions to the robot's typical action profile. For instance, when carrying an object cooperatively with a robot, the human tends to adjust his/her walking pace to match the robot's. Therefore, it is not clear whether the robot's cooperation strategy was successful or the human adaptation compensated the robot's shortcomings.

Another challenging question in pHRI is that the typical profiles for human actions are usually unknown. Moreover, when individual differences are taken into consideration, the challenge is even greater. Take a robotic prosthetic arm as an example. For a person with an amputated arm, a robotic prosthetic arm needs to cooperate with his/her other arm to perform activities of daily living (ADLs). Effective cooperation happens when the robotic arm recognizes the human's preferred motion trajectories and preferred force-exchange patterns.

The next challenge in engaging robots in physical interaction with humans is control of the robot. Assume that the human's preferred motion and the expected interaction force are known and the cooperation model is also available. The question then is how to use this information in the robot's control policy. The central claim of this thesis is:

> Including the interaction information in the robot's control policy significantly improves the performance of the robot, when physically interacting with a human.

To validate this claim, we first propose a set of quantitative measures to be able to evaluate the quality of a cooperative interaction between the human and the robot. Then, we propose a model for the human's preferred motion profile and also a model for the expected interaction force during a cooperative interaction. Next we propose robot controllers with and without the knowledge of the interaction. Finally, we evaluate our claim by comparing between the two controllers (statistical analysis) and show that, in fact, including interaction information in designing the controller improves robot's performance.

1.1 Motivation

Among many different applications where a human-like interaction with a robot is essential, our initial motivation for this project was a robotic caregiver for the elderly. Aging population is an emerging issue for many developed countries; confronting them with the problem of how to keep elderly healthy and independent. The elderly need to be motivated (demanded) to engage in their activities of daily living (ADLs) with minimum assistance. It helps the elder person to slow down muscle deterioration (atrophy) and prevents or delays hospitalization. Furthermore, it promotes their mental health and delays cognitive impairment and depression in later life. At the same time, they need constant monitoring, as the risk of a fall and a fracture is considerably higher among the elderly.

Unfortunately, providing the in-home-care for elderly is not a financially sustainable solution for many nations. Even for very rich countries, the population of young caregivers is shrinking and the demand exceeds the resources. Robotic caregivers are expected to be a promising solution for this problem. While a robotic caregiver might not become a reality in the near future, the research in this area paves the way towards this goal.

1.2 Research Questions

In order for a robot to be able to physically interact with a human as naturally as another human, it should be provided with (at least) the same information as a human partner possesses (or infers). In other words, the robot should know: What is the nature of the collaborative task? How, when, where and to what extent should the robot be involved in the task? And what is the human's specific way of performing this collaborative task?

As far as the task, in this research we focus on human manipulative actions. In particular, we study cooperative object manipulation. We also assume that, similar to many scenarios in human-human cooperative object manipulation, the basic characteristics of the task is known to the robot. That is, the robot knows the mechanical properties of the object that is to be manipulated. It also knows the manipulation profile (e.g. start and end configurations).

In regard to the extent of cooperation, there are many interesting works in the literature that target a leader or a follower robotic assistance. In this work however, we focus on cooperative assistance, in which both the robot and the human need to proactively coordinate and adjust to the other party. Our target application (cooperative object manipulation) requires that the robot remains involved during the whole collaboration, similar to a human partner.

Finally, perhaps the the most difficult challenge is that the knowledge about how human will perform the task is not available. Even a human partner does not have this knowledge explicitly. However, he/she implicitly knows that, as humans, they both share an internal model of the way they move and manipulate objects and they both are governed by very similar kinematic models. The robot needs to extract this implicit knowledge and build an explicit model for it in its control policy. In particular, the robot needs to know:

- How to define and to measure the cooperation between the human and the robot?
- What is the human's preferred motion trajectory during this collaborative task?
- What is the human's expected interaction force profile during this collaborative task?
- What robot's control strategy results in a satisfying cooperation with a human? And how is human's satisfaction measured?

In this work, we study each of these questions and introduce possible answers to them. A more detailed discussion follows in Sec. 1.4.

1.3 Our Approach: Mimicking Human Assistance

One promising approach toward determining the answers to the above research questions is to examine them in a physical interaction setting between two humans (instead of a human and a robot). That is, we first replace the robot with another human and study the cooperation profile in human-human physical interaction. The result of the study on the human-human setup would introduce models for the preferred or expected way that humans physically interact. After we obtained the answers to the research questions in a human-human setup, we can reinstate the robot and control it to reproduce the human partner's strategy.

We refer to our approach as "Mimicking Human Assistance", because the robot incorporates human's cooperation models into its controller and responds similarly to another human. While this is a promising approach, it may not result in the best controller. A robot can mimic human assistance, but we are not always happy with our interactions with other people. If the robot can perform optimally (whatever it means) for anyone with whom it interacts (regardless of age, health, culture, etc.), then it would surpass the human performance. In other words, the robot cannot outperform human only by mimicking human assistance. However, in order to empower the robot to perform better than humans, we need to first model the way humans interact and then endow the robot with those models; in other words, the model we obtain in our approach is a prerequisite of more advanced controllers.

1.4 Contributions

The ultimate goal of our research is to propose a control strategy for the robot that mimics the human's strategy. As a result, the human perceives the robot as an acceptable replacement for the human partner. The main contributions of this work in support of the central thesis statement are as follows:

- **Quantitative measures of human-cooperation** (Noohi and Žefran, 2014) introduces a mapping between human perception of the quality of a cooperation and formal and measurable mathematical expressions for such indexes. The indexes can be presented as different dimensions in a feature space, representing the cooperation properties.

- **Human motion trajectory model during cooperation** (Noohi et al., 2015) reveals the preferred motion profile that humans generate when cooperatively manipulating an object. The model explains the nominal behavior of cooperating partners (average over all subjects).

- **Human interaction force model during cooperation** (Noohi et al., 2016; Noohi and Žefran, 2016) introduces the hidden forces that provide a communication channel between the cooperative partners. It is shown that the interaction force and the the motion trajectory model are tightly related. The effectiveness of the model is compared with other existing models using the proposed quantitative measures.

- **Human interaction force properties during cooperation** (Noohi and Žefran, 2017) provide insights on an expected (by human partner) natural interaction with a robot. The interaction force is computed from our proposed model and the properties have been studied statistically.

- **Control policies for robots** (Noohi et al., 2016; Noohi and Žefran, 2017) to enable them to mimic human assistance. The controllers are based on the observed properties of the humans' interaction force. The evaluations on the proposed controllers support the central statement of this dissertation.

In the following chapters, we will discuss each of these contributions in more details.

1.5 Thesis Organization

This thesis is organized into four parts and 12 chapters. Descriptions of each part and each chapter of the dissertation are as follows:

Part I, Preliminaries: This part contains an introduction to the research problem, a review of the existing works and a description of the human study.

Chapter 1: This chapter provides the reader with the motivations for this work and identifies the research questions that the work is focused on. Our approach to these problems is explained and a list of related contributions is included in this chapter, as well.

Chapter 2: In this chapter we review some background that will be referenced later in the thesis, including the minimum-jerk model of human hand movement, polynomial model of applied force for hand movement in a force field and, interaction force formulation in a dyadic manipulation task.

Chapter 3: This dissertation introduces several hypotheses about a natural human-human cooperative manipulation. To be able to evaluate and analyze those hypotheses, a human study is conducted. This chapter explains the details of this study, including the experimental setup, manipulation tasks, data acquisition system, cooperation modes and scenarios, experimental procedure, recruitment procedure, the questionnaire and data analysis procedure. To provide the reader with an insight on the results of our proposed models, a few example graphs are presented in this chapter as well.

Part II, Models: This part contains our first three contributions: a motion model, a force model and a cooperation model for cooperative dyadic object manipulation.

Chapter 4: This chapter provides an abstract model for cooperative manipulation between humans and proposes a set of features that quantitatively describe the cooperation. The model is based on the human study and its associated questionnaire, discussed in Chapter 3. It is also argued that a lack of a model for the interaction force would limit the usefulness of the proposed measures.

Chapter 5: This chapter introduces a model for motion of an object, while being manipulated cooperatively. It is based on the human study, discussed in Chapter 3. The role of time coordination between the subjects (movement synchronization) is explored and presented in this chapter, as well.

Chapter 6: The interaction force model, as one of the core contributions of this dissertation, is presented in this chapter. We show that the interaction force can be modeled by utilizing the information about the movement model. As a case study, we take the movement model discussed in Chapter 5 and derive the associated model for the interaction force. The results of employing the proposed model on the interaction data, collected during our human study (Chapter 3), are described in this chapter, as well.

Chapter 7: This chapter evaluates the performance of the proposed interaction force model (in Chapter 6) and compares it with some existing models in the literature. The statistical evaluation is performed using the data collected in Chapter 3 and performance metrics proposed in Chapter 4.

Part III, Controllers: This part introduces a set of robot controllers for effective interaction with humans, using the interaction force model introduced in the previous part.

Chapter 8: This chapter highlights several features of interaction forces during dyadic object manipulation. The statistical analysis is performed using the data collected in Chapter 3 and the interaction force model proposed in Chapter 6. Using the observed properties of human interaction forces, a simplified cooperation policy (controller) is proposed in this chapter that associates the robot's force with the object's velocity.

Chapter 9: This chapter presents another important contribution of this work: the robot performance is statistically significantly higher when interaction information is included in the robot's controller. In this chapter, a general control scheme is proposed for a successful human-robot collaborative manipulation that considers feedforward injection of the interaction force into the controller. Again, the statistical analysis is performed using the data collected in Chapter 3 and the interaction force model proposed in Chapter 6.

Chapter 10: This chapter extends the controller scheme described in Chapter 9 and proposes an online feedback controller scheme. An online controller requires an estimation of the interaction force, because the proposed model in Chapter 6 is non-causal. We present our prediction of future human forces and compute an estimation of the interaction force. The performance of the resulting causal controller is statistically evaluated, as well

Part IV, Conclusion: This part contains open problems and concluding remarks.

Chapter 11: This chapter discusses a few possible extensions of our work and also reviews related open problems. In particular, we discuss potential extensions to our motion model and our interaction force model. We also suggest exploring new interaction models, such as interaction torque and interaction impedance. The idea of applying different tools, such as Hidden Markov Model, HMM, and Artificial Neural Network, ANN, is discussed in this chapter, as well.

Chapter 12: A concluding summary of the thesis is presented in this chapter.

1.6 Reader's Guide

The thesis is organized in such a way that each chapter provides foundation for the following chapters. As such, it is expected to be read in the order presented. However, in some parts of the dissertation, a brief preview of the results has been provided to motivate the approach and provide the reader with additional insight. If the reader is interested in the shape of the collected signals, referring to Fig. 6 – Fig. 10 and Fig. 17 – Fig. 19 can be helpful. Also, examples of the computed interaction forces have been presented in Fig. 27 and Fig. 31.

Part I
Preliminaries

CHAPTER 2

BACKGROUND AND NOTATION

Parts of this chapter have been presented in (Noohi et al., 2016). Copyright © 2016, IEEE.

2.1 Motion Trajectory during Reaching Movement

Human Reaching movements have been studied extensively. During the reaching task, a person moves his/her hand from point A to point B in a straight line. The motion is fast and occures over a short distance. When performing the single arm reaching movement, it has been shown that humans generate a smooth trajectory with the well-known bell-shaped curve for hand velocity (Flash and Hogan, 1985). More specifically, the hand trajectory minimizes the *minimum jerk* cost function:

$$\begin{aligned} H(t_i, t_f, x) &= \frac{1}{2}\int_{t_i}^{t_f} \left\| \frac{\mathrm{d}^3 x(t)}{\mathrm{d}t^3} \right\|^2 \mathrm{d}t \\ x^*(t) &= \underset{x(t)}{\operatorname{argmin}} \left(H(t_i, t_f, x) \right) \end{aligned} \tag{2.1}$$

where $x(t)$ is the position trajectory of the hand, t_i is the start time of the motion and t_f is the end time. If we take the assumption that the hand is at rest at the start and at the end of the reaching movement (i.e. zero boundary conditions), the minimum of the cost function would be: $H^* = 360L^2$, and the optimal trajectory is: $x^*(\tau) = x_i + (6\tau^5 - 15\tau^4 + 10\tau^3)(x_f - x_i)$, where $\tau = (t - t_i)/(t_f - t_i)$. Here, $x_i = x(t_i)$ and $x_f = x(t_f)$ are the positions of the hand at the start point and the end point, respectively.

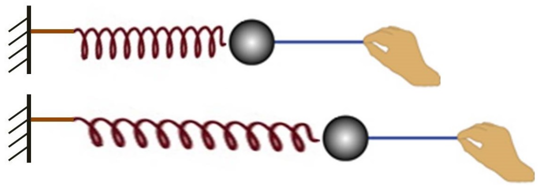

Figure 1: Reaching movement under spring-like force field. Copyright © 2016, IEEE.

2.2 Applied Force during Reaching Movement

If the reaching movement is disturbed by an external force field, the hand trajectory will deviate from the optimal trajectory. It has been shown that, after a sufficient number of learning trials, humans can adapt to the external force field and return to their original trajectories (Shadmehr and Mussa-Ivaldi, 1994; Flash and Gurevich, 1997; Melendez-Calderon et al., 2015). Consider the situation where a subject performs a reaching movement while a spring resists his/her forces, see Fig. 1. The spring introduces the position-dependent force field $F = -k_s\,(x(t) - x_0)$, where k_s is the stiffness of the spring and, x_0 is the position of the spring's end when no force is applied to it. After the adaptation period, the subject learns to cancel the force field and returns to the optimal trajectory, $x^*(t)$, for the reaching movement (Flash and Gurevich, 1997). More interestingly, the force that the subject needs to apply at the end effector (to cancel the force field) is $F^*(t) = -k_s\,(x^*(t) - x_0)$. In other words, the applied force follows a smooth minimum-jerk trajectory. Since $\mathrm{d}^3x(t)/\mathrm{d}t^3 = (-k_s^{-1})\,\mathrm{d}^3F(t)/\mathrm{d}t^3$, we can rewrite (2.1) as:

$$F^*(t) = \underset{F}{\operatorname{argmin}} \left(\frac{1}{2} \int_{t_i}^{t_f} \left\| \frac{\mathrm{d}^3 F(t)}{\mathrm{d}t^3} \right\|^2 \mathrm{d}t \right) \tag{2.2}$$

Eq. (2.2) states that, in a *spring-like force field*, the applied force minimizes the squared-jerk cost function. Applying the calculus of variations techniques on (2.2), it is easy to show that the 6th derivative of $F^*(t)$ is zero (Shadmehr and Wise, 2005). Therefore, the applied force can be represented as a 5th order polynomial:

$$F^*(t) = \sum_{k=0}^{5} c_k t^k \tag{2.3}$$

Note that, if the hand is at rest at the start and at the end of the reaching movement, the applied forces are, too. In the general case that the hand is not at rest, to determine the c_k coefficients in (2.3), the minimization problem of (2.2) should satisfy the boundary conditions.

2.3 Interaction Force Formulation

Consider a dyadic object manipulation task. Let f_1 and f_2 refer to the forces that are applied to the manipulated object and $F_{sum} = f_1 + f_2$ be the resultant force that is associated with the task. Each applied force can be decomposed into the effective force (f_1^* and f_2^*) and the interaction force (F^i) as:

$$\begin{aligned} f_1 &= f_1^* + F^i \\ f_2 &= f_2^* - F^i \end{aligned} \tag{2.4}$$

The interaction force can be used to secure the grasp or to communicate with the other person (van der Wel et al., 2011; Reinkensmeyer et al., 1992). It can compress or stretch the object, but it does not influence the object's equations of motion. As a result, all force components that lie in the null space of F_{sum} (orthogonal to it) are part of interaction force. That is:

$$f_1^* = \alpha F_{sum}$$
$$f_2^* = (1-\alpha) F_{sum} \tag{2.5}$$

and therefore,

$$F^i = (1-\alpha) f_1 - \alpha f_2 \tag{2.6}$$

where α denotes the contribution of each person in performing the task.

Note that (2.4) is an under-determined system of equations and, any arbitrary value of α, $(0 \leq \alpha \leq 1)$ introduces a valid decomposition. According to (2.5) and (2.6), the only situation in which the system has a unique solution is when $F_{sum} = 0$. In such instances, $F^i = f_1 = -f_2$ and $f_1^* = f_2^* = 0$. In all other situations, to be able to uniquely determine the interaction force, one needs to introduce an additional constraint to the system (e.g. introducing specific values for α). Note that, we take the general case where both hands can apply pure torque to the object and thus, the direction of the interaction force is not necessarily aligned with the grasp configuration (no additional torque constraints).

Fig. 2 shows two possible decomposition examples for a single pair of applied forces. Note that in Fig 2b, the interaction force has both orthogonal and parallel components (w.r.t. F_{sum}). While obtaining the orthogonal component is straightforward, finding a computational model for the parallel component is challenging. That is the reason why we only focus on the parallel components of f_1, f_2 and F^i in this work. We will refer to these parallel components as the applied forces (f_1 and f_2) and interaction force (F^i), hereafter. After the interaction force is computed, it will be augmented with the orthogonal component.

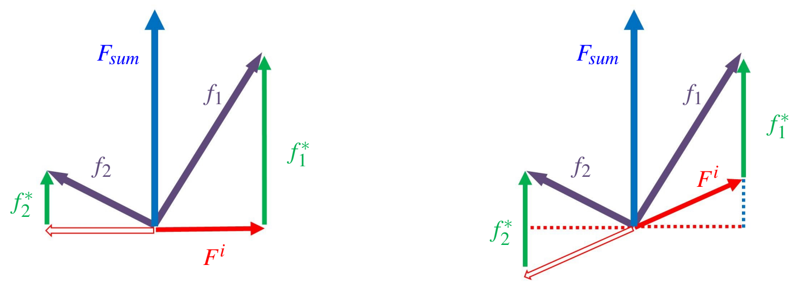

(a) Orthogonal

(b) Non-orthogonal

Figure 2: For a single pair of forces, f_1 and f_2, the orthogonal (a) and a non-orthogonal (b) decompositions are illustrated. Note that the orthogonal decomposition matches the minimum-energy model and the non-orthogonal decomposition matches the virtual linkage model.

It is worth mentioning that the interaction force has been introduced in a few different other forms, as well. For instance:

$$F^i = \frac{1}{2}(f_1 - f_2) - (\alpha - \frac{1}{2})F_{sum} \tag{2.7}$$

or if the orthogonal component is ignored,

$$F^i = \beta F_{sum} \tag{2.8}$$

While they look different, it is easy to see that they are equivalent to (2.6). One just needs to plug (2.5) into (2.4), properly.

As discussed above, for a given set of applied forces, f_1 and f_2, computing the interaction force, F^i and the value of α are two sides of the same problem. However, since α is also related to the contribution

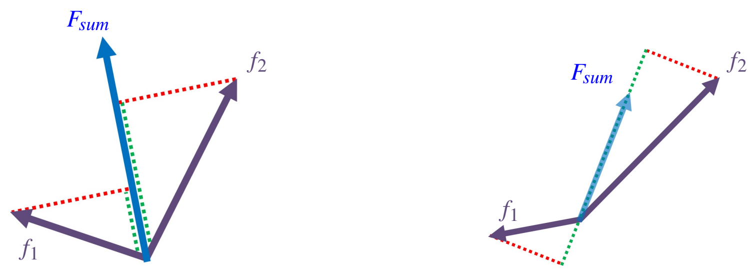

(a) Cooperative (b) Non-cooperative

Figure 3: Cooperative interaction and non-cooperative interaction. Copyright © 2014, IEEE.

of each person to the total task, it can inform us more about the interaction. Fore instance, earlier we discussed that any arbitrary value of α introduces a valid decomposition. However, we restricted the values to the range: $(0 \leq \alpha \leq 1)$. This constraint guarantees that each person provides a positive contribution to the task and the effective forces do not cancel each other. This was in fact an attempt to define a cooperative interaction. In other words, we can identify non-cooperative interactions, when the value of α is out of that range; or equivalently, one effective force cancels the whole other effective force. Fig. 3 provides an illustration for these interaction types.

One last point tat we want to make here is on practical issues with computing the interaction force. We mentioned earlier that any component of forces that lie in the null space of F_{sum} is part of the interaction force. We also mentioned that when $F_{sum} = 0$, the applied forces represent the interaction force. However, for non-zero small vectors of F_{sum}, the measurement noise can significantly change the direction of the vector and the computed null space would be wrong. Therefore, it is important to consider how noise would affect the computation of the interaction force, when introducing a new model for the interaction force.

2.4 Notation

In this section we list the variables that we will keep referring to in the following chapters:

t_i	the start time of the motion
t_f	the end time of the motion
t_m	the time in the middle of the motion, where $F_{sum} = 0$
$x_i = x(t_i)$	the positions of the hand at the start point
$x_f = x(t_f)$	the positions of the hand at the end point
f_1	the applied force to the manipulated object by agent one
f_2	the applied force to the manipulated object by agent two
$F_{sum} = f_1 + f_2$	the resultant force applied to the object
f_1^*	the effective force for agent one
f_2^*	the effective force for agent two
F^i	the interaction force
$\alpha = f_1^*/F_{sum}$	contribution ratio for agent one
$\delta = \frac{1}{2} - \alpha$	cooperation index

CHAPTER 3

HUMAN STUDY

Parts of this chapter have been presented in (Noohi et al., 2016), (Noohi and Žefran, 2016), (Noohi et al., 2015) and (Noohi and Žefran, 2014). Copyright © 2014-2016, IEEE.

As discussed in Chapter 1, we follow a human-inspired approach in modeling a cooperative pHRI. That is, we set up an experiment with human subjects and studied their cooperative manipulation behaviors in order to develop a model for cooperation between humans. We chose a co-manipulation task and collected interaction data for both bimanual and dyadic object manipulation. In single-person-bimanual (SPB) mode, the subjects were asked to grasp an object with both hands and move it horizontally. In dyadic mode, the subjects were grouped into pairs and asked to perform cooperative manipulation. In both cases, the grasps were power grasps and the subjects could apply independent forces and torques to the object.

In this chapter, we present the details of our experiment. Throughout this dissertation, we will introduce various hypotheses and report several observations. The experiment described in this chapter provides data and evidence to validate those hypotheses. In executing this human study, we followed a protocol (#2011-0579) that was reviewed and approved by our IRB at the University of Illinois at Chicago. The protocol is presented in Appendix A and its approval notice, the approved consent document, recruitment material and the questionnaire can be found in Appendix B to Appendix E.

3.1 Experimental Setup

We chose an aluminum pot ($w < 22N$) as the object to be carried bimanually. To collect the forces applied by the subjects, we used two SI-65-5 ATI Gamma force sensors (ATI, 2014). The force sensors were placed in between each handle and the pot. The forces are then sampled by a computer through two PCI-6034E NI data acquisition boards (NI, 2014) at the frequency of 1 KHz. The acquired data is then transformed to the earth reference frame. This requires the orientation of the pot to be measured. We used a 9DOF-Sensor-Stick SparkFun IMU to measure the pot's orientation and acceleration (Sparkfun, 2014). The sampling frequency for the IMU is set to 100 Hz. The IMU is interfaced with the computer through an Arduino Mega microcontroller board (Arduino Mega, 2014). All data collection is managed through a Matlab GUI that we have developed. Fig. 4 shows the experimental setup and its components. To eliminate the high frequency noise, a low pass FIR smoothing filter with the cutoff frequency of 12.5 Hz is applied to the signals.

3.2 Manipulation Task

Each trial of the experiment consisted of three subtasks; lifting the pot from the table at the start point (point A), moving the pot horizontally towards the destination point (point B) and putting the pot down on the table at the end point. Studies have shown that gravity plays a significant role in single-arm vertical reaching movements (Sabes et al., 1998; Crevecoeur et al., 2009). Therefore, in this study we focus on the horizontal movements and discard the first and last subtasks in each trial.

The start point and the end point were marked to provide x_i and x_f. The configurations of the start points and the end points were designed in such a way that we have two types of horizontal motions. In type 1 motions, the direction of the motion is perpendicular to the line connecting the handles. There-

Figure 4: Experimental setup. The force sensors are installed between the handles and the container. The IMU is interfaced with a Arduino board and placed in a box that is glued to the inside bottom of the pot. The sampled data is collected by a GUI in Matlab. Copyright © 2016, IEEE.

fore, the grasp force has small components in the motion direction. In type 2 motions, the direction of the motion is parallel with the line connecting the handles and, grasp force has dominant components in this direction, see Fig. 5. Also, the distances between the start points and the end points were selected such that both short-range and long-range motions were included. In the short-range motions, the horizontal distance between the start point and the end point was 28 cm and, in the long-range motions it was 83 cm.

3.3 Data Acquisition System

To facilitate data annotation, we programmed the data-acquisition software to play a beep at certain points in time. The subjects were instructed to perform the subtasks immediately after hearing the beep. That is, they held the handles, waiting for a beep. After hearing the beep, they picked up the pot from point *A* and waited there for the next beep. When the next beep was played, they moved the

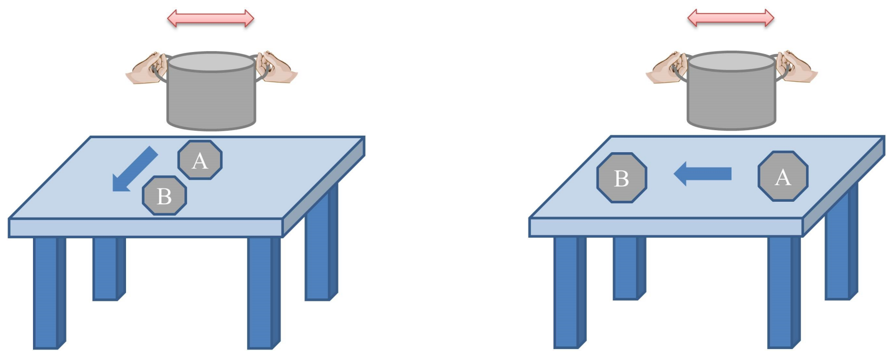

(a) Type 1 motion

(b) Type 2 motion

Figure 5: Type 1 and type 2 motions. In SPB manipulation the person stands behind the table and grabs the handles. In dyadic manipulation, the subjects stand on the opposite sides of the table and grab the handles. The blue arrow on the table shows the motion direction and the red double arrow is the grasp force. Copyright © 2016, IEEE.

pot horizontally towards the point *B* and waited there. Finally, by hearing the last beep, they put the pot down on the table at point *B*. The participants followed the same instructions in all trials (including different modes and different tasks).

The Matlab GUI is capable of recording the forces applied to the pot by the subjects, the inertial information of the pot and a video of the experiment. The camera was installed at the ceiling and had a top view of the experiment trials. The cables (force sensors and Arduino) were pulled up and hanged to the ceiling so that they have minimum interference with the manipulation task.

3.4 Cooperation Modes

We study three different cooperation scenarios in this work. In the first scenario, each subject performs a bimanual reaching movement, alone. We will refer to this case as single-person bimanual (**SPB**) scenario. The next two scenarios correspond to cooperative dyadic reaching movement. In one, a leader and a follower role is assigned to the subjects in each pair. The leader is initiating all the subtasks, while the follower is told to follow his/her lead. This case is referred to as leader-follower (**L/F**) scenario.

To study the effect of the lag between the leader and the follower (at the beginning of the movement in L/F scenario), we introduce a synchronized-cooperation scenario. In this last scenario, the subjects are told to execute each subtask right after hearing the beep (no roles are assigned to the subjects). Therefore, the start time of the reaching movement is known by both subjects and the lag between the subjects at the beginning would disappear. Note that there still might be a small time lag due to the difference between individuals' response times. However, since the tone is played at fixed points in time, the start time is predictable and the synchronization would be accurate. This case is referred to as the synchronized (**Sync**) scenario.

3.5 Experimental Procedure

First, each subject was given enough familiarization trials (as much as they needed). Then, he/she performed three trials in SPB scenario, including a short-range type 1 motion, a short-range type 2 motion and a long-range type 2 motion. The long-range type 1 motion was skipped, because it was not within the range of human-arm reachable space. The subjects stood on the long-sides of the table.

Therefore, they performed type 2 motion tasks along the direction of the length of the table and the type 2 motion task along the direction of the width of the table.

Then the subjects were grouped into pairs (dyadic mode), no subject was in more than one pair. Subjects in each pair stood on the opposite long-sides of the table and performed three trials in Sync scenario followed by two more trials in L/F scenario, summing up to five trials of dyadic interaction. In the Sync scenario, the short-range type 2 motion was excluded. That was due to the fact that, unlike all other trials, this motion was a retracting motion for one subject and extension for the other subject. In all other tasks, the arm movement was an extension motion for both arms. Finally, In the L/F scenario, each pair performs a long-range type 1 motion. Then the subjects switched the roles and repeated the task. The motion direction in all trials was along the length of the table. To generate different motion types, the pot was yawed to be parallel with or orthogonal to the motion direction.

In all of the eight trials, no repeated measurements were collected. Following each trial, the subjects were asked to complete a questionnaire and assess their interaction performance. The questionnaire helps us to evaluate our performance metrics and tailor them towards human perception of interaction performance. Since the set of potential answers to some of these questions had less than 5 items to choose from, and also since we had a limited number of participants, we used a Visual Analogue Scale (VAS) questionnaire instead of a Likert scale to achieve a higher precision in self-assessment results. The questionnaire can be found in Appendix E. A list of these questions have been included at the end of this chapter, too.

3.6 Recruitment Procedure

According to our IRB protocol, we were allowed to recruit participants, using flyers and emails. The approved flyers were posted in buildings around the University of Illinois at Chicago (UIC) campus. Also, a recruitment email was sent to the Graduate Student list server at UIC. As a result, the participants belonged to the body of the UIC students, staff and their acquaintances. Among all volunteers, we recruited 22 adult subjects (12 men and 10 women), ranging in age from 19 to 35. The only criterion for inclusion or exclusion was for the volunteer to be a healthy adult.

The data collection was performed in the Robotics Lab at the University of Illinois at Chicago (UIC). The experiment were scheduled over the course of 10 days, according to the participant's availability. The subjects were randomly paired and assigned to a specific session. In each session, after briefing the participants about the project goals, benefits and risks, they signed the consent forms. Then, the task was explained and demonstrated to them, including different modes (bimanual vs dyadic), different scenarios (SPB, Sync and L/F) and different tasks (motion types and motion ranges). Each session took less than an hour and each participant were paid upon completion of all of the tasks.

3.7 Data Analysis

With 22 participants, we collected 63 trials (21×3 in SPB scenario) in bimanual mode (one of the participants refused to complete the task in this mode) and 55 trials in dyadic mode (11×3 in Sync scenario plus 11×2 in L/F scenario). Then, the collected data was analyzed to identify the measurement errors. The errors were mainly due to the hysteresis error that the sensors exhibited randomly. We examined the value of F_{sum} to identify the measurement error. For instance, if the pot was not moving (according to the IMU readings), a constant large value in F_{sum} would indicate the presence of the

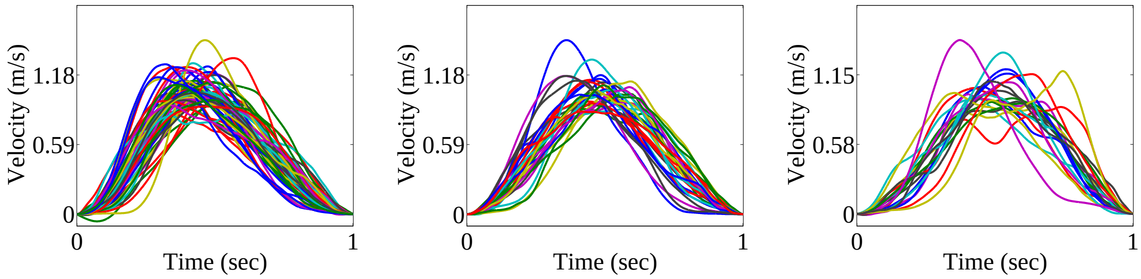

(a) SPB scenario (b) Sync scenario (c) Leader/Follower scenario

Figure 6: Time trajectory for normalized velocity samples in (a) SPB, (b) Sync and (c) L/F scenarios. Copyright © 2015, IEEE.

hysteresis error. As a result, five trials in bimanual and three trials in dyadic mode (two in Sync scenario and one in L/F scenario) were marked as corrupted signals. After the corrupted trails were excluded, the data was processed and employed to validate our hypotheses.

We observed a huge range of variability in the applied forces by the subjects. As such, an illustration of the collective signals won't be informative. We will present a few examples of the applied forces in the following section. However, the object's velocity follows a more regular behavior. Figure 6 shows a collective illustration of the normalized velocity of the object for all trials in different scenarios. As it is clear, there is a regularity in the signals and we will explore a model for that in Chapter 5

3.8 A Glance at the Results

Before we introduce our proposed models for the interaction force, it would be helpful to present the results of employing that model to the collected signals. Here, we only present an exhaustive qualitative

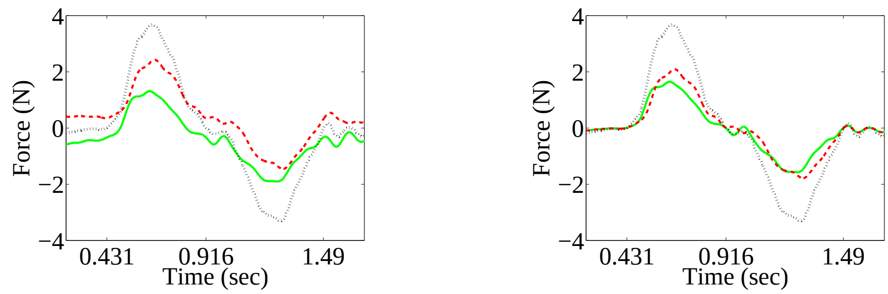

(a) Applied forces (S13)

(b) Effective forces (S13)

Figure 7: Good cooperation: force interaction in SPB manipulation, type 1 motion. a) The red dashed line represents f_1 and green solid line represents f_2. b) The red dashed line represents f_1^* and green solid line represents f_2^*. In both graphs, the black dotted line represents F_{sum}. Copyright © 2017, Springer.

evaluation on all recorded data and leave the more elaborated quantitative evaluation of the model for the following chapters.

Let us start with the SPB manipulation. In type 1 motions, where the interaction force is very small, we expect that both hands of each subject apply similar forces, i.e. $f_1^* \approx f_2^* \approx \frac{1}{2}F_{sum}$. Fig. 7 depicts the applied forces and the effective forces for subject-13 as an example. The results showed that the same high degree of cooperation is presented by all of the subjects in this type of motion.

In SPB type 2 motions, the interaction force is larger and our model plays a more influential role. Again we observed good cooperation between each subject's hands. More than 90% of the subjects applied similar forces, as expected. However, 2 subjects performed the task differently. Fig. 8 shows subject-1 and subject-18's forces where subject-1 examplifies the first group (one of the 90% subjects)

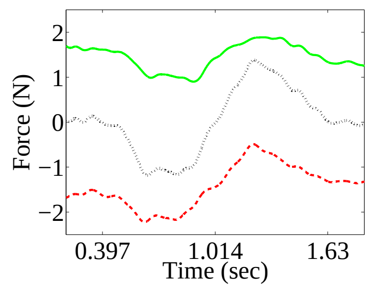

(a) Applied forces (S1)

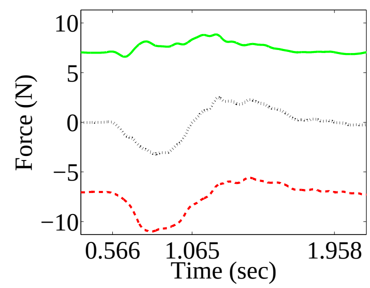

(c) Applied forces (S18)

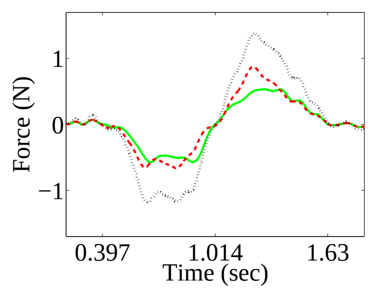

(b) Effective forces (S1)

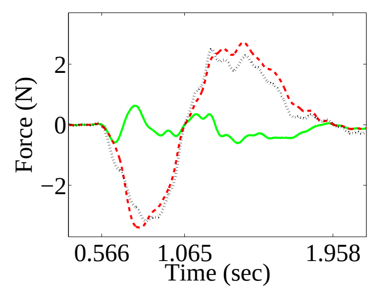

(d) Effective forces (S18)

Figure 8: Specialized cooperation: force interaction in SPB manipulation, type 2 motion for subject-1 and subject-18. a) The red dashed line represents f_1 and green solid line represents f_2. b) The red dashed line represents f_1^* and green solid line represents f_2^*. In both graphs, the black dotted line represents F_{sum}. Copyright © 2017, Springer.

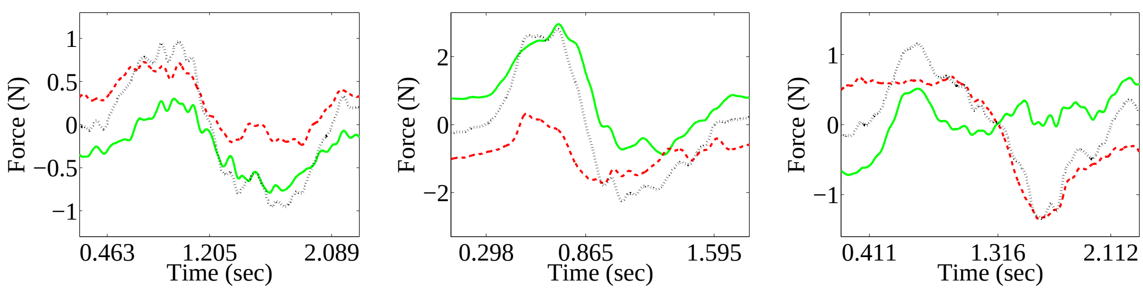

(a) Applied forces (P6)   (c) Applied forces (P7)   (e) Applied forces (P3)

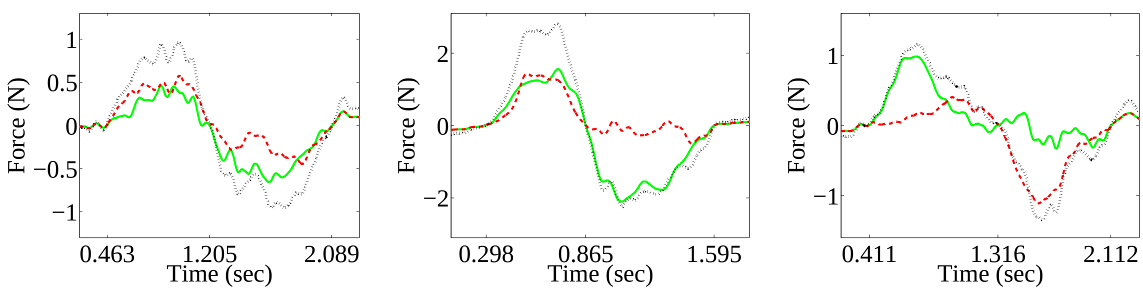

(b) Effective forces (P6)   (d) Effective forces (P7)   (f) Effective forces (P3)

Figure 9: Role development: force interaction in dyadic manipulation, type 1 motion for pairs 6, 7 and 3. a,c,e) The red dashed line represents f_1 and green solid line represents f_2. b,d,f) The red dashed line represents f_1^* and green solid line represents f_2^*. In all graphs, the black dotted line represents F_{sum}. Copyright © 2017, Springer.

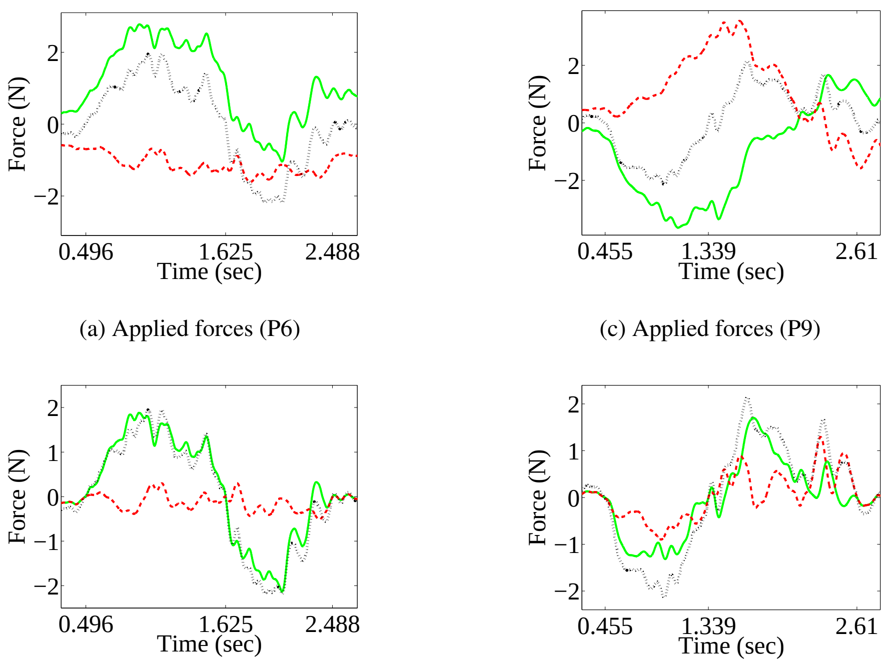

(a) Applied forces (P6)

(c) Applied forces (P9)

(b) Effective forces (P6)

(d) Effective forces (P9)

Figure 10: Force interaction in dyadic manipulation, type 2 motion. Pairs 6 and 9 are shown. a,c) The red dashed line represents f_1 and green solid line represents f_2. b,d) The red dashed line represents f_1^* and green solid line represents f_2^*. In all graphs, the black dotted line represents F_{sum}. Copyright © 2017, Springer.

and subject-18 presents one of the different signals. The graph reveals that the subject-18's hands took different roles: one hand generates a coarse trajectory for the whole task while the other hand only introduces fine tuning to the path. The specialization of human hands in collaborative tasks has been reported previously (Guiard, 1987).

Now, let's consider dyadic manipulation. Here, the synchronization between subjects is not as good as during SPB manipulation. Nevertheless, 55% of the groups still demonstrated good cooperation (e.g. pair-6). The other 45% of the groups demonstrated some kind of specialization (e.g. pair-7). Fig 9 shows the graphs for these pairs. In one interesting case (pair-3), the subjects extended their specialization and developed roles. As illustrated in the fiugure, one subject only contributed in accelerating the object, while the other subject only contributed in decelerating it. The acceleration/deceleration roles in collaborative tasks have also been reported in the literature (Reed et al., 2006).

Finally, in type 2 motion of dyadic manipulation, due to the imperfect synchronization and larger interaction forces, pairs demonstrate a wide range of collaboration types. That is, in addition to the good cooperation, specialization and role development, switching between these behaviors during the manipulation were also observed. Figure 10 shows interaction forces for pairs 6 and 7 as two examples.

Please note that the purpose of this section was to provide the reader with a glance of how the model would work. The qualitative assessments presented here in this section should not be considered as proof of validity of the model. We will discuss this later in Chapter 6.

3.9 Questionnaire Details

While the actual questionnaire form can be found in Appendix E, here the list of questions and answers is presented for your reference:

1. How fast was the whole manipulation task?

   The whole collaboration experience was ...

   (a) too slow; I would do it faster myself!

   (b) slower than I prefer; but not annoyingly.

   (c) very good; it matched my natural speed.

   (d) faster than I prefer; but not annoyingly.

   (e) too fast; I would prefer to do it slower myself!

2. How do you characterize your relative speeds?

   My partner was ...

   (a) too slow; I had to push him/her to go faster!

   (b) slower than me; but not annoyingly.

   (c) pleasant; in the same speed range as me.

   (d) faster than me; but not annoyingly.

   (e) too fast; I had to slow him/her down!

3. How do you feel about the nature of your partner's effort? I felt my partner was ...

   (a) resisting my actions during the whole experience!

   (b) forcing his actions over mine during the task!

   (c) exerting some pushes/pulls, but they were not annoying.

   (d) quite cooperative; no pushes/pulls.

4. How fair do you feel the collaboration was? I feel ...

    (a) he/she applied most of the effort; I had a free ride

    (b) we contributed equally in performing the task

    (c) I did most of the work and he/she enjoyed a free ride

5. How do you characterize the cooperative nature of this collaborative task? I felt ....

    (a) I was leading the task the whole time

    (b) we were switching the roles, but I was leading most of the time

    (c) we both actively cooperated

    (d) we were switching the roles, but I was following most of the time

    (e) I was following him/her the whole time

6. How natural do you feel the motion trajectory was?

    I feel ....

    (a) it was even smoother than I would do it alone!

    (b) it was as smooth as if I did it alone.

    (c) there were some unusual pauses/accelerations, but overall fine

    (d) it was totally abnormal way of performing the task, I would never do it like this!

7. How much attention (mental workload) did the task demand, compared to doing the manipulation on your own?

    I feel the task needed ...

(a) no attention; I just moved naturally

(b) little attention to synchronizing our motions

(c) a lot of mental involvement due to the need to synchronize our actions

Part II
Models

CHAPTER 4

QUANTITATIVE MEASURES FOR HUMAN-COOPERATION

While assisting with ADLs, robots would naturally be expected to engage in dyadic collaboration. One of the main challenges in deploying robots in collaborative tasks is for the robot to behave in a natural human-like way. For instance, in a physical Human-Robot Interaction (pHRI), because people have different motion preferences for the exact same manipulation task, the robot is expected to recognize these differences and to engage in the manipulation task accordingly. Robotic caregivers for elderly are an interesting example where a broad range of motion profiles may appear in a simple dyadic ADL due to the diverse physical capabilities among the elderly.

Lack of a model for physical collaboration tasks has motivated many researchers to attempt describing different aspects of the collaboration. In this chapter, we present a set of metrics that describe different aspects of a collaborative object manipulation task, namely: effectiveness, efficiency, fairness, comfort and similarity. These metrics can be used as an abstract model of how humans cooperate. Using the results of an empirical study with human subjects, we examine the effectiveness of the proposed model and the validity of the metrics. Furthermore, these metrics will be employed as an assessment tool to quantify the performance of different interaction models in Chapter 7. These measures can also be used to evaluate the performance of a robot in a collaborative pHRI task.

4.1 Related Work

A thorough understanding of Human-Human Interaction enables us to successfully employ robots in place of human assistants. Due to the diversity of preferred behavior among people, modeling Human-Human Interaction (HHI) is assumed to be a promising approach. There are many factors, e.g. mental, social, gender-specific etc., affecting the quality of an HHI. In this chapter, we focus on evaluating the quality of physical Human-Human Interaction (pHHI) in order to understand the requirements of an acceptable pHRI. More specifically, we study the quantitative measures for evaluating the performance of a pHHI during a dyadic object manipulation task.

To introduce quantitative measures for human performance in manipulation tasks, (Abdel-Malek and Yang, 2005) models human limbs/joints as robotic linkages/joints in robotic manipulators. The measures that are introduced therein, e.g. reachability, dexterity and weighted-sum-of-joint-displacements, are reformulations of well-explored robotic measures, i.e. workspace, manipulability and accuracy, respectively. Although these measures are well established for single chain manipulators (Yoshikawa, 1985), parallel manipulators (Merlet, 2006) and closed-chain manipulators (cooperative robots) (Bicchi and Prattichizzo, 2000), they are not suitable for measuring human performance. For example, the proposed model is too simple to describe the dexterity differences between the dominant hand and non-dominant hand of the same person.

In a more promising approach, human motions are modeled using the empirical studies. For instance, minimum jerk path (Flash and Hogan, 1985) and Fitts' law (Fitts, 1954) are two widely recognized models for human arm motions. These models are then exploited to introduce new performance measures. An example of this approach is (Garvin et al., 1997), where minimum jerk model is extended to describe motion profiles of two-arm manipulation tasks. The authors present two kinematic models for two physically coupled arms manipulating an object.

To the best of our knowledge, there exists no acceptable model for pHHI in the literature. Moreover, very little has been done in studying the performance of a pHHI (American National Standard, 2000). Effectiveness is an example of a common performance measure among pHHI researchers (Ganesh et al., 2014; van der Wel et al., 2011). Root-mean-square error (RMSE) is another common metrics, which is usually used when deviation from a desired behavior is studied (Groten et al., 2009).

On the other hand, to evaluate the performance of a robot in an HRI task, a wide range of quantitative measures have been proposed (Singer and Akin, 2011; Madhavan et al., 2009; Steinfeld et al., 2006). In particular, in a pHRI problem, using completion time, team-effort (energy) and accuracy (RMSE) is an acceptable practice (Mörtl et al., 2012; Feth et al., 2009). However, none of these metrics can describe the cooperative quality of a pHRI.

4.2 Performance Measures

Among many human performance measures, we choose the ones that are applicable in ADLs and also are of the most interest in both pHHI and pHRI, namely effectiveness, efficiency, cooperativeness, similarity, fairness and comfort. Each performance measure is introduced both subjectively and objectively. The qualitative (subjective) description of each measure is specified by associating it with a set of questions. Subsequently, a quantitative expression for that measures is proposed that relates the subjective concept to the perceived interaction efforts. To make the measures task independent and easy to be compared, most of our proposed objective measures are normalized between zero and one.

4.2.1 Cooperativeness

In a collaborative task, each person may take a different role in performing the task. They may also negotiate over the roles and switch the roles according to the negotiation result. The cooperativeness represents the degree at which the dyad members help each other. The cooperativeness can be measured by answering questions like:

How do you characterize your cooperation?

Did you take complementary roles in performing the task?

Did you mostly lead the task or follow the other person?

In a dyadic manipulation task, each person contributes a certain amount of the effective effort to the total effective effort F_{sum}. Cooperativeness measures the amount of each person's share in the total effort. However, subject shares in a dyadic task are complementary to each other, see (2.5). Let's introduce $\delta = \frac{1}{2} - \alpha$. Therefore,

$$\begin{aligned} f_1^*(t) &= \left(\tfrac{1}{2} - \delta\right) F_{sum} \\ f_2^*(t) &= \left(\tfrac{1}{2} + \delta\right) F_{sum} \end{aligned} \tag{4.1}$$

δ is called the *cooperation index*. When $\delta = 0$ we have $f_1^*(t) = f_2^*(t) = \frac{1}{2}F_{sum}$; that is each person carries out half of the task by contributing exactly half of the total effective effort required. When $|\delta(t)| \leq 0.5$, both persons help in performing the task by contributing positively in direction of the required effective effort, see Fig. 11a. In this situation, we define the collaboration to be in a *cooperative mode*, meaning a successful negotiation in role assignment.

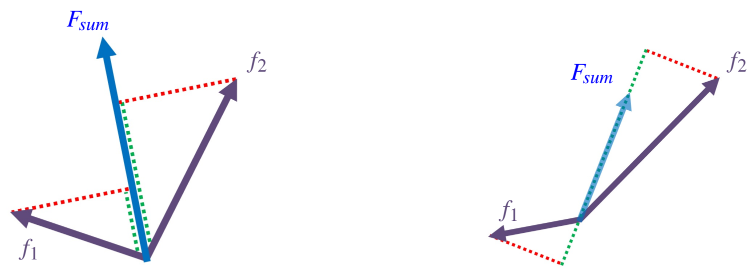

(a) Cooperative (b) Non-cooperative

Figure 11: Cooperative mode vs non-cooperative mode. Copyright © 2014, IEEE.

On the other hand, when $|\delta(t)| > 0.5$, one person's effort is in the reverse direction of F_{sum}, see Fig. 11b. Therefore the other person needs both to cancel the negative effort and to provide the whole required effort. In such a situation, the negotiation on role assignment has failed and we define the collaboration to be in a *non-cooperative mode*.

4.2.2 Collaboration Effectiveness

The effectiveness of a collaborative task is defined as the degree of optimality of performing the task. It can be measured by answering questions like:

How natural do you feel the motion trajectory was?

Was the motion as smooth as when you do it alone?

Did it match your natural speed or it was faster/slower?

Recall that for the reaching task, which is under study in this work, the optimality is measured by minimizing the jerk function. Let $H(t)$ denote the cost function, and $H^*(t)$ be it's minimum value (the optimal solution). The effectiveness index is defined by:

$$I_{effectiveness}(t) = \frac{H^*(t)}{H(t)} \tag{4.2}$$

Since $H^*(t) = min\{H(t)\}$, the effectiveness index is suitably bounded, i.e. $0 \leq I_{effectiveness}(t) \leq 1$. Using our proposed effort decomposition in previous section, we can rewrite the cost function as following:

$$H(t_i, t_f) = \frac{1}{2m^2} \int_{t_i}^{t_f} \left\| \dot{F}_{sum} \right\|^2 \mathrm{d}t \tag{4.3}$$

where m is the object's mass. Note that $F_{sum} = F_{net} - mg$, and therefore $\dot{F}_{sum} = \dot{F}_{net} = m\dot{a}$.

4.2.3 Collaboration Efficiency

As a result of a disagreement on the motion trajectory, it is not uncommon in a dyadic task that one person's efforts are partially canceled by the other's. The efficiency of a collaborative task is defined as the percentage of the amount of the efforts that is not canceled during performing a task. It can be measured by answering questions like:

How do you feel about the exchanged efforts?

Did you receive some unusual pushes or pulls?

Did the other person cancel some of your efforts?

We introduce three different quantitative expressions for measuring collaboration efficiency, namely individual efficiency, team efficiency and negotiation efficiency.

4.2.3.1 Individual Efficiency

For a person $k\,(k = 1, 2)$ in the team, the measure is defined as:

$$M_{ie_k}(t) = \frac{\|f_k^*(t)\|}{\|f_k(t)\|} \tag{4.4}$$

Recall that $f_k(t) = f_k^*(t) \pm F_{normal}(t)$, and therefore individual efficiency is bounded, i.e. $0 \leq M_{ie_k}(t) \leq 1$.

4.2.3.2 Team Efficiency

The percentage of effective team-effort is defined as:

$$M_{te}(t) = \frac{\|F_{sum}(t)\|}{\|f_1(t)\| + \|f_2(t)\|} \tag{4.5}$$

It is obvious that $0 \leq M_{te}(t) \leq 1$ and the performance is maximum, $M_{te}(t) = 1$, only when no effort is wasted, $\|F_{normal}(t)\| = 0$. The team efficiency will be zero, when the dyad members cancel each others' effort, $\|F_{sum}(t)\| = 0$. Also, note that if individual efficiency of both members of the dyad are equal, $M_{ie_1}(t) = M_{ie_2}(t)$, the team efficiency is equal to the individual efficiency.

Team Efficiency Index is defined as the average value of the team efficiency, measured over the period of performing the task:

$$I_{te}(t_i, t_f) = \frac{1}{t_f - t_i} \int_{t_i}^{t_f} M_{te}(t)\,\mathrm{d}t \tag{4.6}$$

4.2.3.3 Negotiation Efficiency

This measure represents the extent of disagreement of the dyad members in performing the task. The negotiation efficiency measure is defined as:

$$M_{ne}(t) = \frac{\|F_{sum}(t)\|}{\|f_1^*(t)\| + \|f_2^*(t)\|} \tag{4.7}$$

Note that the measure is properly bounded, $0 \leq M_{ne}(t) \leq 1$. This is due to the fact that according to (4.1) we have:

$$\|f_1^*(t)\| + \|f_2^*(t)\| = \left(\left| \frac{1}{2} - \delta(t) \right| + \left| \frac{1}{2} + \delta(t) \right| \right) \|F_{sum}\|$$

or

$$\|f_1^*(t)\| + \|f_2^*(t)\| = \begin{cases} 2\delta(t)\|F_{sum}\| & \delta(t) > 0.5 \\ \|F_{sum}\| & -.5 \leq \delta(t) \leq 0.5 \\ -2\delta(t)\|F_{sum}\| & \delta(t) < -.5 \end{cases}$$

Therefore, (4.7) can be rewritten as:

$$M_{ne}(t) = \begin{cases} 1 & |\delta(t)| \leq 0.5 \\ \frac{1}{2|\delta(t)|} & |\delta(t)| > 0.5 \end{cases}$$

When the collaboration is in a cooperative mode ($|\delta(t)| \leq 0.5$), the negotiation has been successful and $M_{ne}(t) = 1$. On the other hand, when the collaboration is in a non-cooperative mode ($|\delta(t)| > 0.5$), the negotiation efficiency decreases as the disagreement increases: $M_{ne}(t) = (2|\delta|)^{-1} < 1$. The *Negotiation Efficiency Index* is defined as the average value of the negotiation efficiency, measured over the time period of performing the task:

$$I_{ne}(t_i, t_f) = \frac{1}{t_f - t_i} \int_{t_i}^{t_f} M_{ne}(t)\, \mathrm{d}t \tag{4.8}$$

4.2.4 Similarity of Efforts

Many dyadic tasks, including the one we study in this work, have sort of a symmetry such that swapping the dyad efforts would have no effect on performing the task. In such tasks, it is logical to assume that the effective efforts of dyad members are similar. Similarity can be measured by answering questions like:

How do you characterize your relative speeds?

Do you feel your motions were in sync?

Consequently, the measure of similarity is defined as:

$$M_s(t) = 1 - \left| \frac{\|f_1^*(t)\| - \|f_2^*(t)\|}{\|F_{sum}(t)\|} \right| \tag{4.9}$$

Note that the measure is properly bounded, $0 \leq M_s(t) \leq 1$. This is due to the fact that according to (4.1) we have:

$$\|f_1^*(t)\| - \|f_2^*(t)\| = \left(\left| \frac{1}{2} - \delta(t) \right| - \left| \frac{1}{2} + \delta(t) \right| \right) \|F_{sum}\|$$

or

$$\|f_1^*(t)\| - \|f_2^*(t)\| = \begin{cases} -\|F_{sum}\| & \delta(t) > 0.5 \\ -2\delta(t)\|F_{sum}\| & -.5 \leq \delta(t) \leq 0.5 \\ +\|F_{sum}\| & \delta(t) < -.5 \end{cases}$$

Therefore, (4.9) can be rewritten as:

$$M_s(t) = \begin{cases} 1 - 2|\delta(t)| & |\delta(t)| \leq 0.5 \\ 0 & |\delta(t)| > 0.5 \end{cases}$$

When the collaboration is in a non-cooperative mode ($|\delta(t)| > 0.5$), the similarity measure is zero. However, in a cooperative mode ($|\delta(t)| \leq 0.5$), the measure increases: $M_s(t) = 1 - 2|\delta(t)|$. Maximum similarity ($M_s(t) = 1$) happens only when effective effort of both persons are exactly the same (or equivalently $\delta(t) = 0$).

The *Similarity Index* is defined as the average value of the similarity measure over the period of performing the task:

$$I_s(t_i, t_f) = \frac{1}{t_f - t_i} \int_{t_i}^{t_f} M_s(t)\,\mathrm{d}t \tag{4.10}$$

4.2.5 Fairness of Collaboration

Another important performance measure in a collaborative task is fairness. During the whole task, the dyad members continuously negotiate on their contribution in effective effort. A collaborative task is performed fairly, when both members of the dyad contribute the same total amount of the effective effort. Fairness can be measured by answering questions like:

How fair do you feel the collaboration was?

Did you contribute equally in performing the task?

Or one did most of the task and other enjoyed a free ride?

The fairness index represents the inequality of their attempts as follows:

$$I_f(t_i,t_f) = 1 - \left| \frac{N_1 - N_2}{N_{sum}} \right| \tag{4.11}$$

in which:

$$\begin{aligned} N_1(t_i,t_f) &= \textstyle\int_{t_i}^{t_f} \|f_1^*(t)\| \,\mathrm{d}t \\ N_2(t_i,t_f) &= \textstyle\int_{t_i}^{t_f} \|f_2^*(t)\| \,\mathrm{d}t \\ N_{sum}(t_i,t_f) &= \textstyle\int_{t_i}^{t_f} \|F_{sum}(t)\| \,\mathrm{d}t \end{aligned} \tag{4.12}$$

Note that the index is properly bounded, $0 \leq I_f(t_i,t_f) \leq 1$. This is due to the fact that (4.11) can be rewritten as:

$$I_f = 1 - \left| \frac{\int_{t_i}^{t_f} \|f_1^*(t)\| \,\mathrm{d}t - \int_{t_i}^{t_f} \|f_2^*(t)\| \,\mathrm{d}t}{\int_{t_i}^{t_f} \|F_{sum}(t)\| \,\mathrm{d}t} \right|$$

$$I_f = 1 - \left| \frac{\int_{t_i}^{t_f} (\|f_1^*(t)\| - \|f_2^*(t)\|) \,\mathrm{d}t}{\int_{t_i}^{t_f} \|F_{sum}(t)\| \,\mathrm{d}t} \right|$$

or

$$I_f(t_i,t_f) = \begin{cases} 1 - \frac{\left|\int_{t_i}^{t_f} 2\delta(t) \|F_{sum}(t)\| \,\mathrm{d}t\right|}{\int_{t_i}^{t_f} \|F_{sum}(t)\| \,\mathrm{d}t} & |\delta(t)| \leq 0.5 \\ 0 & |\delta(t)| > 0.5 \end{cases}$$

For a collaboration in cooperative mode ($|\delta(t)| \leq 0.5$), if both dyad members apply equal amount of total effective effort, the collaboration is fair and the index is maximized ($I_f = 1$). However, when the collaboration is in a non-cooperative mode ($|\delta(t)| > 0.5$), the index is zero. It's because one person is actually doing the whole task and additionally, compensating the other person's inappropriate effort.

4.2.6 Collaboration Comfort

According to a well-respected hypothesis in neuroscience, human motions are executed in a feedforward fashion (Kawato, 1999). The main justification of this hypothesis is that our sensory system suffers from a huge delay, which makes a real-time feedback control scheme impractical. However, when the actual motion differs from the intended motion (feedforward plan), due to an unexpected/external disturbance, the feedback control system is engaged to reduce the error. The feedback loop demands some degree of mental computations, which makes us uneasy. The Measure of Comfort represents the degree of mental demand in a collaborative task and can be measured by answering questions like:

How much attention did the task demand?

Was the task as easy as doing it alone?

Or did the task demand a lot of mental involvement?

In a collaborative object manipulation task, each person's effort can be perceived as an external disturbance by the other. The only way that a person can execute a feedforward motion plan here, is that he/she perceives the other person's effort as a constant mass. Let's take a 10 kg object for an example. Also, let P refer to the person's feedforward plan (when he/she performs the task alone) for an 8 kg object. The person can execute P in a dyadic collaborative task (and obtain the same trajectory), only if the other person's effort properly compensates the extra 2 kg. In this case the ratio of their effective effort is constantly 4. Therefore, the most comfortable collaboration happens when the effective efforts are proportional, $f_1^*(t) \propto f_2^*(t)$. According to (4.1) we have $(\frac{1}{2}+\delta(t))f_1^*(t) = (\frac{1}{2}-\delta(t))f_2^*(t)$. Therefore, maximum comfort happens when $\delta(t) = \text{const}$. We took the extent of the variation of the *cooperation index* as a measure of comfort:

$$M_c(t) = \|\dot{\delta}(t)\| \tag{4.13}$$

Using the variation of the *cooperation index* as an indicator of the degree of mental demand is motivated by the assumption that humans perform manipulation tasks in a (sub-) optimal manner. Accordingly, the resultant trajectory (or equivalently the resultant effort F_{sum}) may be considered as a solo manipulation plan, a feedforward plan P. Any variations in δ means a new debate on the amount of dyad contributions in F_{sum}, which comes with mental computation costs.

The measure is zero, when the collaboration is the most comfortable and increases as the comfort decreases. The *Comfort Index* is defined as the average value of the comfort measure over the period of performing the task:

$$I_c(t_i, t_f) = \frac{1}{t_f - t_i} \int_{t_i}^{t_f} M_c(t)\, \mathrm{d}t \tag{4.14}$$

4.3 Discussion

While effectiveness, individual efficiency and team efficiency are task-oriented measures, other measures focus on cooperation characteristics of a collaborative task. To be able to highlight different aspects that different measures are evaluating, we choose a simple collaborative reaching task. The object's motion is assumed to follow the optimal (minimum-jerk) trajectory along a straight line (say x-axis). Fig. 12 depicts the value of required effort, F_{sum}, along x-axis. Note that for easier comparison, the task parameters (mass, path length and collaboration time) are adjusted in such a way that F_{sum} is bounded between -1 and $+1$.

4.3.1 Cooperation Mode

Fig. 13 illustrates four different examples of collaborations in cooperative mode. A perfect cooperation is depicted in Fig. 13a, in which cooperation index is zero, $\delta = 0$. Here, each dyad member applies the exact same effort; $f_1^* = f_2^* = \frac{1}{2}F_{sum}$. Therefore, the similarity index and fairness index both are maximum; $I_s = 1$ and $I_f = 1$. Also, the comfort index is minimum; $I_c = 0$.

On the other hand, a marginal cooperation is depicted in Fig. 13b, where $\delta = -0.5$. Here, the whole task is performed by one person and the other person enjoys a free ride. Accordingly, both similarity and fairness indices are minimum; $I_s = 0$ and $I_f = 0$. However, since no negotiation happens during the task (δ is fixed), the comfort index is still minimum; $I_c = 0$.

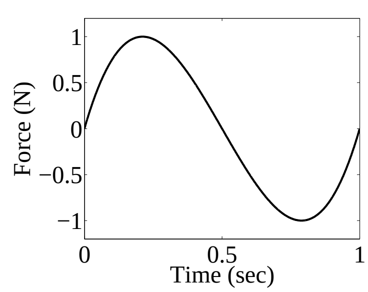

Figure 12: The minimum-jerk force required to move a mass of $1kg$ over a straight line which is $L = 17.32cm$ long during a period of $t_f - t_i = 1sec$. Copyright © 2014, IEEE.

Fig. 13c depicts a cooperative collaboration, where $\delta = -0.3$. Here, one person applies four times more effort than the other person. Therefore, similarity and fairness indices are: $I_s = 0.4$ and $I_f = 0.4$; which follows the unbalanced nature of cooperation. Again, $I_c = 0$.

Note that when cooperation index is constant, the similarity and fairness indices are the same, $I_s = I_f = 1-2|\delta|$, and comfort index is zero (as it appeared in above three cases). Fig. 13d depicts a situation where δ changes form -0.5 to $+0.5$ in the middle of cooperation. In this case, one person is responsible for accelerating the object in the first half of the path and the other is responsible for decelerating it on the second half. The role assignment is fair and each dyad member applies half of the total required effort and therefore, $I_f = 1$. However, their efforts are not similar; i.e. $I_s = 0$. Also, note that $I_c = 1$, which indicates a less comfortable cooperation. These trajectory emerges in specific tasks, where dyads learn to take accelerating/decelerating roles (Reed et al., 2006). The increase in I_c reflects the learning cost (or equivalently increase in complexity).

Fig. 14 illustrates two examples of non-cooperative collaboration, where $|\delta(t)| > 0.5$. In both cases, dyad members apply forces in different directions, partly canceling other person's effort. Fig. 14a shows collaboration with constant cooperation index, $\delta = 1$. Accordingly, $I_s = I_f = I_c = 0$. On the other hand, Fig. 14b illustrates the effect of cooperation index variations in non-cooperative mode. Here, $I_s = 0$, $I_f = 1$ and $I_c = 2$; indicating a fair but complicated collaboration.

4.3.2 Grasp Force

In an object manipulation task, parts of the applied efforts are exerted to secure the object in a grasp. Since we do not have a model for the interaction force yet, let's assume that it is mainly comprised the grasp force. In Chapter 2, we showed that in addition to a normal component, the grasp forces can

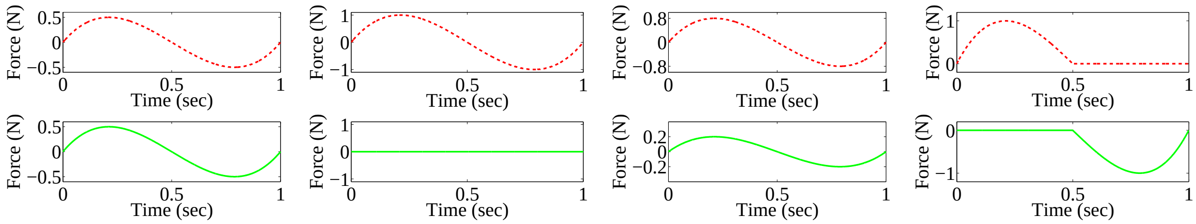

(a) Perfect cooperation (b) Marginal cooperation (c) Unbalanced cooperation (d) Role taking cooperation

Figure 13: Collaborations in cooperative mode. In each pair of graphs, the red signals (dashed line on top) is f_1^* and the green one (solid line on bottom) is f_2^*. a) perfect cooperation ($\delta = 0$). b) marginal cooperation ($\delta = -0.5$). c) unbalanced cooperation ($\delta = -0.3$). d) acceleration/deceleration role taking. Copyright © 2014, IEEE.

have components aligned with the effective effort, F_{sum}, too. These components act as a low-frequency time-varying bias that can affect the cooperation index variations adversely. For instance, when the magnitude of F_{sum} is small, these bias will result in a large δ. A more promising model that may take this bias into account is:

$$\begin{aligned} f_1^*(t) &= \left(\tfrac{1}{2} - \delta(t)\right) F_{sum} - F_{bias}(t) \\ f_2^*(t) &= \left(\tfrac{1}{2} + \delta(t)\right) F_{sum} + F_{bias}(t) \end{aligned} \tag{4.15}$$

Fig. 15 exemplifies a situation where the negotiation is succeeded, both dyad members apply equal contributions on top of their grasp force components, and the collaboration results the optimal solution (minimum-jerk) for F_{sum} (with the same assumptions as in Fig. 12). Ignoring the grasp forces, our model suggests that the collaboration is in a non-cooperative mode and δ would diverge in the middle point (where $F_{sum} = 0$). Following the model introduced in (4.15), we get $\delta(t) = 0$ and the collaboration

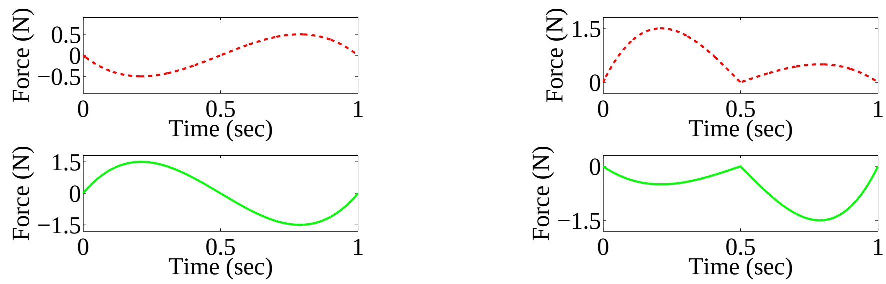

(a) Constant δ

(b) Varying δ

Figure 14: Collaborations in non-cooperative mode. In each pair of graphs, the red signals (dashed line on top) is f_1^* and the green one (solid line on bottom) is f_2^*. a) $\delta = 1$. b) δ changes form -1 to $+1$ in the middle. Copyright © 2014, IEEE.

is in a perfect cooperation mode. As mentioned earlier, unfortunately, there is no sufficient information to uniquely determine $F_{bias}(t)$ here.

To tackle this issue, note that when F_{sum} is very small, both f_1^* and f_2^* are mainly representing grasp forces. Therefore, the amounts of the grasp forces are known for a few points during manipulation, where $F_{sum} = 0$. We observed that the variations of the grasp force ($F_{bias}(t)$) between these isolated points resemble a line. Therefore, we used linear interpolation to estimate the grasp forces in between the known points. Applying these estimated grasp force in (4.15) will result in more accurate values for δ.

4.4 Survey on Human Collaboration

Following the human-study protocol explained in Chapter 3, we collect interaction force signals and motion trajectories of bimanual and dyadic object manipulation tasks. The signals are then filtered

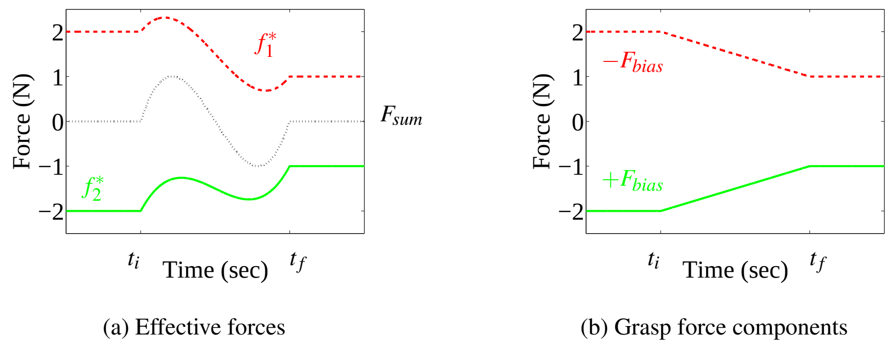

Figure 15: The effect of grasp bias on the effective forces. a) The dyad members' effective forces result in an optimal effective effort (F_{sum}). b) The low-frequency time-varying grasp force components (F_{bias}), which is aligned with the effective effort. Copyright © 2014, IEEE.

(a Savitzky-Golay smoothing filter with polynomial degree of 7 and window size of 201). Following the model proposed in (4.15), effective forces and the interaction force have been computed. These components are then utilized to calculate the values of the proposed quantitative measures.

To evaluate the proposed measures, we provided a self-assessment questionnaire and asked each subject to fill it after each trial. The questions are those appeared in Sec. 4.2. Since the set of potential answers to some of these questions had less than 5 items to choose from, and also since we had a limited number of participants, we used a Visual Analogue Scale (VAS) questionnaire instead of a Likert scale to achieve a higher precision in self-assessment results. The questionnaire can be found in Appendix E.

4.5 Qualitative Assessment

Fig. 16 illustrates six examples of different types of force interactions that may appear in a subtask. In Fig. 16a a successful cooperation is presented, where $\delta(t) < 0.5$ during the whole task. While this type of collaboration happens mainly in *synchronized mode*, a few successful cooperation were recorded in *follower mode* too. However, in one instant, the follower stated that he could read the leader's intention to move and could predict the beginning of the motion by watching her eyes. In this type of collaboration, both subjects stated that they contributed equally and interacted cooperatively.

Fig. 16b shows an example of the role taking type of cooperation, where one subject mainly accelerate the pot and the other decelerate it. To cancel the grasp force, we used the model in (4.15). Again, both subjects stated that they contributed equally and interacted cooperatively. A common complain that was reported in this type of collaboration was about the internal force exchange. Both subjects stated that the other person exerted some pushes/pulls during the task. These internal forces were evaluated by the team efficiency measure.

Fig. 16c exemplifies the marginal cooperation type of collaboration. Both subjects agreed that most of the task was performed only by one subject and the other one had a free ride. The fairness measure agreed with this assessment. Fig. 16d-16f illustrate non-cooperative collaborations. They are common cases in the *follower mode*. Fig. 16d shows the situation in which the follower reacted with a delay and exerted an opposing force. The common complain in this type of collaboration was the speed mismatch. Each subject stated that the other person was faster/slower than his/her natural speed. However, we observed that most of the times, the follower could catch up with the leader and perform a successful cooperation in the second half of the task.

Another interesting type of collaboration is presented in Fig. 16e, where both subjects actively negotiate in collaboration. If the model in (4.15) is applied to the signals in this figure, they will become a role taking cooperation. However, unlike that type of collaboration, here subjects declare different

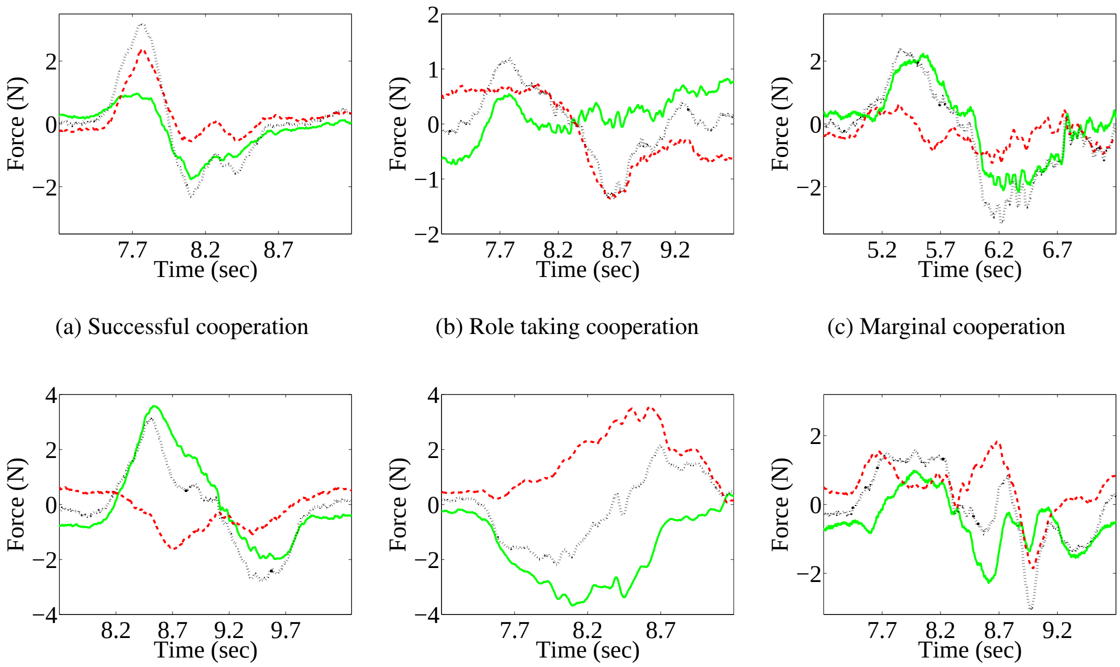

(a) Successful cooperation (b) Role taking cooperation (c) Marginal cooperation

(d) Opposing collaboration (e) Active negotiation (f) Non-smooth collaboration

Figure 16: Different types of collaborations. In all graphs, red signal (dashed line) is f_1^*, green signal (solid line) is f_2^* and black signal (dotted line) is F_{sum}. Copyright © 2014, IEEE.

amount of contributions to the task. For instance, in the case of this particular figure, both subjects agreed that all of the work is done by the person applying green signal (solid line). This assessment is very similar to the marginal cooperation type of collaboration. We speculate that the difference in subjective assessments is related to the characteristics of the exchanged internal force.

The last common type of collaborations that we observed is exemplified in Fig. 16f. As the graph shows and also the assessments agree, there exists unusual pause/accelerations during the task. As a result, the shape of the signal is very different from the expected minimum-jerk signal. The smoothness of the motion is evaluated by the effectiveness measure.

4.6 Conclusion

As illustrated in the previous section, taking the grasp force as the interaction force would reveal some information about the interaction. However, there are cases where the grasp force alone does not provide enough information. Take Fig. 16e as an example. Here the interaction seems to be very smooth and a minimum-jerk motion is taking place. However, the grasp forces both at the beginning and at the end of motion are very small. Thus, canceling the grasp forces would not reveal anything new about the nature of the interaction. In this chapter we suggested that a linear interpolation of the grasp force can provide information about the interaction force. In Chapter 6 we present our proposed model for the interaction force. It is argued that the interaction force would follow a 5th order polynomial in this specific task. In fact, "taking the linear interpolation of the grasp forces as the interaction force" is a low-order approximation of the proposed interaction force model. This is the reason why it performs well in certain trials and fails in some others.

CHAPTER 5

OBJECT MOTION MODEL

Parts of this chapter have been presented in (Noohi et al., 2015). Copyright © 2015, IEEE.

While hand trajectory has been successfully modeled for single arm reaching movement, few works have considered the bimanual reaching movement and no study has modeled the dyadic reaching movement. In a bimanual task, both hands belong to the same person, while in a dyadic task each hand belongs to a different person. In this chapter, we study both bimanual and dyadic reaching movements and show that the motion trajectory follows the minimum-jerk trajectory. Furthermore, we show that our model is consistent with the existing theories on single arm motions, when applied to each of the cooperating arms.

5.1 Related Work

As a result of the extensive body of research on human movements, many theories and predictive models have been developed. While proposing a model that accounts for trial-to-trial variations of the motion trajectory is a very challenging research problem, the average motion trajectory has been described successfully with several models and theories. It has been shown that many biological movement profiles possess certain regularities.

In a large class of complex movements, drawing a curved path for instance, Lacquaniti et al. (Lacquaniti et al., 1983) showed that the angular velocity, $\alpha(t)$, and the path curvature, $\kappa(t)$, are in a power relation as: $\alpha(t) = a \times \kappa(t)^{2/3}$. This relation, which is also known as the 2/3rd power law, can equivalently be expressed as a relation between the velocity and the curvature, as: $v(t) = b \times \kappa(t)^{-1/3}$. Also, in grasping and reaching movements, the movement time, MT, is related to the target's size (width), W, and the distance to the target, D. By defining the Index of difficulty as $ID = log_2(\frac{2D}{W})$, Fitts (Fitts, 1954) showed that a linear relation exists between the movement time and the Index of difficulty, $MT = a + b \times ID$, also known as Fitts' law. The parameters a and b depend on the task.

The most successful class of models for biological movements is arguably the optimal control models (Todorov, 2004). These models suggest that the human sensorimotor system optimizes a certain cost function in order to perform specific movements. Anderson and Pandy (Anderson and Pandy, 2001) showed that metabolic energy minimization reproduces the salient features of normal gait (for walking on level ground). In reaching movements, such as pointing, grasping and eye movements, it has been shown that the trajectory smoothness is of the most importance. Flash and Hogan (Flash and Hogan, 1985) showed that a minimum-jerk model accurately describes trajectories of the reaching movements. This model generates the well-known bell-shape velocity profile and can describe the relation between the velocity and the curvature, even more accurately than the 2/3rd power law (Todorov, 2004).

Another criterion related to the smoothness is the minimum torque change (MTC), proposed by (Uno et al., 1989) and (Nakano et al., 1999). In this model, the nonlinear dynamics of the arm is considered and the motion trajectory is obtained by minimizing the variations of the applied joint torques. MTC can explain the mirror asymmetry that appears in some via-point tasks, while minimum-jerk model fails to do so.

In addition to smoothness, the accuracy of the final position in reaching movement (wrt. the target point) is proposed as another optimization criterion. Since the motor noise is known to be signal-dependent, the sequence of muscle activation commands will contribute to the final position error. Therefore, minimizing the final position error leads to the optimal control policy. Harris and Wolpert (Harris and Wolpert, 1998) suggested that the optimal trajectory minimizes the final position variance, also known as minimum variance model. The model is shown to be very successful in describing speed profiles of saccadic eye movements. The reaching trajectories introduced by minimum variance model are in agreement with those of the MTC model. Also, minimum variance model is consistent with both Fitts' law and the power law.

While there exists a rich literature on modeling single arm reaching movement, bimanual and dyadic movements are far less studied. Guiard (Guiard, 1987) suggested that in bimanual tasks, while one arm performs the majority of the workload, the other arm is responsible for fine tuning and corrections. He discussed this role assignment in tasks like swinging a golf club or writing a letter. Reed et al. (Reed et al., 2006) observed similar arm specialization in a dyadic task where one person is contributing more to acceleration and the other person to deceleration. In a different approach in modeling the bimanual and dyadic movements, quantitative metrics were proposed to measure the performance of the task. Noohi and Žefran (Noohi and Žefran, 2014) proposed a set of measures that evaluate the performance of physically-coupled subjects and cross-validated those metrics with the subjects' self-assessments. Groten et al. (Groten et al., 2009) studied the efficiency of a virtual pursuit tracking task for haptically-coupled subjects (in a virtual reality environment). Ganesh et al. (Ganesh et al., 2014) reported that haptically-coupled subjects demonstrate better motor performance in virtual pursuit tracking task than a single person. Similarly, van der Wel et al. (van der Wel et al., 2011) showed that physically-coupled subjects demonstrate better coordination in an object manipulation task than a single person.

In all of these works, certain features in the bimanual and dyadic reaching movements were studied and modeled at an abstract level. Very few works have considered a computational model for bimanual movement trajectory. For instance, Tresilian and Stelmach (Tresilian and Stelmach, 1997) showed that the aperture and transport components of a unimanual reach-to-grasp task is very similar to the bimanual performance of the same task. Garvin et al. (Garvin et al., 1997) studied the bimanual reaching movement and proposed an extension to the minimum-jerk model by incorporating the rotational jerk of the object into the optimization constraint. Diedrichsen (Diedrichsen, 2007) studied bimanual reaching movement in one-cursor and two-cursor conditions. He showed that the change in the control and in the adaptation are both optimal and task-dependent.

5.2 Data Collection

Following the human-study protocol explained in Chapter 3, we collect interaction force signals and motion trajectories of bimanual and dyadic object manipulation tasks. The signals are then introduced to a low pass filter with the cutoff frequency of 12.5 Hz to eliminate the high frequency noise. The filter is a Savitzky-Golay smoothing filter (Schafer, 2011), with polynomial degree of 7 and window size of 201. The velocity of the object is obtained by integrating its acceleration. The total force that is applied to the object is obtained by adding the forces that each hand applies to the object to the object's gravitational force. The total force is then projected onto the direction of motion. Note that in the horizontal movements, this projection cancels out the gravitational force. We will refer to this projected total force by F_{sum}. Additionally, to be able to compare these signals across different motion types and different scenarios, we normalize the signals in both time and magnitude. That is, the motion duration and the traveled distance are both normalized to 1.

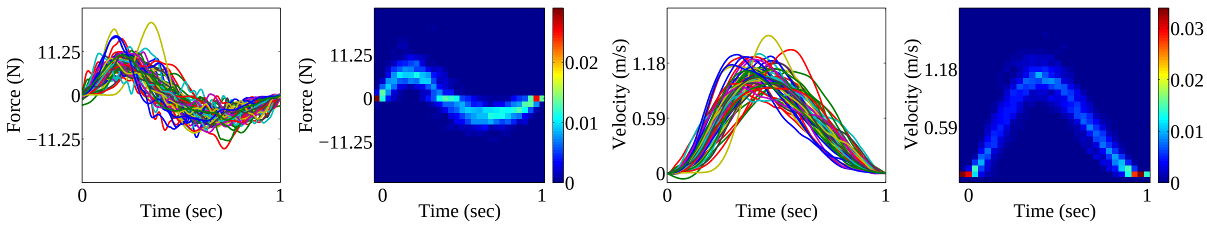

(a) Normalized F_{sum} samples for SPB (b) Normalized velocity samples for SPB

Figure 17: Time trajectory and 2D histogram of SPB samples. Copyright © 2015, IEEE.

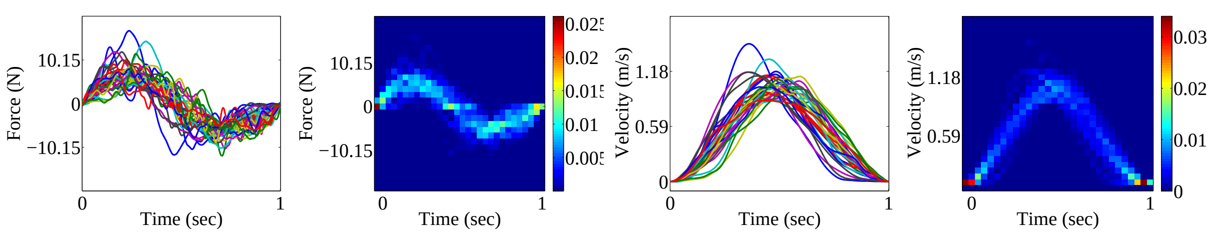

(a) Normalized F_{sum} samples for Sync (b) Normalized velocity samples for Sync

Figure 18: Time trajectory and 2D histogram of Sync samples. Copyright © 2015, IEEE.

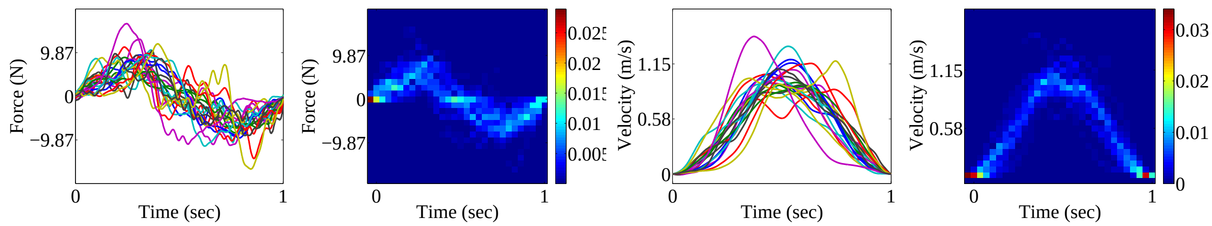

(a) Normalized F_{sum} samples for L/F (b) Normalized velocity samples for L/F

Figure 19: Time trajectory and 2D histogram of L/F samples. Copyright © 2015, IEEE.

5.3 A Minimum-Jerk Model for Cooperation

Fig. 17 shows the time trajectory and 2D histogram for both the normalized F_{sum} and the normalized velocity of the object in the SPB scenario. It is worth mentioning that while *averaging* potentially eliminates important information of the signals, *2D histograms* conserve these information and provide a better representation. Fig. 18 and Fig. Fig. 19 show the same graphs for the signals in the Sync and L/F scenarios, respectively. Both force and velocity signals resemble a minimum-jerk trajectory for the object. In this section we study our hypothesis that:

Motion Trajectory Hypothesis:

In a dyadic or a bimanual reaching movement, the object's motion trajectory is highly correlated with the minimum-jerk trajectory.

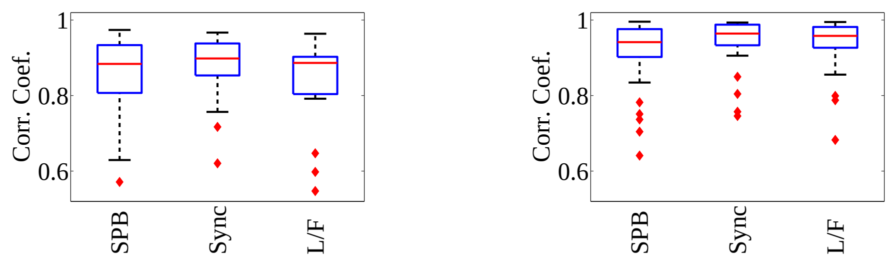

(a) Force samples (b) Velocity samples

Figure 20: Pearson correlation coefficients for a) the normalized samples of F_{sum} and b) the normalized samples of object's velocity. Copyright © 2015, IEEE.

To evaluate this hypothesis, the similarity between the signals and the minimum-jerk trajectory should be quantified.

To measure the similarity between two signals, it is a common practice to use Pearson correlation coefficient, r, (Shadmehr and Mussa-Ivaldi, 1994; Hwang et al., 2003). The value of r is calculated between every velocity (force) sample and the minimum-jerk velocity (force) signal. Box-and-whisker plots in Fig. 20 demonstrate the distribution properties of the correlation coefficients. Fig. 20a illustrates the distribution of r for force samples in SPB, Sync and L/F scenarios. The same is presented in Fig. 20b for the velocity samples. According to these box plots, 87.5% of force samples and 100% of velocity samples have correlation coefficient $r > 0.8$, when the outliers are excluded.

The mean and standard-deviation of r for force and velocity samples in different scenarios are reported in Table I. Considering the skewness of the distribution of the correlation coefficients, we use

	Velocity		Force	
	Mean ($\bar{x}$)	SD (s)	Mean ($\bar{x}$)	SD (s)
SPB	0.92	0.08	0.86	0.09
Sync	0.94	0.07	0.88	0.08
L/F	0.93	0.08	0.84	0.11

TABLE I: MEAN AND STANDARD-DEVIATION OF THE PEARSON CORRELATION COEFFICIENTS FOR FORCE AND VELOCITY SAMPLES IN DIFFERENT SCENARIOS.

	Velocity		Force	
	$\hat{\rho}$	$95\% CI$	$\hat{\rho}$	$95\% CI$
SPB	0.95	[0.935, 0.963]	0.89	[0.863, 0.906]
Sync	0.97	[0.951, 0.978]	0.90	[0.872, 0.919]
L/F	0.96	[0.933, 0.977]	0.87	[0.820, 0.902]

TABLE II: THE ESTIMATED VALUES OF PEARSON CORRELATION COEFFICIENTS AND THEIR 95% CONFIDENCE INTERVALS.

Fisher's z-transformation to map the samples to an approximately-normal distribution (Fisher, 1915). Table II reports the estimated correlation coefficients and their 95% confidence intervals. Note that all estimated correlation coefficients for velocity (force) signals are greater than 95% (87%). Also, the lower limits of the 95% confidence intervals for the velocity (force) signals are greater than 93% (82%). It supports the hypothesis that there exists a strong correlation between the object's motion trajectory in dyadic/bimanual reaching movements and the minimum-jerk trajectory.

5.4 Analysis of Skewness in Cooperation

A closer look at Fig. 17 reveals that the motion profiles in SPB are slightly skewed to the left. This skewness is more recognizable if the average of the signals in each scenario is plotted against the minimum-jerk signals, see Fig. 21. As can be seen in this figure, SPB signals and Sync signals are noticeably skewed to the left. However, the average of the signals can be misleading and the skewness may only be the result of some outliers.

Similar left-skewness has been reported in the case of single arm reaching movements (Jeannerod, 1988; Milner and Ijaz, 1990). Many researches take the duration of the acceleration phase as a measure of the skewness. However, this method is not accurate, particularly when considering the submovements and the noise. Here, we took a different approach. As discussed in the previous section, the object's motion trajectory is highly correlated with the minimum-jerk trajectory. As a result, the first order approximation of the skewness is the time-shift between the signal and the minimum-jerk trajectory. That is, canceling the time-shift between a signal and the minimum-jerk signal will result in the maximum correlation coefficient r between them. Fig. 22 illustrates the result of such a compensation for the signals in the Sync scenario.

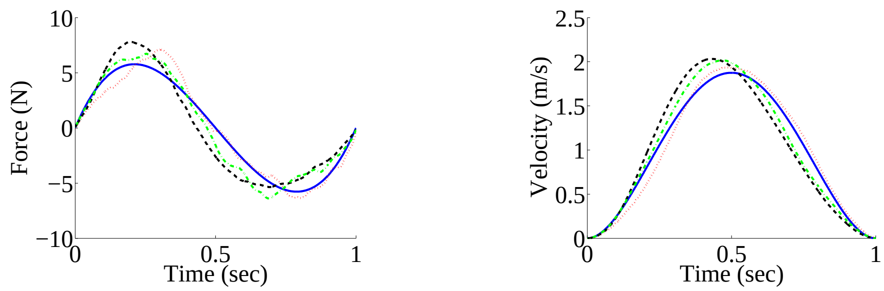

(a) Skewness in force

(b) Skewness in velocity

Figure 21: Skewness of the motion trajectories in different scenarios wrt the minimum-jerk trajectory. The dashed line signal (black) is the average of the SPB signals. The dash-dot line signal (green) and the dotted line signal (red) are for Sync and L/F signals respectively. The solid line signal (blue) is the minimum-jerk optimal trajectory. Copyright © 2015, IEEE.

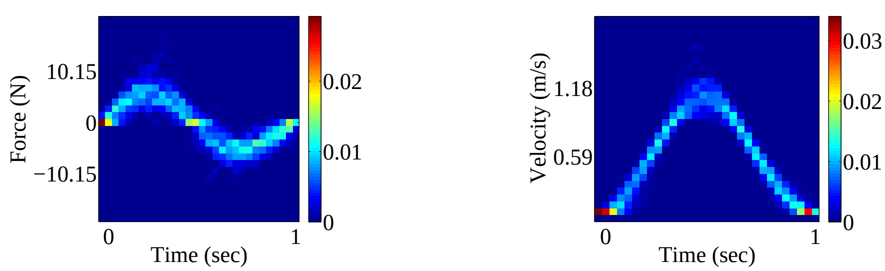

(a) Unskewed F_{sum} samples

(b) Unskewed velocity samples

Figure 22: 2D histogram of Sync samples after skewness enhancement. Copyright © 2015, IEEE.

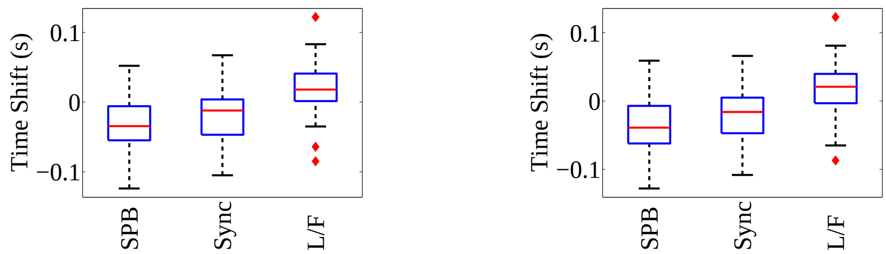

(a) Force samples (b) Velocity samples

Figure 23: Cross-correlation time-shift for a) the normalized samples of F_{sum} and b) the normalized samples of object's velocity. Copyright © 2015, IEEE.

The time-shift is computed by maximizing the cross-correlation between each signal and the minimum-jerk signal. Box-and-whisker plots in Fig. 23 demonstrate the distribution properties of these time-shifts. According to these box plots, while 75% of the time-shifts in SPB and Sync scenarios are negative (left skewed), 75% of the time-shifts in L/F scenario are positive (right skewed). This observation suggests the following hypotheses:

H^1: Time-shifts in SPB samples are negative. The null hypothesis here is "$H_0 : \mu_{SPB} = 0$" against the alternative hypothesis "$H_a : \mu_{SPB} < 0$".

H^2: Time-shifts in Sync samples are negative. The null hypothesis here is "$H_0 : \mu_{Sync} = 0$" against the alternative hypothesis "$H_a : \mu_{Sync} < 0$".

H^3: Time-shifts in L/F samples are positive. The null hypothesis here H^3 is "$H_0 : \mu_{L/F} = 0$" against the alternative hypothesis "$H_a : \mu_{L/F} > 0$".

To test the normality of the distributions, we used Shapiro-Wilk test, Anderson-Darling test, Kolmogorov-Smirnov test, Lilliefors test and Jarque-Bera test. All tests fail to reject the hypothesis that the data is distributed normally. For instance in Kolmogorov-Smirnov test, all p-values were $p > 0.63$, for both force and velocity samples in all scenarios. Therefore, we can safely use the one-sample t-test for testing the above hypotheses.

Regarding H^1, the velocity time-shift (-0.037 ± 0.038) was statistically significantly lower than zero $(95\% CI = [-0.047, -0.027]$, $t(57) = -7.3$, $p = 5.0e{-10})$. The force time-shift (-0.032 ± 0.037) was also significantly lower than zero $(95\% CI = [-0.042, -0.023], t(57) = -6.7, p = 5.7e{-9})$. Similarly for H^2, the velocity time-shift (-0.020 ± 0.042) was statistically significantly lower than zero $(95\% CI = [-0.035, -0.0047], t(30) = -2.6, p = 0.006)$. The force time-shift (-0.018 ± 0.041) was also significantly lower than zero $(95\% CI = [-0.033, -0.0035], t(30) = -2.5, p = 0.009)$.

These results indicate that, in both H^1 and H^2, very strong evidences exist in favor of the alternative hypotheses and we can strongly reject the null hypotheses at $\alpha = 0.05$. However for H^3, only weak evidences exist in favor of the alternative hypothesis and the test fails to reject the null hypotheses at the given significance level $(\alpha = 0.05)$. The velocity time-shift (0.017 ± 0.048) was not statistically significantly different from zero $(95\% CI = [-0.0051, 0.0387], t(20) = 1.6, p = 0.063)$. The force time-shift (0.017 ± 0.046) was not statistically significantly different from zero, too $(95\% CI = [-0.0037, 0.0384]$, $t(20) = 1.7$, $p = 0.051)$.

Another interesting observation in Fig. 23 is the similarity of distributions of SPB and Sync samples. Furthermore, based on the above statistical analysis, their mean values are close to each other (less than half a σ apart) and their standard deviations are similar. These observations suggest the following hypotheses:

H^4: Time-shifts in SPB samples are equal to the time-shifts in Sync samples. The null hypothesis for testing H^4 is "$H_0 : \mu_{SPB} = \mu_{Sync}$" against the alternative hypothesis "$H_a : \mu_{SPB} \neq \mu_{Sync}$".

H^5: Time-shifts in SPB samples are smaller than the time-shifts in L/F samples. The null hypothesis for testing H^5 is "$H_0 : \mu_{SPB} = \mu_{L/F}$" against the alternative hypothesis "$H_a : \mu_{SPB} < \mu_{L/F}$".

H^6: Time-shifts in Sync samples are smaller than the time-shifts in L/F samples. The null hypothesis for testing H^6 is "$H_0 : \mu_{Sync} = \mu_{L/F}$" against the alternative hypothesis "$H_a : \mu_{Sync} < \mu_{L/F}$".

To evaluate the similarity between the time-shifts in SPB, Sync and L/F scenarios, we used a one-way ANOVA test. The test results indicate that a statistically significant difference exists between scenarios. In case of the velocity signals, $F(2,107) = 12.92$ and $p = 9.4e{-}6$. And for the force signals, $F(2,107) = 11.98$ and $p = 2.0e{-}5$.

To evaluate the above hypotheses we performed a Tukey post-hoc test. The test results revealed that no statistically significant difference exists between the time-shifts in SPB scenario and Sync scenario (H^4). In the case of the velocity signals, $p = 0.17$ and the $95\%CI = [-0.038, 0.0052]$. For the force signals, $p = 0.25$ and the $95\%CI = [-0.035, 0.007]$. In both cases, H^4 fails to reject the null hypotheses at the given significance level.

On the other hand, in the case of H^5 and H^6, very strong evidence exists in favor of the alternative hypotheses. That is, the time-shifts in L/F scenario was statistically significantly greater than both SPB scenario and Sync scenario. Regarding H^5, in the case of the velocity signals, $p = 4.9e{-}6$ and the

$95\% CI = [-0.079, -0.028]$. For the force signals, $p = 1.0e{-5}$ and the $95\% CI = [-0.074, -0.025]$. Similarly for H^6, we got $p = 0.006$ and the $95\% CI = [-0.065, -0.009]$ for the velocity signals and $p = 0.005$ and the $95\% CI = [-0.063, -0.008]$ for the force signals.

To summarize, based on the results of H^1 test, we infer that the samples in SPB scenario are skewed to the left with respect to the optimal minimum-jerk signals. H^2 test also indicates a left-skewness for Sync samples. The results of H^3 test show no significant skewness in L/F samples. Similarly, H^4 test shows no significant difference between the skewness of SPB and Sync scenarios. On the other hand, H^5 and H^6 indicate that samples in both SPB and Sync scenarios are left-skewed compared to the samples in L/F scenario.

Trajectory Skewness Hypothesis:

In both dyadic and bimanual reaching movements, when the movement start time is well-coordinated (SPB and Sync scenarios), the object's motion trajectory is left-skewed compared with a minimum-jerk trajectory. However, when coordination is imperfect (L/F scenario), no skewness is observed.

5.5 Discussion

It is well-known that the single arm reaching movements follow the minimum-jerk trajectory (Flash and Hogan, 1985). In this work, for the first time, we showed that bimanual and dyadic reaching movements are also strongly correlated with the minimum-jerk trajectory. This finding is in agreement with existing theories of human arm movements. In particular, it is well-known that a human can adapt to the external force field and his/her arm motion trajectory will return to the minimum-jerk trajectory after the learning trials; see (Shadmehr and Mussa-Ivaldi, 1994; Hwang et al., 2003; Flash and Gurevich, 1997). In a dyadic reaching movement, each person acts as an external disturbance force to the other person and thus observing a minimum-jerk trajectory is highly expected.

We also found out that there is a statistically significant left-skewness in single-person bimanual reaching movements (SPB scenario). On the other hand, no such skewness was observed in dyadic reaching movement (leader/follower scenario). However, when the dyad members are synchronized with an audible marker (Sync scenario), the left skewness appeared again. More interestingly, no statistically significant differences were observed between the skewness of the samples in Sync and SPB scenarios. These observations are also in agreement with the existing theories of human arm movements as discussed below.

The left-skewness in reaching movements has been observed in goal-directed reaching tasks (Jeannerod, 1988; Milner and Ijaz, 1990). In the tasks like reaching-to-grasp, a prolonged deceleration phase provides enough time for error corrections and accuracy improvements. In our experimental setup, we asked the participants to move the pot from point A to point B; therefore, the task is qualified as a goal-directed task. This explains the left-skewness in SPB and Sync scenarios.

In the L/F scenario on the other hand, due to the lag between the leader and the follower, the subjects need to perform the corrections from the beginning of the movement. Therefore, instead of a prolonged deceleration phase, the whole task duration is extended. The emergence of several sub-movements during the motion trajectory and the prolonged movement duration are evidences of such corrections in L/F scenario. The lack of skewness in L/F scenario can therefore be related to these distributed corrections.

The similarity of the samples in SPB scenario and Sync scenario is also anticipated. In the Sync scenario, the subjects agree on the start time of the motion. Furthermore, the fixed pace of the synchronizing beep enables them to predict the start time very accurately. Therefore, when each person performs his/her left-skewed reaching movement, the resulting trajectory remains left skewed. The similarity of these scenarios supports the hypothesis that the proposed synchronization eliminates the necessity for the corrections at the beginning of the movement.

The collected data includes samples for vertical reaching movement, which we excluded from this study due to the effect of gravity on the task. Based on our observations for horizontal movement, we speculate that patterns similar to those of a single arm vertical reaching movements will be found in bimanual and dyadic vertical reaching movement. Also, the skewness of the motion trajectory in vertical reaching movement would be interesting to be studied. Another interesting aspect that needs further investigation is the effect of the object's weight on the dyadic motion trajectory and its skewness.

CHAPTER 6

INTERACTION FORCE MODEL

Parts of this chapter have been presented in (Noohi et al., 2016). Copyright © 2016, IEEE.

During collaborative object manipulation, the interaction forces provide a communication channel through which humans coordinate their actions. In order for the robots to engage in physical collaboration with humans, it is necessary to understand this coordination process. Unfortunately, there is no intrinsic way to define the interaction forces. In this chapter, we propose a model that allows us to compute the interaction force during a dyadic cooperative object manipulation task. The model is derived directly from the existing theories on human arm movements.

6.1 Introduction

Many robotic applications require proactive physical interaction between a human and a robot. For instance, consider a robotic caregiver in the elderly care application. It has been shown that home care aides are most effective when they actively involve the elderly in physical activities (Hughes et al., 2004; Szulc et al., 2005). That is, it is important that the caregiver does not simply perform the task for the elder person, the elderly should be asked to proactively contribute in performing the task. Cooperative object manipulation (e.g. moving a table) is another example where proactive interaction is necessary. In general, in cases of cooperative physical interaction, successful completion of the task requires a coordinated force-exchange between the human and the robot.

While the human can usually amplify the cooperation performance by adjusting to the robot's actions, in many applications the human is not capable of such an adjustment. For instance, in elderly care, rehabilitation, or childcare, the human is either an elderly person, a physically challenged patient or a toddler. In such applications, the human is not expected to adjust to the robot. Instead, the robot's actions need to be as natural to the human as possible. Therefore, modeling the characteristics of natural human movements and the properties of the exchanged forces would significantly contribute to designing better robot control strategies in such applications.

In order to build a model for a natural (human-like) interaction, researchers have studied human-human collaborative tasks and proposed different models for the exchanged forces between humans. However, due to the physics of the task, there is an inherent ambiguity in trying to recover the interaction forces from the forces exerted by the humans. In other words, since the interaction force (the portion of the applied force that does not contribute to the motion of the object) is unknown, obtaining the effective portion of the applied force for each individual is challenging. To resolve this ambiguity, different models for the interaction force have been proposed (Williams and Khatib, 1993; Groten et al., 2009; Rahman et al., 2000; Evrard and Kheddar, 2009; Reed et al., 2005). In all of these models (including ours) the ambiguity is resolved by introducing additional constraints in the interaction model.

The existing models compute the interaction force for every isolated pair of force vectors and ignore the time dependencies among the force pairs during the task. In contrast, our approach considers the whole trajectories of the force vectors to compute the interaction force. More specifically, the interaction force is obtained by exploiting a computational motion model of the nominal movement trajectory during the cooperation. In fact, the knowledge of the motion model serves as the constraint that resolves the ambiguity.

In this chapter, by exploiting the motion model associated with the task, we propose a descriptive model for the interaction force. The key advantage of the proposed model compared to other models is that it only requires one of the applied forces to be measured in order to compute the interaction force. As a result, during a human-robot collaborative task, the robot can model the interaction force by measuring only the force applied by the human. In turn, this significantly simplifies the robot's controller. Details are given in Sec. 6.3.

6.2 Related Works

To uniquely determine the interaction force, researchers have considered different approaches. In case of the human-robot collaboration, some researchers tackle this problem by assigning the leader/follower roles to the human and the robot ($\alpha = 0$ or $\alpha = 1$), e.g. (Rahman et al., 2000). Mörtl et al. (Mörtl et al., 2012) studied the exchange of the leader/follower roles between the human and the robot and observed that dynamic role assignments resulted in a considerably larger interaction force. Evrard and Kheddar (Evrard and Kheddar, 2009) suggested that a continuous homotopy switching happens between the leader and the follower roles during the collaboration (for each agent independently). However, they did not identify the homotopy function for dyadic tasks. Leader/follower schemes are very successful in the tasks that the human steers the task and the robot provides the whole workload and follows the human.

Unlike leader/follower schemes, in this work we are interested in cooperative object manipulation task where both human and robot are actively contributing in performing the task. One of the most appreciated approaches is to take the mechanical internal force as the interaction force. For instance, while proposing a hybrid position/force control scheme for two coordinated robots, Uchiyama and Dauchez (Uchiyama and Dauchez, 1988) described the interaction between the robots by the internal force/moment vector. Using this vector, the authors manage to describe the object deformation (including twisting, bending and shearing) during manipulation. Williams and Khatib (Williams and Khatib, 1993) introduced a more general framework to properly design the interaction forces for multi-contact robot-robot collaborative tasks, namely "*virtual linkage*" model. They suggested that an acceptable interaction force would minimize the *engineering strain* (minimum deformation of the object). They used the internal forces as the interaction force in multi-robot object manipulation. In case of two robots, the force decomposition would become:

$$\begin{aligned} f_1^* = f_2^* = \tfrac{1}{2} F_{sum} \\ F^i = \tfrac{1}{2}(f_1 - f_2) \end{aligned} \tag{6.1}$$

or $\alpha = 0.5$. Taking the difference of the applied forces as the interaction force, as expressed in (6.1), is a common practice in the human-robot interaction literature as well, e.g. (Reed et al., 2005).

Another interesting assumption in the literature, proposed by Groten et al. (Groten et al., 2009), is that human minimizes the energy of the interaction force during the collaboration. They studied the dominance distribution in a dyadic haptic collaboration and implicitly exploited the minimum-energy model. The assumption is based on the intuition that when only one force is applied to an object, the interaction force should be zero. Fig. 24 illustrates this intuitive assumption in comparison with the

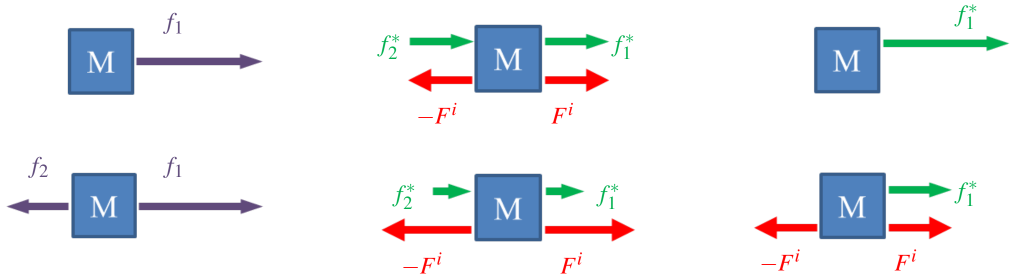

(a) Applied forces (b) Virtual Linkage (c) Minimum energy

Figure 24: Force decomposition of the applied forces (a), based on the virtual linkage model (b) and the minimum-energy model (c). Note that when only one force acts on the object, minimum energy model suggest zero interaction force, while virtual linkage model does not. Copyright © 2016, IEEE.

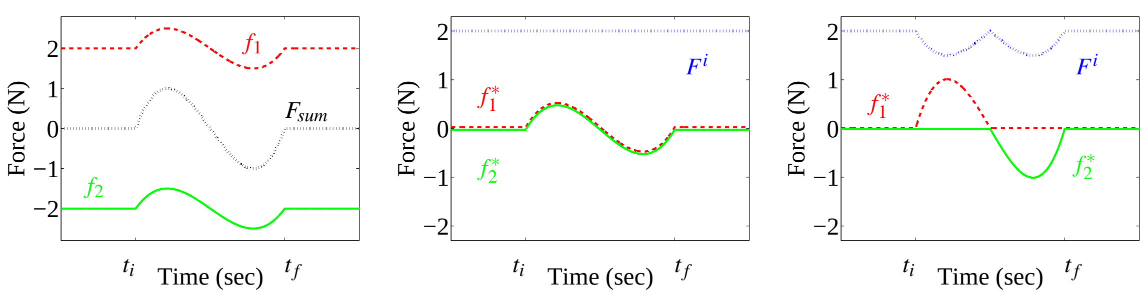

(a) Applied forces (b) Virtual Linkage (c) Minimum energy

Figure 25: A comparison on different assumptions in a 1-D object manipulation task. a) Applied forces and the total force. b) Virtual linkage assumption c) Minimum-energy assumption. In both b) and c) f_1^*, f_2^* and F^i are dashe, solid and dotted lines respectively. Copyright © 2016, IEEE.

virtual linkage model. This model finds a solution for (2.5) and (2.6) in which the magnitude of the interaction force is minimum. In other words:

$$\alpha(t) = \underset{\alpha}{\operatorname{argmin}} \left(||F^i|| \right) \tag{6.2}$$

Fig. 25a shows a typical example of a bimanual object manipulation in 1-D. The interaction force before the start of the motion ($t \leq t_i$) and after the end of the motion ($t \geq t_f$) is $F^i = 2$, which is the grasp force to hold the object. Fig. 25b shows the interaction force and the effective forces obtained from virtual linkage model. Here, $F^i = 2$ and $f_1^* = f_2^* = \frac{1}{2}F_{sum}$. The model suggest a perfect load-sharing cooperation, which is a likely behavior in a single-person-bimanual manipulation. Fig. 25c depicts the interaction force and the effective forces based on the minimum-energy assumption. Under this assumption, the first (second) hand applies the whole required force (F_{sum}) to move the object in the acceleration (deceleration) phase of the manipulation, while the other hand applies zero force. Taking the accelerating/decelerating roles is an expected behavior in dyadic collaborative tasks (Reed et al., 2006). We will compare our proposed model with these two models in the following sections.

6.3 Proposed Model for the Interaction Force

In this section, we first compute the interaction force in a mass-spring system. Then, we discuss how a mass-spring system generalizes a rigid body model for a solid body. Next, we propose our model for the interaction force, using the knowledge of the task. Finally, we discuss different aspects of the proposed model and list its key features.

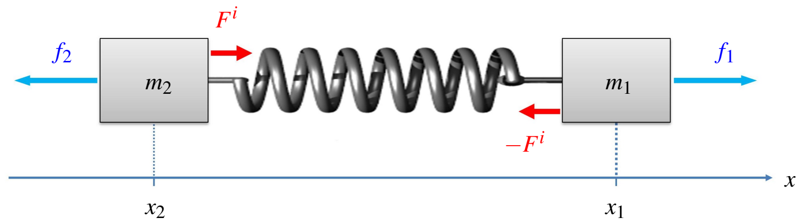

Figure 26: A Mass-Spring system in a cooperative manipulation task. The spring is assumed to be massless and linear. The force f_1 (f_2) is applied to the mass m_1 (m_2). The position of the center of mass m_1 (m_2) is x_1 (x_2). The system is one-dimensional; that is, applied forces are parallel with x-axis. Copyright © 2016, IEEE.

6.3.1 Interaction Force in a Mass-Spring System

Consider the cooperative manipulation of the mass-spring system in Fig. 26. The masses m_1 and m_2 are coupled with a spring and the forces f_1 and f_2 are applied to them, respectively. The positions of the masses m_1 and m_2 are referred to by x_1 and x_2 ($x_1 > x_2$), respectively. The task is to move the masses from their initial configurations (x_{i_1} and x_{i_2}) to the goal configurations (x_{f_1} and x_{f_2}) on a straight line (aligned with the x-axis).

If the position variables are available (or can be measured), the interaction force that the spring introduces to the system is computed as:

$$F^i(t) = -k_s\left(x_1(t) - x_2(t) - L_0\right) \tag{6.3}$$

where k_s is the stiffness of the spring and L_0 is the length of the spring when no force is applied to it.

On the other hand, if x_1 and x_2 are not available but the applied forces f_1 and f_2 are, then the interaction force would be computed from the equations of motion. For the above mass-spring system, the equations of motion can be expressed as:

$$\begin{aligned} m_1\,\ddot{x}_1(t) &= f_1(t) - F^i(t) \\ m_2\,\ddot{x}_2(t) &= f_2(t) + F^i(t) \end{aligned} \tag{6.4}$$

By combining the equations in (6.4), we will have:

$$m_1\,m_2\,(\ddot{x}_1 - \ddot{x}_2) = m_2\,f_1 - m_1\,f_2 - (m_1 + m_2)\,F^i \tag{6.5}$$

Taking the second derivative of (6.3) would result in:

$$\ddot{F}^i(t) = -k_s\,(\ddot{x}_1(t) - \ddot{x}_2(t)) \tag{6.6}$$

And plugging (6.6) into (6.5) would introduce the interaction force only in terms of the applied forces:

$$C\,\ddot{F}^i(t) + F^i(t) = (1-\alpha)f_1(t) - \alpha f_2(t) \tag{6.7}$$

where

$$C = \frac{-m_1 m_2}{k_s(m_1+m_2)} \quad \text{and} \quad \alpha = \frac{m_1}{m_1+m_2} \tag{6.8}$$

Equations (6.7) and (6.8) describe the interaction force in the form of a dynamical equation when f_1, f_2 and the system parameters (m_1, m_2 and k_s) are available,

6.3.2 Mass-Spring System vs. Rigid Body

Modeling objects as a rigid body is a common practice in many problems, due to its simplicity and effectiveness. It is based on the fact that deformation of a solid body in response to small (or moderate) forces is negligible for many materials. This is especially true when the applied forces are within the range of a human-human cooperative manipulation. However, using the rigid body model and ignoring the deformation of the solid body is in part the source of the ambiguity in computation of the interaction force (as discussed in Sec. 2.3).

The mass-spring system generalizes the rigid body model by including object deformation in the model (the spring). For instance, if we replace the spring with a massless rigid rod (or equivalently $k_s \to \infty$ in the spring), the mass-spring system becomes one rigid object (with two separated masses). Since the rod is rigid, we have $x_1 = x_2 + L_0$ and therefore, (6.5) becomes the same as (2.6), where α is defined in (6.8).

Although the generalization introduced by mass-spring system seems promising, unfortunately, neither (6.3) nor (6.7) can be used to compute the interaction force in a solid body. In case of (6.3), although the position variables (x_1 and x_2) are assumed to be available, accurate measurement of these variables is practically infeasible. Furthermore, the value of k_s in a solid body is very large. As a result, any small noise in the measurement of x_1 and x_2 would result in a large error in the computation of F^i.

Similarly, exploiting (6.7) to compute the interaction force in a solid body is impractical. Here, the large value of k_s would not be a problem and, in fact, it results in a negligible value for C in (6.8) and thus, would transform (6.7) to be the same as (2.6), as expected. The problem is that any arbitrary values for m_1 and m_2 would work in the mass-spring system and generate a valid model for the solid body. For instance, if $m_1 = m_2$, we get $\alpha = 0.5$ in (6.8) and it would represent the virtual linkage model. Or similarly, when $m_1 = 0$ ($\alpha = 0$), the mass-spring system represents the leader/follower model in which f_1 leads the task. In other words, the mass-spring system cannot disambiguate the interaction force model in (2.6), if (6.7) is being exploited.

In contrast, we will show that by including the information about the task, we can tackle both aforementioned problems. That is, the proposed model for the interaction force is both non-ambiguous and robust to the measurement noise. To tackle the ambiguity issue, it implicitly takes advantage of the position variables. And to address the noise problem, it exploits the measurements of the applied forces. In other words:

Interaction Force Hypothesis:

Incorporating the information about the task in modeling the interaction force, in particular the motion information, will disambiguate the system and results in a unique and robust computation of the interaction force.

6.3.3 Task-Aware Interaction Model: A Polynomial Model

Let us assume that the mass-spring system is being manipulated cooperatively, in a cooperative reaching movement task. That is, the subjects move the masses from their initial configurations (x_{i_1} and x_{i_2}) to their final configurations (x_{f_1} and x_{f_2}), following a minimum-jerk trajectory. Since each hand experiences disturbing forces through the spring (the interaction force), the reaching movement is performed inside a force field. As discussed in Sec. 2.2, after enough learning trials, cooperating hands learn to compensate for the force field and return to their original minimum-jerk motion trajectories:

$$
\begin{aligned}
x_1(\tau) &= x_{i_1} + (x_{f_1} - x_{i_1})(6\tau^5 - 15\tau^4 + 10\tau^3) \\
x_2(\tau) &= x_{i_2} + (x_{f_2} - x_{i_2})(6\tau^5 - 15\tau^4 + 10\tau^3)
\end{aligned}
\tag{6.9}
$$

where $\tau = (t - t_i)/(t_f - t_i)$ and t_i and t_f are the start time and the end time of the cooperative manipulation. As a result, $\Delta x(t) = x_1(t) - x_2(t)$ would also be a minimum-jerk trajectory:

$$
\Delta x = \delta_i + (\delta_f - \delta_i)(6\tau^5 - 15\tau^4 + 10\tau^3) \tag{6.10}
$$

where $\delta_i = (x_{i_1} - x_{i_2})$ and $\delta_f = (x_{f_1} - x_{f_2})$. Let us rewrite (6.3) as $F^i(t) = -k_s(\Delta x(t) - L_0)$. Similar to the discussions in Sec. 2.2, when $\Delta x(t)$ is a minimum-jerk trajectory, the interaction force would also be a minimum-jerk trajectory:

$$
F^i(t) = \underset{F}{\operatorname{argmin}} \left(\frac{1}{2} \int_{t_i}^{t_f} \left\| \frac{\mathrm{d}^3 F(t)}{\mathrm{d}t^3} \right\|^2 \mathrm{d}t \right) \tag{6.11}
$$

or equivalently, the interaction force can be expressed as:

$$
F^i(t) = \sum_{k=0}^{5} c_k t^k \tag{6.12}
$$

For a complete model, we need to determine the coefficients, c_k. As explained in Sec. 2.3, when $F_{sum} = 0$, the value of $F^i = f_1$ is known. According to Chapter 5, F_{sum} is associated with a minimum-jerk trajectory (bell-shaped velocity profile). That is, it has exactly one zero crossing point, namely t_m. Therefore, $F_{sum} = 0$ for $t \le t_i$, $t = t_m$ and $t \ge t_f$, see Fig. 25a. This constructs three constraints for the interaction force:

$$\begin{aligned} F^i(t_i) \ &= f_1(t_i) \\ F^i(t_m) &= f_1(t_m) \\ F^i(t_f) \ &= f_1(t_f) \end{aligned} \tag{6.13}$$

Since $F^i(t) = f_1(t)$ for $t \le t_i$ and $t \ge t_f$, we will have $\dot{F}^i(t_i^-) = \dot{f}_1(t_i^-)$ and $\dot{F}^i(t_f^+) = \dot{f}_1(t_f^+)$. And since both signals are smooth signals:

$$\begin{aligned} \dot{F}^i(t_i) \ &= \dot{f}_1(t_i) \\ \dot{F}^i(t_f) &= \dot{f}_1(t_f) \end{aligned} \tag{6.14}$$

The five constraints in (6.13) and (6.14) determine five coefficients in (6.12) and the last coefficient is obtained by solving the optimization problem in (6.11). To calculate the coefficients, let $P_4(t)$ denote the 4th order polynomial that satisfies the constraints in (6.13) and (6.14), i.e.:

$$\begin{aligned} &P_4(t) = e_4t^4 + e_3t^3 + e_2t^2 + e_1t + e_0 \\ &P_4(t_i) \ = f_1(t_i) \quad \dot{P}_4(t_i) \ = \dot{f}_1(t_i) \\ &P_4(t_m) = f_1(t_m) \quad \dot{P}_4(t_f) = \dot{f}_1(t_f) \\ &P_4(t_f) \ = f_1(t_f) \end{aligned} \tag{6.15}$$

Thus, any 5th order polynomial that satisfies the constraints in (6.13) and (6.14) can be expressed as:

$$P_5(t,\kappa) = P_4(t) + \kappa(t-t_i)^2(t-t_m)(t-t_f)^2 \tag{6.16}$$

The interaction force is the 5th order polynomial that satisfies (6.11). Thus, by solving (6.11) for (6.16), the optimal value of κ is obtained as:

$$\kappa^* = \underset{\kappa}{\operatorname{argmin}} \left(\frac{1}{2} \int_{t_i}^{t_f} \left\| \frac{\mathrm{d}^3 P_5(t,\kappa)}{\mathrm{d}t^3} \right\|^2 \mathrm{d}t \right) \tag{6.17}$$

And the interaction force will be:

$$F^i(t) = P_5(t,\kappa^*) \tag{6.18}$$

Equations (6.15)-(6.18) provide the computational model for the interaction force during a dyadic reaching movement. In other words:

Polynomial Trajectory Hypothesis:

The interaction force for a ballistic point-to-point movement of an object that is being manipulated cooperatively can be explained as a 5th order polynomial function in terms of time.

6.4 Discussion

To better understand different aspects of the proposed model, we provide a list of the characteristics of the model:

6.4.1 Assumption

As discussed in Sec. 2.3, to uniquely determine the interaction force, one needs to introduce a new constraint to the system. The proposed polynomial model assumes that the characteristics of the task is given in the form of a computational model for the motion profile (here the minimum-jerk trajectories). As a result of this assumption, the model does not depend on the value of the object's stiffness, k, or the selection of m_1 and m_2.

6.4.2 Limitation

The proposed interaction force model is based on the motion model of the cooperative hands. As a result, the level of precision of the model is determined by the precision of the motion model. Since minimum-jerk model (the motion model we applied) is the nominal model of hand movement, the resulting polynomial model describes the nominal profile of the interaction force. This approximating behavior will be observed in Chapter 7.

6.4.3 Advantage

Unlike the interaction force models discussed in Sec. 2.3, the polynomial model does not require the whole trajectory of applied forces (f_1 and f_2) to obtain the interaction force. More importantly, it can extract the interaction force based on only one of the applied forces, e.g. f_1 in (6.15). This is particularly important when the robot engages in a cooperative task with a human. We will further exploit this in Chapter 9.

6.4.4 Disadvantage

The interaction force models discussed in Sec. 2.3 can compute the value of F^i at time t only by measuring f_1 and f_2 at the same time, t. The proposed model, however, depends on the values of f_1 in the future times (i.e at boundary points). This would be a major issue when the robot needs to compute the interaction force in real-time. We will further discuss this in Chapter 10.

6.4.5 Extension

The mass-spring model relates the interaction force to the deformation of the object. Since elastic deformation appears in many different forms (such as compression, tension, shear and torsion), one might suggest a more general form of linear relation between the interaction force and the deformation strain. For instance, the model can simply be extended to a more general case by using a mass-spring-damper system. Taking k_d as the damping coefficient, the interaction force would be expressed as $F^i(t) = -k_s(x_1(t) - x_2(t) - L_0) - k_d(\dot{x}_1(t) - \dot{x}_2(t))$. It is easy to see that, if the motion profiles of x_1 and x_2 are available, the interaction force would be obtained as a linear combination of these profiles and their derivatives. In case of the reaching movement, the resulting interaction force would again be a 5th order polynomial.

6.5 Proposed Model in Action

It is insightful to illustrate an example of the interaction force when the proposed model is employed. Considering the collected data from the human study (applied forces f_1 and f_2), we can process and compute the interaction force, F^i, using (6.15)-(6.18). Then, the effective forces, f_1^* and f_2^*, is obtained from (2.4). Fig. 27 demonstrates the result of this procedure for a single sample trial. The collected applied forces and computed interaction force are shown in panel (a) and the effective forces along with F_{sum} are presented in panel (b). It is worth mentioning that the optimization problem in (6.17) was solved numerically, using the optimization toolbox in Matlab. In order to compute interaction force for virtual linkage model and minimum energy model, the above data processing procedure should be performed again, using (6.1) for the virtual linkage model and (6.2) for the minimum energy model.

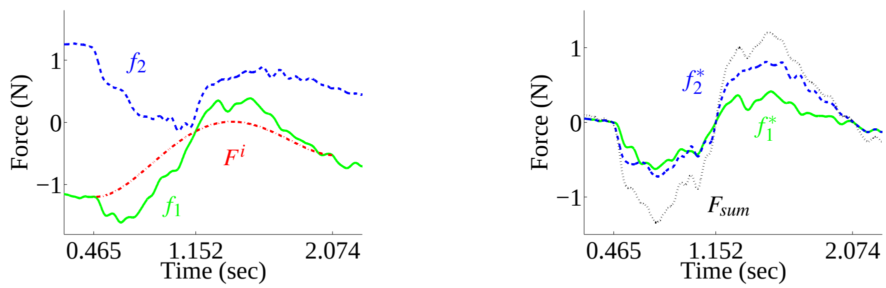

(a) Applied forces

(b) Effective forces

Figure 27: An example of calculating interaction force and effective forces. The solid green signal is f_1 (f_1^*), the dashed blue signal is f_2 (f_2^*), the dotted black signal is F_{sum} and the dash-dotted red signal is F^i. In this example, $t_i = 0.46\ s$, $t_m = 1.15\ s$ and $t_f = 2.07\ s$. Copyright © 2016, IEEE.

CHAPTER 7

EVALUATION OF THE INTERACTION MODEL

Parts of this chapter have been presented in (Noohi and Žefran, 2016). Copyright © 2016, IEEE.

7.1 Evaluation Metrics: Review

To be able to quantitatively compare different models of the interaction force, we employ the performance metrics, introduced in Chapter 4. However, to be able to provide a better visualization of the comparison results, we modified the metrics and normalized them to be bounded between zero and one. In this section, we quickly review the measures and introduce the modified version of the metrics.

7.1.1 Cooperation Index

Let us define:

$$I_\delta = \frac{1}{t_f - t_i} \int_{t_i}^{t_f} \delta(t)\,\mathrm{d}t \tag{7.1}$$

This index measures the average value of δ during the task, and is related to the average interaction force that is present. Since the index is not bounded, we need to map it to the range of zero and one. Using the maximum value among all the calculated samples, we have:

$$I_c = 1 - \frac{I_\delta}{\max(I_\delta)} \tag{7.2}$$

We will refer to this normalized index (I_c) as the Cooperation index, hereafter. The higher values of the Cooperation index indicate a better cooperation among the subjects (smaller δ).

7.1.2 Comfort Index

We define the Comfort index based on the Difficulty index. The Difficulty index is defined as:

$$I_d = \frac{1}{t_f - t_i} \int_{t_i}^{t_f} M_d(t)\,\mathrm{d}t \tag{7.3}$$

where $M_d(t) = \|\dot{\delta}(t)\|$. The index evaluates the difficulty of the task by measuring the degree of required mental demand. The higher values of the index indicate more difficult task. The Comfort index is defined by normalizing the Difficulty index. That is:

$$I_o = 1 - \frac{I_d}{\max(I_d)} \tag{7.4}$$

The higher values of the Comfort index indicate simpler tasks with less mental demands ($I_o = 1$ when $\delta(t) = \text{const.}$).

7.1.3 Efficiency Index

Let us define:

$$I_e = \frac{1}{t_f - t_i} \int_{t_i}^{t_f} M_e(t)\,\mathrm{d}t \tag{7.5}$$

where

$$M_e(t) = \frac{\|F_{sum}(t)\|}{\|f_1^*(t)\| + \|f_2^*(t)\|}$$

This measure represents the extent of disagreement of the dyad members in performing the task. The higher values of the index indicate less wasted efforts. The index is suitably bounded between zero and one ($0 \leq I_e \leq 1$), see Chapter 4.

7.1.4 Similarity Index

Let us define:

$$I_s = \frac{1}{t_f - t_i} \int_{t_i}^{t_f} M_s(t)\,\mathrm{d}t \tag{7.6}$$

where

$$M_s(t) = 1 - \left| \frac{\|f_1^*(t)\| - \|f_2^*(t)\|}{\|F_{sum}(t)\|} \right|$$

This index measures the similarity of the effective forces (symmetry with respect to the task). Higher values of the index indicates more symmetry between the effective forces. The index is suitably bounded between zero and one, see Chapter 4.

7.1.5 Fairness Index

Let us define:

$$I_f = 1 - \left| \frac{N_1 - N_2}{N_{sum}} \right| \tag{7.7}$$

where

$$\begin{cases} N_1 = \int_{t_i}^{t_f} \|f_1^*(t)\|\,\mathrm{d}t \\ N_2 = \int_{t_i}^{t_f} \|f_2^*(t)\|\,\mathrm{d}t \\ N_{sum} = \int_{t_i}^{t_f} \|F_{sum}(t)\|\,\mathrm{d}t \end{cases}$$

It measures the inequality between the effective efforts in terms of the signal-energy. The higher values of the index indicate smaller differences between the contributions of the subjects (in terms of signal-energy of the forces). The index is suitably bounded between zero and one ($0 \leq I_f \leq 1$), Chapter 4.

7.2 Comparison Results

We recruited 22 adult subjects, consisting of 12 men and 10 women between 19 and 35 years of age. Discarding the corrupted measurements, we collected 58 trials in SPB scenario, 31 trials in Sync scenario and 21 trials in L/F scenario (a total of 52 trials in dyadic mode). We then applied our proposed polynomial model (Poly), the internal force model (IntF) and the minimum energy model (MinE) to the collected signals for all trails (f_1 and f_2) and obtained all interaction forces, $F^i(t)$, and effective forces for each model. To calculate the performance indexes, we applied (7.1)-(7.7) to these interaction and effective forces. Therefore, we obtained 110 samples for each index per model.

We looked into the effect of two factors in the data: cooperation and coordination. Since only one brain controls both hands in bimanual mode (vs. two brains in dyadic mode), it is expected that the properties of F^i are different between the two modes (effect of cooperation type). On the other hand, since the subject share the start time in Sync scenario, we expect that their performance is different (better) than the L/F scenario. Also, we do not expect that the synchronization mechanism improves the performance as high as the SPB performance.

To study these hypotheses, we set up a repeated measures ANOVA test. We used Mauchly's test to validate the sphericity assumption. The test showed that the assumption had been violated ($\chi^2(989) > 10000$, $p < .0001$), and therefore, a Greenhouse-Geisser correction ($\hat{\varepsilon} = 0.086578$) was applied. The repeated measures ANOVA with a Greenhouse-Geisser correction determined that a statistically significant interaction exists between the "cooperation mode" and the "interaction model" ($F(0.173, 3.983) = 187.21$, $p < 0.0019$). The significance level was $\alpha = 5\%$ in this test. No any other statistically significant interaction was observed ($p > 0.05$ for all). No significant main effect was ob-

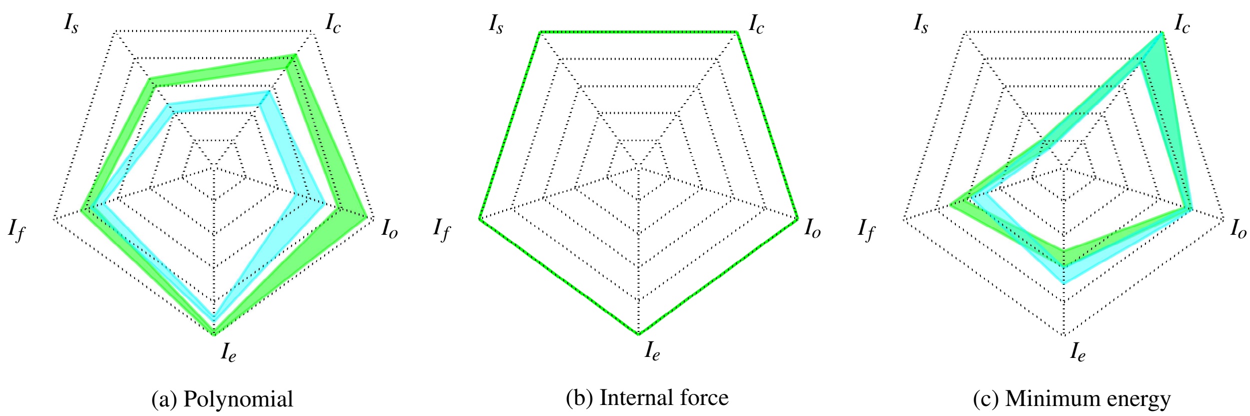

Figure 28: Radar charts of the confidence intervals of all five indexes obtained for different models. The green and cyan charts represent the stats for the bimanual and dyadic modes, respectively. Copyright © 2016, IEEE.

served, except for the cooperation mode ($F(0.173, 3.983) = 187.21$, $p < 0.0019$) which was shadowed by its significant interaction with "interaction model".

A pairwise multiple comparisons post-hoc test with the Bonferroni correction was performed. We observed significant differences between the means of the Poly, IntF and MinE, when the cooperation mode was bimanual ($p < 0.0001$ for all). In case of the dyadic cooperation, while significant difference between the mean of IntF and the means of the Poly and MinE were observed ($p < 0.0001$ for both), no significant difference was observed between the means of Poly and MinE ($p > 0.88$). On the other hand, a significant difference between the means of bimanual and dyadic groups was observed in Poly model ($p < 0.0001$), while no significant difference was observed in case of IntF and MinE models ($p > 0.76$).

The former test results indicate that, regardless of the cooperation mode, IntF model introduces a statistically significantly different F^i than Poly and MinE. Furthermore, Poly and MinE introduce statistically significantly different F^i in bimanual mode. However, no enough evidences existed to draw the same conclusion in dyadic mode. This is a fairly expected conclusion, considering the difference between the assumptions taken by different models.

The latter test results indicate that the interaction forces (F^i) appearing in bimanual mode are statistically significantly different from the ones appearing in dyadic mode, when the Poly model is employed. For the other two models, there is no enough evidence to draw similar conclusions. This observation does not strongly support our hypothesis and the test failed to reject the null hypothesis, when IntF or MinE is employed.

Quantitative Measures Observation:

The polynomial model captures the essential features of collaboration and reveals the collaboration type, while the other two models fail to do so.

To better understand this observation, we have visualized it in Fig. 28. Panels (a), (b) and (c) in this figure show these results for the Poly model, IntF model and MinE model, respectively. In all charts, the green patches are associated with bimanual mode and the cyan patches present stats of the dyadic mode. The depicted stats are the *confidence intervals* for the performance indexes. Recall that since the indexes are bounded between zero and one, and the higher index values are associated with higher performance, the charts axes are all between zero to one, with zero at the center of the chart.

As illustrated in Fig. 28a, when proposed model is employed, bimanual and dyadic modes are statistically significantly different in all metrics (except I_f). However, when IntF model is used, no discrepancy exists between the metrics, see Fig. 28b. That is due to the fact that $f_1^* = f_2^*$ and $\delta = 0$ when the IntF model is employed (see (6.1)). Plugging these values in (7.1)-(7.7) would give a constant value of one for all metrics. Finally, Fig. 28c shows that the confidence intervals in bimanual and dyadic modes overlap (except for I_f) when MinE model is used. The test results suggest an interesting conclusion: Poly would effectively capture the difference between the bimanual mode and the dyadic mode, IntF would always fail to do so and no enough evidence existed that MinE can do the same. In other words, considering existing sample population, the proposed polynomial model captures the critical information of the interaction better than the other two models.

Fig. 29 depicts the pairwise multiple comparisons post-hoc test results regarding different scenarios. Panels (a) and (b) in this figure show these results for the Poly model and MinE model, respectively. We excluded the chart for IntF model, because its results were constant in all tests. In both charts, the green, blue and red patches are associated with SPB, Sync and L/F scenarios, respectively. According to the test results, the proposed model suggests significantly (for I_c, I_e), strongly (I_s) or weakly (I_o) performance differences between the scenarios, but no significant difference on I_f. On the contrary, MinE model only suggest a significant difference between SPB and L/F for I_f ($p = 0.001$). As illustrated in Fig. 29a, the Poly model clearly uncovers the performance improvement trend, resulted by the coordination mechanism. It suggests that the average performance in the synchronized scenario (Sync) is higher than dyadic leader-follower scenario (L/F), but not as high as a single person in SPB scenario.

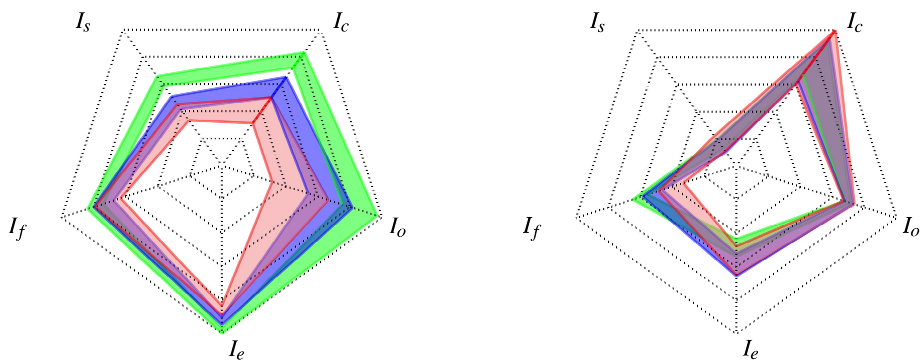

(a) Polynomial (b) Minimum energy

Figure 29: Radar charts of the confidence intervals of performance indexes considering different scenarios. The green, blue and red charts represent the stats for the SPB, Sync and L/F scenarios, respectively. Copyright © 2016, IEEE.

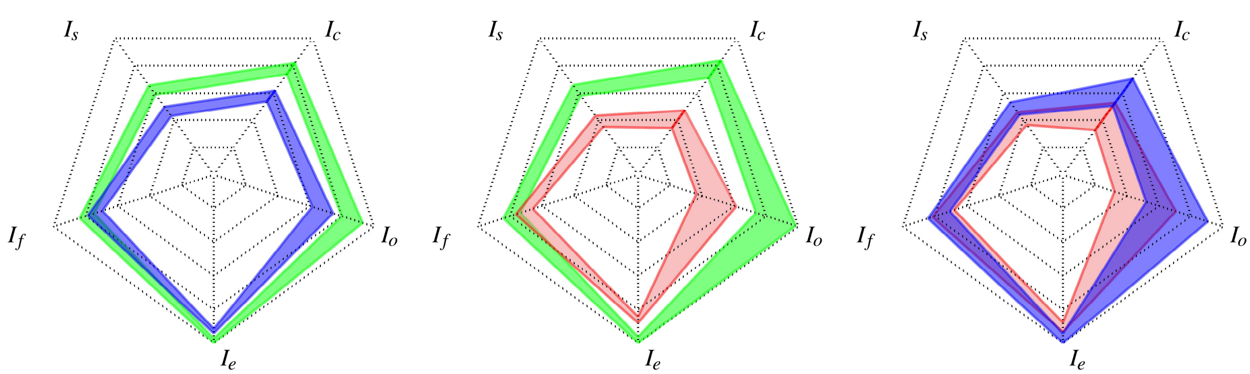

(a) SPB vs Sync (b) SPB vs L/F (c) Sync vs L/F

Figure 30: Radar charts comparing different scenarios, based on the proposed model. The green, blue and red charts represent the stats for the SPB, Sync and L/F scenarios, respectively. Copyright © 2016, IEEE.

To better visualize the trends that exists between different scenarios, Fig. 30 presents three spider charts, comparing different pairs of scenarios with each other. Similar to previous figure, The green, blue and red charts represent the stats for the SPB, Sync and L/F scenarios, respectively. As depicted, the proposed model effectively identifies the significant performance superiority of SPB scenario over both Sync and L/F. It also suggests a performance improvement trend for Sync scenario compared with L/F as hypothesized.

7.3 Conclusion

In this chapter, we employed five performance metrics to explore different aspects of cooperation, namely: cooperativeness, similarity, fairness, efficiency and difficulty. We showed that when our proposed polynomial model is employed, a significantly higher performance is observed in bimanual mode and also an improvement trend is associated with the coordination process. We also discussed that while our model can effectively uncover human behavior, the alternative models fail to do so.

After modeling the interaction force and validating the model, the next step would be to design a controller that utilizes this model. We will discuss our approach in designing different controllers in the following chapters. Our controllers are designed based on the properties of the interaction force that we observed in the collected data.

Part III

Controllers

CHAPTER 8

INTERACTION FORCE PROPERTIES

In this Chapter we study the statistical properties of the interaction force during a dyadic manipulation task. We show that while many properties vary between different scenarios, a certain component is strongly correlated with the object velocity. We will use this component as an abstract model for the human intent and accordingly will propose a cooperation strategy at the end of this chapter.

For the signals to be comparable in different motion types and in different scenarios, they are normalized in both time and magnitude. That is, motion duration is scaled to be exactly 1 second and the traveled distance is also scaled to be exactly 1 meter. The normalization scaling factors are calculated for F_{sum} and then applied to f_1, f_2 and F^i. We used G*Power software (Faul et al., 2009) to calculate the statistical power. The number of trials were high enough to provide a power of $1-\beta > 0.95$ for all scenarios. All other statistical figures were obtained using Matlab. Following the model explained in Sec. 6.3, we first calculated the interaction forces, $F^i(t)$, for all trials. Then we studied the variations and magnitude of the interaction forces among different scenarios. Fig. 31 shows the interaction forces in SPB and Sync scenarios as two examples. As exemplified in this figure, the interaction forces in bimanual mode are larger than those in dyadic mode. The results of the statistical analysis of these signals appear in the following sections.

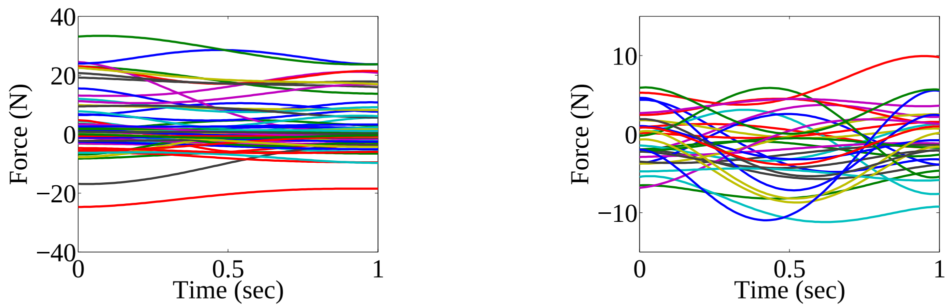

(a) SPB scenario

(b) Sync scenario

Figure 31: interaction forces exemplified with two scenarios. Copyright © 2017, Springer.

8.1 Initial Grasp-Force Magnitude

Before the movement is initiated, the interaction force is equivalent to the grasp force. Our statistical analysis shows that the magnitude of the initial grasp force ($\|F^i(0)\|$) is significantly larger in bimanual mode compared with the dyadic mode. For a significance level of $\alpha = 0.05$, we observe that $\mu_{bimanual} > \mu_{dyadic}$ with a p-value of $p = 0.0001$. The 95% confidence interval for $\mu_{bimanual}$ is $CI = [5.42, 9.71]$ and for μ_{dyadic} is $CI = [2.34, 3.89]$. The same trend exists in all scenarios, $\mu_{SPB} > \mu_{Sync}$ ($p = 0.0008$) and $\mu_{SPB} > \mu_{L/F}$ ($p = 0.019$). The variations of the initial grasp force are also significantly larger in bimanual mode compared with the dyadic mode. That is, $\sigma_{bimanual} > \sigma_{dyadic}$ with a p-value of $p < 0.0001$ for $\alpha = 0.05$.

8.2 Final Grasp-Force Magnitude

Immediately after the movement is finished, the applied forces sum up to zero and therefore, the interaction force would be the grasp force again. Similar results are observed for the magnitude of the final grasp force ($\|F^i(1)\|$). That is, the final grasp force (and its variations) is significantly larger in bimanual mode compared with the dyadic mode. For a significance level of $\alpha = 0.05$, we observe that $\mu_{bimanual} > \mu_{dyadic}$ with a p-value of $p = 0.004$. Also $\sigma_{bimanual} > \sigma_{dyadic}$ with a p-value of $p < 0.0001$. The same trend exists in all scenarios, $\mu_{SPB} > \mu_{Sync}$ ($p = 0.01$) and $\mu_{SPB} > \mu_{L/F}$ ($p = 0.05$). The 95% confidence interval for $\mu_{bimanual}$ is $CI = [4.25, 7.77]$ and for μ_{dyadic} is $CI = [2.4, 4.12]$.

8.3 interaction force Energy

Similarly, the average energy of the interaction force signals ($\int_0^1 \|F^i(t)\|^2 dt$) are significantly higher in bimanual mode compared with the dyadic mode. For $\alpha = 0.05$, we observe that $\mu_{bimanual} > \mu_{dyadic}$ with a p-value of $p = 0.001$. Also $\sigma_{bimanual} > \sigma_{dyadic}$ with a p-value of $p < 0.0001$ and the power of $1 - \beta = 0.999$. The same trend exists in all scenarios, $\mu_{SPB} > \mu_{Sync}$ ($p = 0.008$) and $\mu_{SPB} > \mu_{L/F}$ ($p = 0.04$). The 95% confidence interval for $\mu_{bimanual}$ is $CI = [47.4, 137.2]$ and for μ_{dyadic} is $CI = [10.5, 30.2]$.

A Discussion on the Grasp Force

Above observations can be combined and expressed as the following hypothesis:

> **Grasp Force Hypothesis 1:**
>
> Humans apply larger grasp forces in bimanual mode compared to the dyadic mode. The variations of the grasp forces are also larger in bimanual mode.

While we showed statistical evidence in favor of the above hypothesis, it seems completely counter intuitive. In bimanual mode, both hands belong to the same person and both are controlled with the same brain. So, the movement is expected to be smoother compared to the dyadic mode and the interaction force is expected to be negligible. However, the results show that, in fact, the average energy of the interaction force signals are significantly higher in bimanual mode than in dyadic mode. We speculate that the higher energy is an artifact of the higher initial (final) grasp-force. In other words, if these grasp forces are compensated, the remaining signals have less energy in bimanual mode than in dyadic mode.

To test this hypothesis, we need to study the variations of the interaction force in more detail. We first consider the difference between the initial grasp-force and final grasp-force, i.e. $\Delta F = F^i(1) - F^i(0)$. Then the initial grasp-force is canceled, i.e. $F_c^i = F^i - F^i(0)$. Finally, both initial and final grasp forces will be canceled.

8.4 Difference between Initial and Final Grasp-Forces

In this test, no statistically significant difference is observed for $\Delta F = F^i(1) - F^i(0)$. That is, no strong evidence exists to reject the null hypothesis that $\mu_{bimanual} = \mu_{dyadic}$ and the p-value of the test is $p = 0.19$. The same trend exists for all scenarios, $\mu_{SPB} = \mu_{Sync}$ ($p = 0.39$) and $\mu_{SPB} = \mu_{L/F}$ ($p = 0.23$). In addition, the data fails to reject the null hypothesis that the $\Delta F = 0$. Particularly, the 95% confidence interval for $\mu_{bimanual}$ is $CI = [-2.26, 0.48]$ and for μ_{dyadic} is $CI = [-0.8, 1.28]$. These observations can be summarized as the following hypothesis:

Grasp Force Hypothesis 2:

Regardless of the manipulation mode (in both dyadic and bimanual), the initial and final grasp forces are not significantly different.

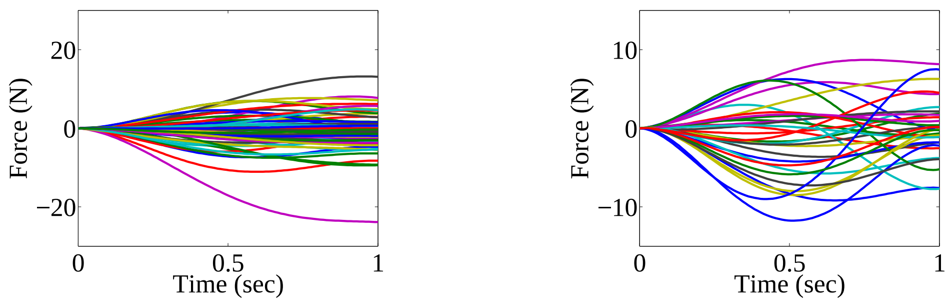

(a) SPB scenario

(b) Sync scenario

Figure 32: interaction forces variations exemplified with two scenarios. Copyright © 2017, Springer.

8.5 interaction force Variation

In order to study the interaction force variations, first the initial grasp-force is canceled, $F_c^i = F^i - F^i(0)$. Fig. 32 shows F_c^i in SPB and Sync scenarios as two examples. The statistical analysis shows that the average energy of F_c^i is not significantly different in bimanual mode compared with the dyadic mode. That is, no strong evidence exists to reject the null hypothesis that $\mu_{bimanual} = \mu_{dyadic}$ and the p-value of the test is $p = 0.53$. The 95% confidence interval for $\mu_{bimanual}$ is $CI = [5.27, 25.80]$ and for μ_{dyadic} is $CI = [7.98, 15.99]$. The same trend exists in all scenarios, $\mu_{SPB} = \mu_{Sync}$ ($p = 0.79$) and $\mu_{SPB} = \mu_{L/F}$ ($p = 0.49$).

On the contrary, the variation of average energy is significantly larger in bimanual mode compared with the dyadic mode. For a significance level of $\alpha = 0.05$, we observe that $\sigma_{bimanual} > \sigma_{dyadic}$ with a p-value of $p < 0.0001$. The same trend exists in all scenarios, $\sigma_{SPB} > \sigma_{Sync}$ ($p < 0.0001$) and $\sigma_{SPB} > \sigma_{L/F}$ ($p < 0.0001$).

8.6 Negotiation Force

In order to cancel both the initial grasp-force and the final grasp-force, we propose to decompose the interaction force into two components. According to the model discussed in Sec. 6.3, the interaction force is obtained by satisfying the boundary conditions. These boundary conditions are the results of the negotiation of two hands on the timing of the reaching movement, see (6.13). The initial and final grasp-forces are two of these boundary conditions. If there had been no other boundary conditions, the interaction force would have followed the minimum-jerk trajectory. Such smooth force can be expressed as:

$$F_s^i = F^i(0) + (F^i(1) - F^i(0)) \times (6t^5 - 15t^4 + 10t^3) \tag{8.1}$$

If we take this smooth force as the first component of the interaction force, the remaining force would be the negotiation component, that is:

$$F_n^i = F^i - F_s^i \tag{8.2}$$

Fig. 33a exemplifies the decomposition of two signals and figures 33b and 33c show the negotiation components for the SPB and Sync scenarios as two examples. As it is illustrated, both initial and final grasp-forces have been canceled in F_n^i.

As expected, the average energy of the negotiation component is significantly lower in bimanual mode compared with the dyadic mode. For $\alpha = 0.05$, we observe that $\mu_{bimanual} < \mu_{dyadic}$ with a p-value of $p = 0.0015$. Also $\sigma_{bimanual} < \sigma_{dyadic}$ with a p-value of $p < 0.0001$. The same trend exists in all scenarios, $\mu_{SPB} < \mu_{Sync}$ ($p = 0.0004$) and $\mu_{SPB} < \mu_{L/F}$ ($p = 0.03$). The 95% confidence interval for $\mu_{bimanual}$ is $CI =$

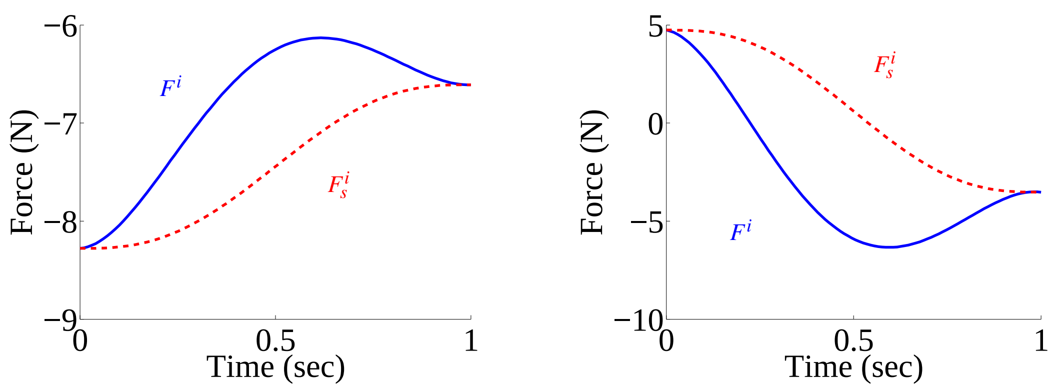

(a) interaction force decomposition examples

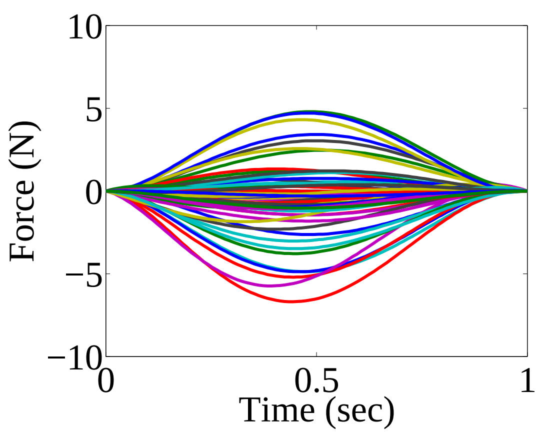

(b) SPB scenario

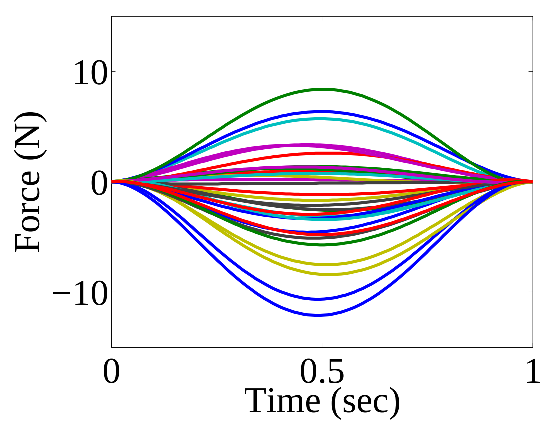

(c) Sync scenario

Figure 33: Negotiation forces exemplified with two scenarios. Copyright © 2017, Springer.

$[1.23, 3.22]$ and for μ_{dyadic} is $CI = [4.39, 11.51]$. These observations can be summarized as the following hypothesis:

Negotiation Force Hypothesis 1:

The average energy of the negotiation force is significantly smaller in bimanual mode compared with the dyadic mode.

8.7 Negotiation Force vs. Object Velocity

A closer look at Fig. 33 reveals that the negotiation forces are very similar to the velocity profile in the reaching movement. As an accepted practice (Shadmehr and Mussa-Ivaldi, 1994; Hwang et al., 2003), we use Pearson correlation coefficient, r, to measure this similarity. The correlation between the normalized object velocity and the negotiation force is calculated for each trial. The values of r show a strong correlation between the two signals. For instance, the average value of r for the negotiation forces in Fig. 33c is $\bar{r} = 0.91$ and its standard-deviation is $s = 0.1$. More specifically, the 95% confidence interval for $\mu_{bimanual}$ is $CI = [0.75, 0.87]$ and for μ_{dyadic} is $CI = [0.84, 0.93]$. The results strongly support the hypothesis that:

Negotiation Force Hypothesis 2:

The negotiation force is strongly correlated with the velocity of the object.

8.8 Proposed Cooperation Policy

In this section we propose a cooperation policy for a robot, collaborating with a human in a dyadic reaching movement. The robot needs to apply forces to the object in such a way that the human perceives a natural (human-like) physical interaction. An important component of this physical interaction is the interaction force. While the interaction forces do not contribute to the motion trajectory of the object, they play an important role in how natural the interaction is.

The interaction force model discussed in Sec 6.3 cannot be implemented in a real-time robot controller. For instance, the model needs the value of the grasp force in between the movement to construct the interaction force. This kind of information is available only after the movement is over. Here, we propose a cooperation policy that eliminates the need for this information and generates a natural interaction force. The proposed policy is based on the two-component decomposition of the interaction force, discussed in Sec. 8.6. Accordingly to (8.2), $F^i = F^i_s + F^i_n$.

To fully determine F^i_s, the values of initial and final grasp-forces ($F^i(0)$ and $F^i(1)$) are required, see (8.1). As discussed in Sec. 8.4, strong evidence exists suggesting that $\Delta F = 0$, or equivalently $F^i(0) = F^i(1)$. Therefore, we propose to select the same value for both the initial grasp-force and the final grasp-force. Let F_G refer to this value. By plugging $F^i(0) = F^i(1) = F_G$ in (8.1), the first component of the interaction force is obtained as, $F^i_s = F_G$.

For the second component, F_n^i, we exploit the observation in Sec. 8.7. As discussed there, F_n^i is strongly correlated with the normalized object velocity. That is, we can approximate the negotiation force as $F_n^i = \kappa \cdot v$, in which κ is a scaling factor. As a result,

$$F^i = F_G + \kappa \cdot v \tag{8.3}$$

As discussed in Sec. 8.1 and 8.2, the 95% confident interval of the initial and final grasp-forces in dyadic mode are $CI = [2.34, 3.89]$ and $CI = [2.4, 4.12]$, respectively. Thus, F_G belongs to the intersection of these ranges, i.e. $F_G \in [2.4, 3.89]$. The exact value of F_G would be obtained during the initial grasp. On the other hand, the value of κ is obtained by calculating the energy of the signal. According to the observation discussed in Sec. 8.6, the 95% confident interval of the average energy of F_n^i in dyadic mode is $CI = [4.39, 11.51]$. The energy of the normalized velocity profile for a minimum-jerk trajectory is 1.414. As a result $\kappa \in [1.76, 2.85]$. The value of $\kappa = 2.3$ would be considered as a safe choice.

Cosidering (8.3) and (2.4), the robot's contribution to the dyadic task would be:

$$F_R = f_R^* + F_G + \kappa \cdot v \tag{8.4}$$

where f_R^* is the effective force provided by the robot. As discussed in the Introduction section, interesting methods have been proposed in the literature for planing f_R^*. Our proposed policy takes advantage of such strategies and augment them with a model for interaction force (last term in (8.4)).

Fig. 34 shows the block diagram of the proposed real-time policy. The "Robot Controller" block in this figure represents one of the existing strategies in the literature. The "interaction force Model" block

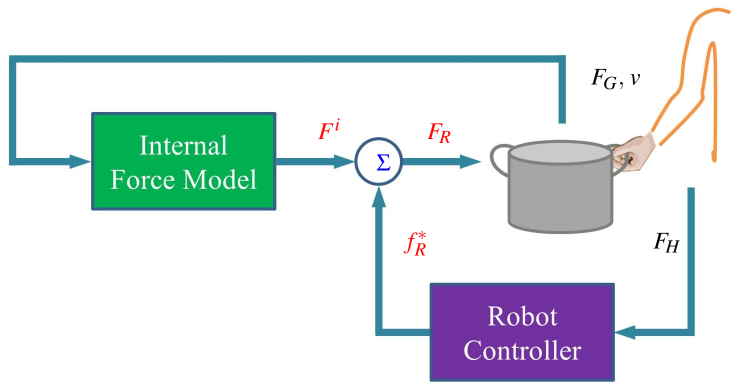

Figure 34: Sketch of the control diagram for the proposed policy. The interaction force block receives the velocity of the pot and the grasp force signals. The robot controller receives the human applied force. Copyright © 2017, Springer.

implements (8.3). By appending the interaction force model into the controller, our cooperation policy can resolve the ambiguity of the haptic channel and introduce a more natural (human-like) interaction force. Merging this policy with the existing cooperation strategies will increase the performance of those strategies, as well. The integrated policy reduces the undesirable push-pull forces and introduces a smoother human-robot interaction.

8.9 Conclusion

In this chapter, we explored different features and patterns in the interaction force signals. We observed that, while the initial and final grasp-forces were both significantly larger in bimanual mode, the difference between these forces were negligible. We also observed that no significant difference existed between bimanual and dyadic mode regarding the average energy of the variations of the interaction force. However, when the interaction force is decomposed into the negotiation force and a smooth force, the average energy of the negotiation component was significantly higher in dyadic mode, as expected. Furthermore, we observed that the negotiation force is strongly correlated with the object's velocity.

The last observation is particularly important. Based on this observation, we proposed a cooperation policy for a human-robot physical collaboration. It was suggested that by merging this policy with existing cooperation strategies, a smoother human-robot interaction would be achieved. Quantifying the performance gain of such an integration will be discussed in the next chapter. Also, in the proposed cooperation policy, we assume that the robot's effective force is available (using existing cooperation strategies). In the next chapter, we propose a complete controller scheme and propose an informed-impedance controller to provide robot's effective force.

CHAPTER 9

ROBOT CONTROLLER AND THE INTERACTION FORCE

In this chapter, we test our hypothesis that the robot performs more efficiently when it is provided with the interaction force. We introduce a controller scheme that exploits the interaction force to generate robot's applied force. The efficiency of the robot is evaluated, using a measure of position error.

Since the controller is based on the *offline computed* interaction force, it is not causal and therefore, it cannot be utilized for a real robot that is interacting with a human in an online fashion. Consequently, the term "robot" in this section stands for a virtual agent (or the controller itself). In the next chapter, we introduce a causal controller that exploits an online estimation of the interaction force instead of the offline computed one.

9.1 Proposed Controller Scheme

Fig. 35 shows the block diagram for the offline controller. The contribution of the robot to the manipulation task is shaped by the "Motion Profile" block. It generates the desired object trajectory x_d that is a minimum-jerk trajectory in our case (see Chapter 5). The "Impedance Control" block generates the controller force F_{ctrl}, which guarantees a stable tracking of this desired trajectory. Thus, F_{ctrl} is the contribution of the robot to the cooperative task. On the other hand, the "Interaction Model" block provides the interaction force F_{intrct}. Thus the robot applied force, F_R, is then construed as:

$$F_R = F_{ctrl} - F_{intrct} \tag{9.1}$$

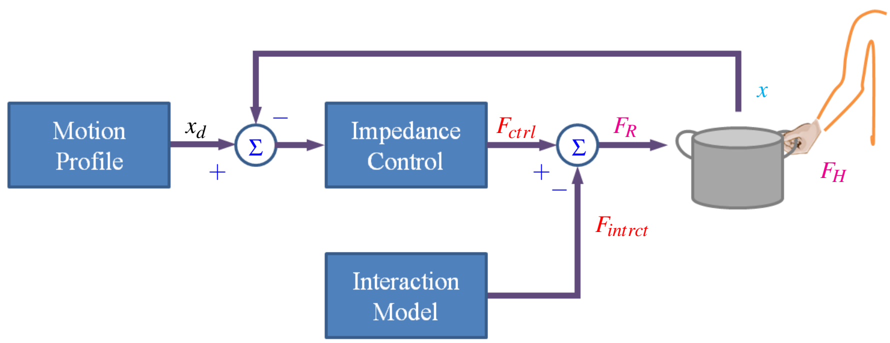

Figure 35: Sketch of the control diagram. The interaction force is introduced in a feed-forward manner. Copyright © 2016, IEEE.

Based on (2.4), "Human-human" cooperation and Human-Robot cooperation can be formulated as:

$$\begin{aligned} F_H &= F_H^* + F^i \qquad & F_H &= F_H^* + F_{intrct} \\ F_h &= F_h^* - F^i \qquad & F_R &= F_{ctrl} - F_{intrct} \end{aligned} \tag{9.2}$$

where F_H (F_H^*) and F_h (F_h^*) are the human applied (effective) forces. More specifically, F_h is the force that we intend to replace with the robot force (F_R) and F_H is the force that the robot wants to cooperate with.

If we take the calculated human interaction force as the human-robot interaction force, $F_{intrct} = F^i$, and if the robot uses the Human-human motion trajectory (x_{Hh}) as the desired trajectory, $x_d = x_{Hh}$, the robot's effective force will follow the other human's effective force, $F_{ctrl} = F_h^*$. Here, we assume that the actual motion trajectory of a Human-human dyadic manipulation (x_{Hh}) is not available to the robot.

Thus, the robot uses the minimum-jerk model as an estimate of the Human-human motion trajectory and therefore, F_{ctrl} approximates F_h^*. The impedance control that provides robot's effective force is:

$$F_{ctrl} = M\,\ddot{x}_d + K_d(\dot{x}_d - \dot{x}) + K_s(x_d - x) - \frac{1}{2}M\,\bar{g} \tag{9.3}$$

where, M is the object's mass, $K_d = 5M$ and $K_s = 6M$. The values of K_d and K_s are selected in such a way that the poles of the closed loop system are small ($p_1 = -2$ and $p_2 = -3$). It allows the robot to interact with the human, while keeping the tracking error small. The last term in (9.3) compensates half of the weight of the object, assuming that the human compensates the other half. Let's apply (9.1), (9.2) and (9.3) to the object's equation of motion, $F_R + F_H + M\bar{g} = M\,\ddot{x}$. Therefore,

$$M\,\ddot{e} + K_d\,\dot{e} + K_s\,e = \tilde{F}_H \tag{9.4}$$

where, $e = x - x_d$ and $\tilde{F}_H$ is the human's gravity-compensated effective force, $F_H^* = \tilde{F}_H - \frac{1}{2}M\,\bar{g}$. Eq. (9.4) shows that the controller is BIBO stable and the tracking error is a function of human effective force.

9.2 Simulation Setup

To measure the performance of these models, we propose the following scenario. First, the applied forces during performing a dyadic (or bimanual) object manipulation task are assumed to be available (our recorded data). Next, we calculate the interaction forces based on all three models (offline). Then, we replace one human (or one hand) with a robot and provide the robot's controller with the computed interaction force. Finally we compare the performance of the human-robot cooperative manipu-

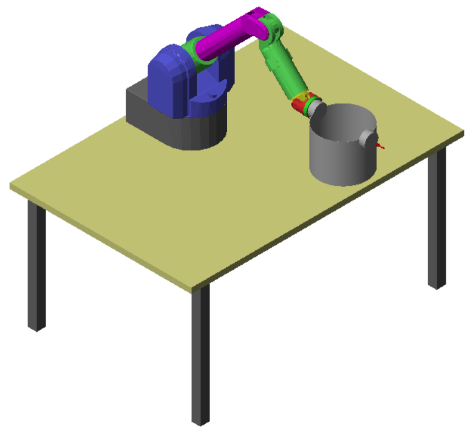

Figure 36: We used a 4 DOF WAM arm to evaluate our proposed model and test the robot's controller with the actual humans' signals. The red arrow at the free pot handle represents the human applied force. Copyright © 2016, IEEE.

lation w.r.t. the human-human dyadic (or bimanual) manipulation, in terms of root-mean-squared-error (RMSE).

To make sure that the measured error reflects the difference between the models (and not dominated by another factor), we take the following steps. We assume that the robot has a full knowledge about the task; that is, x_i, x_f , t_i, t_f and the object's mass, M, are all known to the controller. We chose the impedance control over position control to make the controller responsive to the interaction force. We also assumed that the robot can be controlled perfectly, so that the commanded force appears at the robot's end-effector identically and immediately.

To make sure that the dynamics of the robot and the object will be modeled precisely during our simulations, we used MathWorks' SimMechanics simulation environment. To be faithful to the experimental setup, we used a pot as the to be manipulated object; with the same kinematic and dynamic properties as the actual pot. Fig. 36 shows the simulation setup for the controller evaluation. In this figure, we show a 4 DOF Barrett's WAM robotic arm (Barrett, 2015) as our robot. Since the robot has only 4 DOF, we use a passive ball joint between the robot and the pot. Therefore, the orientation of the pot is controlled only by the human. In the simulation, we used the orientation data that was recorded from IMU during the experiment to reproduce the correct orientation of the pot. The dynamic properties of WAM arm have been provided by the manufacturer in the form of STL files. Following the same approach, any other robotic arm can be selected and employed in our simulations.

9.3 Simulation Results

For each trial of the human study, we consider the applied forces to the pot (f_1 and f_2) and calculate the interaction forces (F^i) based on three models: virtual linkage (VL), minimum energy (ME) and polynomial model (PM). These interaction forces are used in the "Interaction Model" block in the robot controller in Fig. 35. That is, we apply $F_{intrct} = F^i$ for above three models. To study the necessity of including the interaction force in the robot controller, we consider the case where $F_{intrct} = 0$. We will refer to this model by zero-interaction-force (ZF) model.

Fig. 37 illustrates an example of the performance of the robot for different interaction models. The motion trajectory of the Human-human cooperation (x_{Hh}) is considered as the baseline for comparing the performance of the models. In Fig. 37a, this trajectory is marked with small circles (Hh). The motion trajectories of VL, ME and PM closely follow the human-human trajectory. However, the zero-interation-force (ZF) trajectory cannot follow x_{Hh}. This means that, although the impedance controller attempts to contribute to the task and move the pot along the desired trajectory, due to the lack of a good

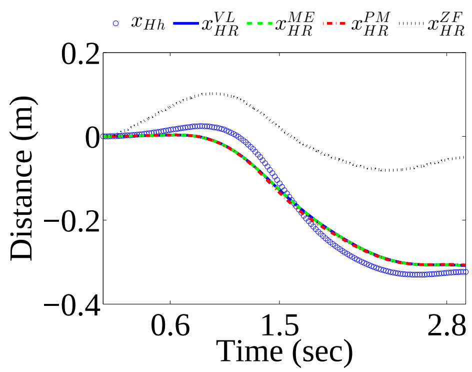

(a) Motion trajectories: x_{Hh} and x_{HR}

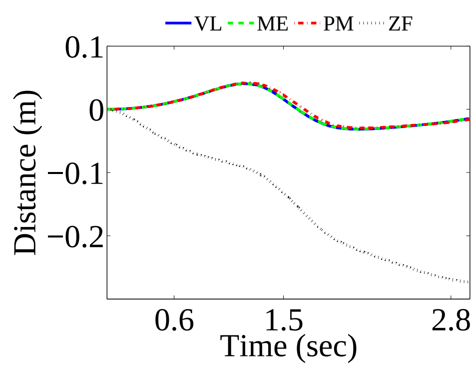

(b) Position error: $x_{Hh} - x_{HR}$

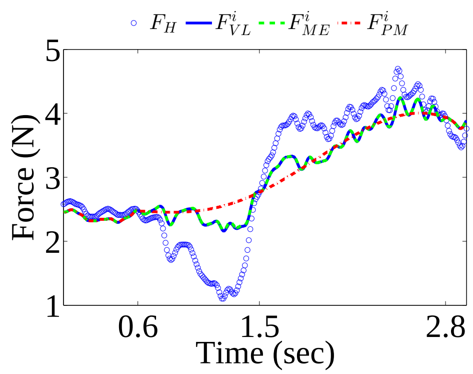

(c) Interaction forces and F_H

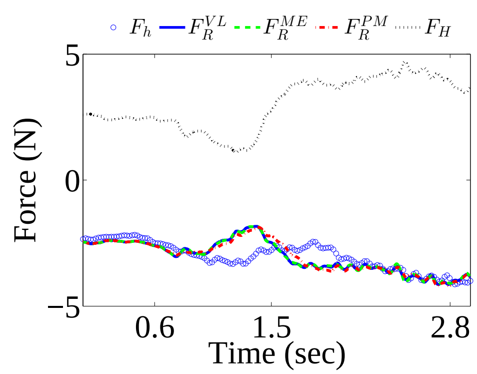

(d) Robot forces, F_h and F_H

Figure 37: An example of the performance of the robot, using different interaction models. a) motion trajectory of Human-human cooperation (x_{Hh}) is compared with human-robot motion trajectory (x_{HR}) using virtual linkage model (VL), minimum energy model (ME), polynomial model (PM) and zero force model (ZF). b) Robot's performance in terms of the position error: $d = x_{Hh} - x_{HR}$. c) Interaction force (F^i) compared with the human force (F_H). d) Robot force (F_R) is compared with both humans forces. F_h is the human force that we intend to replace with the robot force and F_H is the Human force that the robot wants to cooperate with. The presented motion trajectories and forces are all in the direction of motion. Copyright © 2016, IEEE.

model for the interaction force, robot forces conflicts with human's and the whole task fails. It is more evident in Fig. 37b, where the difference between the x_{Hh} and the human-robot motion trajectories (x_{HR}) with different interaction models are illustrated. While the position error for VL, ME and PM are very similar and less than 5 cm, the position error for ZF increases to 28 cm. We will use this error signal to statistically compare these models with each other in the next section.

Fig. 37c shows the human applied force (F_H) and the interaction forces generated by different models. As illustrated here, VL and ME models generate very similar interaction forces and, PM generates a low-order approximation of those interaction forces. These interaction forces shape the robot's applied force (F_R). As it appears in Fig. 37d, the robot's force (F_R) follows the replaced human force (F_h) in all models, as expected. However, there exist a distinct difference between F_R and F_h, due to the difference between robot's desired trajectory and human's original trajectory ($x_d \neq x_{Hh}$).

9.4 Statistical Evaluation

We are interested in studying the effect of different interaction force models (PM, VL, ME, ZF) on the performance of the proposed controller. Comparing the performance requires an evaluation measure to be introduced. Let $d(t)$ be the difference between the human-human motion trajectory and the human-robot motion trajectory, $d(t) = x_{Hh} - x_{HR}$. We used the root-mean-squared of $d(t)$ as the evaluation measure:

$$RMSE = \sqrt{\frac{1}{t_f - t_i} \int_{t_i}^{t_f} \|d(t)\|^2 \, \mathrm{d}t} \tag{9.5}$$

The measure evaluates the performance of the controller in terms of the average position error, given the specific interaction model is used. We use the sample population of the *RMSE* to statistically compare the effect of the interaction models. The mean and standard deviation of the samples for

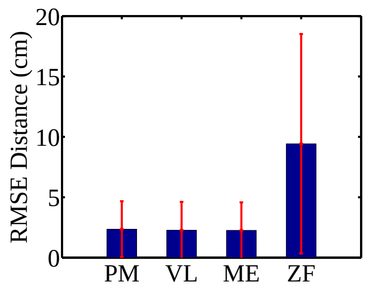

Figure 38: The average performance of the robot, using different interaction models: virtual linkage model (VL), minimum energy model (ME), polynomial model (PM) and zero force model (ZF). Copyright © 2016, IEEE.

different models are: PM:(2.36 ± 2.31), $VL : (2.27 \pm 2.35)$, $ME : (2.25 \pm 2.32)$ and $ZF : (9.43 \pm 9.09)$ all in cm. Fig. 38 shows the mean and standard deviation of RMSE measure, when different interaction models are employed. As it is illustrated in the figure, the ZF model generates larger mean error than other three models and, the average error introduced by PM is not very different from VL's error or ME's error.

In Chapter 7, we discussed that the properties of the interaction force are different among different models. Therefore, it is expected that the performance of the controller would also be different between the models. To evaluate this hypothesis, we set up another repeated measures ANOVA test. The ANOVA model is very similar to the one described in Chapter 7. The between-subjects factor "mode" and the within-subjects factor "task" are the same as before. But, the within-subjects factor "model" has four levels (PM, VL, ME, ZF) here. The test includes a total of 12 (3×4) repeated measurements for each of the 25 subjects.

We used Mauchly's test to validate the sphericity assumption. The test showed that the assumption had been violated ($\chi^2(65) = 894.05$, $p < .0001$), and therefore, a Greenhouse-Geisser correction ($\hat{\varepsilon} = 0.23046$) was applied. A repeated-measures ANOVA determined that the mean RMSE differed statistically significantly among different models ($F(0.6914, 15.9017) = 25.576$, $p < 0.0001$). Furthermore, no statistically significant interaction was observed between "model" and other factors ($p > 0.15$ for all). The significance level was $\alpha = 5\%$ in the test. A pairwise multiple comparisons post-hoc test with the Bonferroni correction was performed. We observed that the mean RMSE error is statistically significantly higher when ZF is used ($p < 0.0003$ for all three pairwise tests). Moreover, no statistically significant difference was observed between the means of PM, VL and ME ($p > 0.82$ for all tests). The test results suggest the following two conclusions.

First, informing the controller about the properties of the interaction force would significantly increase its performance. This conclusion, which is not surprising, would support the exploitation of the interaction force models in designing an online controller (see next section).

Offline Controller Observation:

Providing the controller with the information about the interaction force would increase its performance, significantly.

Second, no enough evidence existed to suggest that the performances of different controllers (with PM, VL and ME models) are statistically significantly different from each other. This is a surprising conclusion, considering our discussion on the differences between the properties of the interaction force among these models (see Chapter 7). We speculate that, the impedance controller block would have partially compensated for the differences between the interaction models and resulted in this observation.

CHAPTER 10

HUMAN-ROBOT COOPERATION STRATEGY

In designing the control scheme in the previous chapter, we argued that taking the human-robot interaction force equal to the calculated human interaction force ($F_{intrct} = F^i$) leads to a human-robot motion trajectory that closely follows the human-human motion trajectory. Thus, we assumed that the interaction force between humans was fully known (calculated offline) and the "Interaction Model" block in Fig. 35 was designed in a feed-forward manner.

In the case of a real-time human-robot interaction, no human-human interaction exists as a reference and therefore, the controller needs to calculate the interaction force only based on the human's applied force F_H. Fig. 39 shows the real-time robot controller block diagram, in which the "Interaction Model" block measures the human force F_H and estimates the interaction force F_{intrct}. The design of the rest of the controller is exactly the same as discussed in the previous section. In the next section, we introduce an algorithm that estimates F_{intrct}, by predicting F_H and utilizing the polynomial model.

10.1 Estimating the Interaction Force

We showed that the polynomial model (PM) demonstrates a satisfactory performance in offline controller. We also discussed that, while other interaction models require both human forces (F_H and F_h) to calculate the interaction force (F^i), PM provides a good approximation for F^i, using only one force (F_H). Moreover, the model requires only five boundary values to identify the interaction force. As

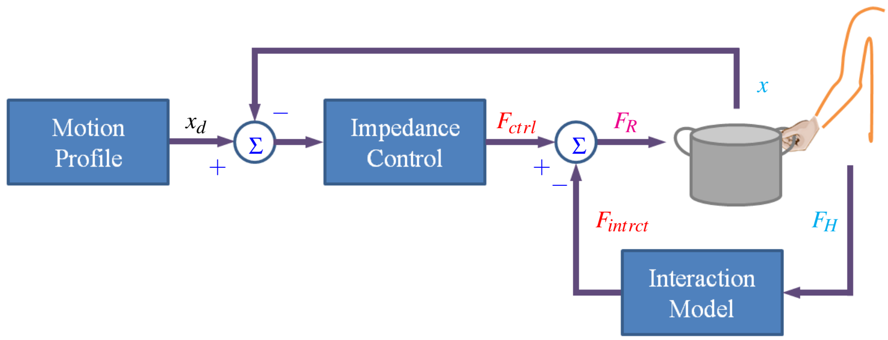

Figure 39: Sketch of the control diagram. The position of the pot and the human applied force are measured and sent to the robot controller. Copyright © 2016, IEEE.

a result, polynomial model is a good candidate for estimating F^i. We will show that, when the estimated interaction force is used, the performance of the robot remains as high as when offline models are being employed.

According to the PM model, (6.15)-(6.18), the interaction force requires the value of F_H to be known at times t_i, t_m and t_f. However, when the robot is calculating $F_{intrct}(t)$ for times $t < t_m$ (or $t < t_f$), the future human force, $F_H(t_m)$ (or $F_H(t_f)$), is not available yet. Therefore, in order to use PM model as an estimator of the interaction force, either the boundary values or the whole future human force need to be predicted.

Let us define the predicted human force $\tilde{F}_H$ as:

$$\tilde{F}_H(\tau, t) = \begin{cases} F_H(\tau) & \tau \leq t \\ F_H(t) & \tau > t \end{cases} \tag{10.1}$$

where τ is the time variable ($0 \leq \tau < \infty$) and t represents the current time. The predictor suggests that human's applied force in future remains constant and equal to the current force value. While it is the simplest prediction of the future values of F_H, it is motivated by the minimum-jerk constraint. It is easy to see that (2.1) minimizes $||\dot{F}_H(t)||^2$ and thus, $\dot{F}_H(t) = 0$ (or $F_H(t) = Const.$) is the optimal solution. However, this justification is based on the assumption that the manipulation task is mainly performed by the robot and human only provides a constant interaction force (e.g. grasp force).

If we plug (10.1) into (6.15)-(6.18), the interaction force that is predicted at time t for the whole task ($t_i \leq \tau \leq t_f$) would be obtained as:

$$\tilde{F}^i(\tau,t) = \text{PolynomialModel}\left(\tilde{F}_H(\tau,t)\right) \tag{10.2}$$

which is a 5th order polynomial, satisfying the predicted boundary values. As a result, the estimated interaction force at time t would be:

$$F_{intrct}(t) = \tilde{F}^i(\tau = t,t) \tag{10.3}$$

Fig. 40a shows the above procedure for the same human force (F_H) as we studied in the previous section. The prediction of human force for $t \geq 1.14$, $\tilde{F}_H$, is shown with blue solid line and the boundary values at $t_m = 1.5$ and $t_f = 2.8$ are marked as magenta dots. The PM model is employed and the predicted interaction force, $\tilde{F}^i(\tau,t)$, is calculated (green dashed line). The estimated interaction force at time t, $F_{intrct}(t)$, is obtained and marked by a red star. Note that the estimated value is very different from the offline calculated interaction force, $F^i(t)$ (red dashed-dotted line). However, as time increases,

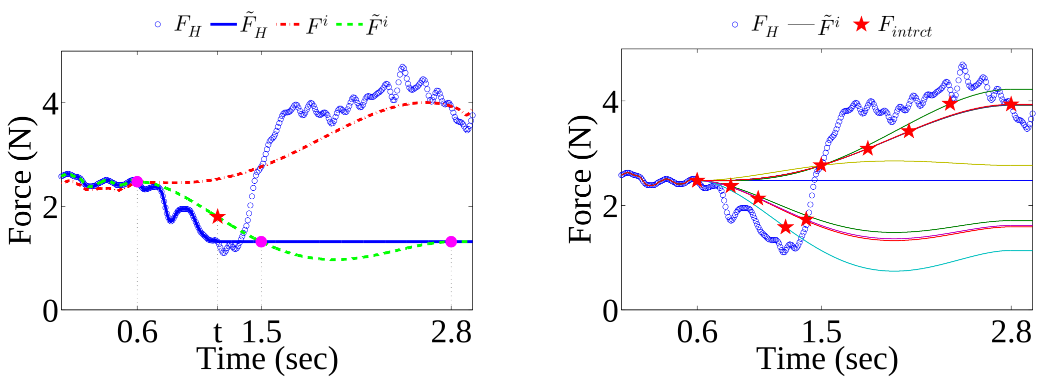

(a) Estimating $F_{intrct}(t)$

(b) Evolution of $\tilde{F}^i$

Figure 40: An example of estimating F_{intrct} at time t. Since neither the human force (F_H) nor the PM interaction force (F^i) is available to the robot after time t, the controller predicts them ($\tilde{F}_H$ and $\tilde{F}^i$ respectively). a) The predicted boundary conditions are marked with magenta dots and the estimated interaction force at time t ($F_{intrct}(t)$) is marked by a red star. b) As time increases, the simulated robot's estimation of F_{intrct} evolves (intermediate curves) and $\tilde{F}^i$ approaches F^i. Copyright © 2016, IEEE.

$\tilde{F}^i$ approaches F^i and the estimated value $F_{intrct}(t)$ gets closer to $F^i(t)$. Fig. 40b shows the evolution of $\tilde{F}^i$ with several intermediate curves. As $\tilde{F}^i$ curves approach F^i, the estimated interaction force values (red stars) get closer to the offline calculated interaction force.

Fig. 41 compares the performance of the online and the offline controllers. Fig. 41a compares the estimated interaction force with the offline-calculated one. Note that the estimated force is the same as the red star marks in Fig. 40b. The motion trajectories of both online and offline controllers are also compared with the human-human motion trajectory. As illustrated in Fig. 41b, while we use a simple prediction for human force, the estimated interaction force results in a high performance. However, it

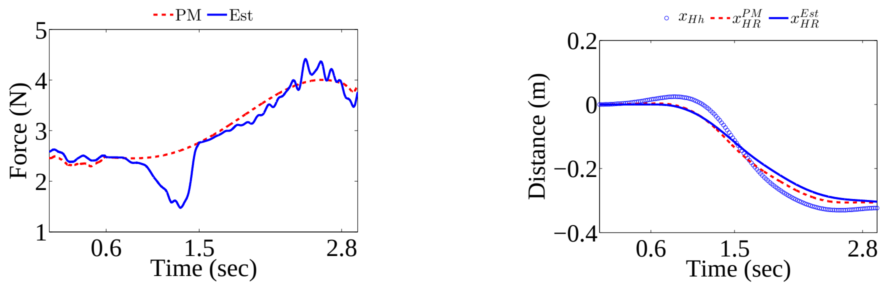

(a) Interaction Forces

(b) Motion Trajectories

Figure 41: An example of the performance of the robot, using the cooperation strategy. a) The simulated online interaction force estimation (Est) is compared with the offline calculated polynomial model (PM). b) The motion trajectory of Human-human cooperation (x_{Hh}) is compared with human-robot motion trajectory (x_{HR}) using polynomial model (PM) and estimated interaction force (Est). Copyright © 2016, IEEE.

does not mean that the predicted human force $\tilde{F}_H$ is a good representative of F_H. It only provides the required information about the boundary values.

Remark

In addition to the simplicity and high performance, the proposed estimator possesses the following interesting features:

1. The proposed estimator guarantees the smoothness of the estimated interaction force (subject to the smoothness of the human applied force)

2. The boundary conditions are always satisfied: $F_{intrct}(t_i) = F_H(t_i)$, $F_{intrct}(t_m) = F_H(t_m)$ and $F_{intrct}(t_f) = F_H(t_f)$. Therefore, as $t \to t_f$, we have $\tilde{F}^i(\tau,t) \to F^i(\tau)$

10.2 Statistical Evaluation

Similar to the implementation in Sec. 9.2, we assumed that the robot has a full knowledge about the task. Also, we assumed that no friction or non-linearity exists in the robot and it can be controlled perfectly. We implemented the control diagram in Fig. 39 as the robot controller. The desired trajectory x_d is a minimum-jerk trajectory, given by (2.1). The impedance controller follows (9.3) and the "Interaction Model" estimator is described by (10.1)-(10.3). To measure the performance of the online controller, the same scenario as in Sec. 9.2 was followed. To evaluate the performance of the online controller, we took the same approach as we discussed in Sec. 9.4 and utilized the same RMSE measure as in (9.5). Let "Est" refer to the population of RMSE error samples obtained in this scenario. The mean and standard deviation for Est is (2.43 ± 2.37) cm.

Consider Fig. 41a; while the estimated interaction force F_{intrct} follows the offline-calculated interaction force F^i, there is a considerable difference between them. Also recall the poor performance of the controller when no information about the interaction force is available (discussed in Sec. 9.4). These observations suggest that the performance of the proposed online controller (using the estimator) would be higher than ZF model, but probably lower than PM model. To study this hypothesis, we set up another repeated measures ANOVA test. The ANOVA model has the same factors as the one described in Sec. 9.4. Except that, the within-subjects factor "model" has five levels (PM, VL, ME, ZF, Est) here. The test includes a total of 15 (3×5) repeated measurements for each of the 25 subjects.

We used Mauchly's test to validate the sphericity assumption. The test showed that the assumption had been violated ($\chi^2(104) = 1154$, $p < .0001$), and therefore, a Greenhouse-Geisser correction ($\hat{\varepsilon} = 0.18648$) was applied. A repeated-measures ANOVA determined that the mean RMSE differed statistically significantly among different models ($F(0.7459, 17.1562) = 25.497$, $p < 0.0001$). Furthermore, no statistically significant interaction was observed between "model" and other factors ($p > 0.15$ for all). The significance level was $\alpha = 5\%$ in the test. A pairwise multiple comparisons post-hoc test with the Bonferroni correction was performed. We observed that the mean RMSE error is statistically significantly higher when ZF is used ($p < 0.0005$ for all four pairwise tests). Moreover, no statistically significant difference was observed between the means of PM, VL, ME and Est ($p > 0.61$ for all six tests).

The test results supports our hypothesis in part. That is, the estimator provides enough information about the interaction, that the performance of the controller is statistically significantly higher than ZF model. However, no enough evidence existed to suggest that the performances of online controller (Est) is statistically significantly different from offline controllers (with PM, VL and ME models). These observations suggest that the human-robot cooperation strategy, proposed by the control scheme in Fig. 39, would be a promising candidate for an effective human-robot cooperative manipulation.

Online Controller Observation:

The proposed online controller scheme, including the prediction-estimation algorithms, can successfully recover enough information about the interaction, such that the performance of the robot is not significantly different from a fully-informed controller.

10.3 Discussion

A key limitation of our simulation approach is that the human applied forces had been recorded during the experiment (between humans) and then they were played back during simulations. In other words, we did not model the possible changes in the human applied forces due to the robot's actions in our simulations. In fact, we do not have access to a model that fully describes how human behavior varies in response to an external force. As a result, although the simulation results are very encouraging, unsatisfactory interactions may appear during an actual human-robot interaction.

On the other hand, human perception is usually noisy. So, if the robot's applied forces are in the range that the human expects to perceive, it may not influence human's behavior. Based on the promising results observed in the simulations, we speculate that the online controller will demonstrate a satisfactory performance in practice as well. But to test this hypothesis, one needs to setup a new study and test the online controller in a real human-robot experimental setup.

Part IV
Conclusion

CHAPTER 11

OPEN PROBLEMS

Throughout this thesis, we introduced a general framework for identifying the interaction force and controlling a robot to co-manipulate an object with a human. To formulate different elements of this framework, we constructed a set of assumptions and constraints. In this chapter, we will go over each element of the framework (i.e. our contributions) and discuss how we can relax some of these constraints or extend some of the models.

11.1 Movement Model

We have introduced a motion model for dyadic object manipulation in Chapter 5. There is a huge body of work on modeling human movements and our model (minimum-jerk) is among simplest computational models for the human movements. In fact, in the same chapter, we observed a significant skewness in some object's velocity profiles that cannot be explained by the minimum-jerk model. One possible extension to this work is to explore more advanced movement models and to examine optimal control models (such as minimum variance model). We speculate that an optimal control model reveals more details about the object's motion trajectory in a dyadic manipulation.

Having a more complex model can also help alleviate some of the constraints that we imposed. For instance, we discarded vertical movements from our study to avoid complications due to the gravitational force, see Sec. 3.2. A more elaborate model can explain the motion in the direction of a force field and relax the constraint of horizontal planar motion.

11.2 Interaction Force Models

One of the core contributions of this work was on how to relate the interaction force with the movement model. We employed the minimum-jerk motion model and derived a 5th order polynomial model for the interaction force. While we discussed the advantages of this model over existing models and showed that our model has good performance, it would be interesting to explore how the same concept works with more advanced movement models. For instance, our model is non-causal and it only provides the nominal human interaction force, which is due to the fact that we used the average motion profile to build our model. A more detailed movement model can potentially provide a better description of the interaction force.

Another aspect of the collaboration that we excluded from our work was the interaction torque model. Due to the specific type of the grasp (power grasp) in our study, the force and torque were decoupled and we could study the force signals without being worried about any constraint imposed by the torque signals. It would be an interesting extension of our work to model the applied torques and how they relate to the object's orientation. Modeling the interaction torque (the amount that cancels out) is crucial, particularly in tasks that involve significant changes in the object's orientation.

11.3 Interaction Impedance Models

There is a school of thought among researchers in human movement science that believes that humans adjust their arm's impedance when interacting with the environment. There is considerable supporting evidence for the hypothesis that humans control their arm's stiffness in order to manage uncertainty. As a result, an extension to our interaction models (motion and force) would be a model for variations of interaction impedance.

As discussed in Sec. 6.3.1, the cooperating parties are haptically coupled and the whole chain introduces the interaction impedance. Instead of using the nominal motion model (average trajectory), one can use the actual trajectory and compute the variations of impedance between arms for each trial. Next, the regularities between the impedance variations can be investigated and a model for the interaction impedance can be formulated. Then, an even more interesting question would be how to relate the impedance of individual arms to each other and to the interaction impedance. This is in fact indirectly related to the interaction force that is canceled.

11.4 Interaction Primitives

As we discussed in our most recent work (Noohi et al., 2017), there exist certain regularities within human movements and human interactions with the environment. We referred to those action-building-blocks as manipulation primitives. It has been shown that taking these primitives into account can assist decyphering the communication between humans (Chen et al., 2015; Javaid et al., 2014). In this work we were mainly focused on the interaction properties of co-manipulation. An interesting extension to this work then could be the development of a set of interaction primitives that can explain more complicated interactions.

The idea here is to map the interaction force into a feature space and to cluster the space in a meaningful way. The candidate features for this mapping are the quantitative measures, proposed in Chapter 4. After the primitives have been identified, a probabilistic framework (such as Hidden-Markov-Model) can be utilized to combine the primitives and generate the natural interaction force. This approach has been proven effective in natural language processing and we speculate that it would be applicable in this context as well.

11.5 Machine Learning Approaches

In recent years, machine learning techniques have shown great potential for solving complex problems in machine vision and artificial intelligence. In this direction, Google has recently released its large-scale interaction data set, used for unsupervised learning of robotic grasping and physical interaction (Levine et al., 2016; Finn et al., 2016). In line with the same efforts, our collected data for human-human co-manipulation interaction can be utilized for developing an artificial neural network that can respond to human forces and produce reaction force signals as well as a human partner. The main challenge here though would be the size of our data set. Usually, an effective learning requires a large data set and therefore repeating the human study may be necessary.

CHAPTER 12

CONCLUSION

In this dissertation, we discussed a critical but less studied application of physical interaction between a human and a robot: cooperative manipulation. We started by studying the definition of the cooperation and followed by exploring the properties of a cooperative manipulation. As discussed in Sec. 1.2, we particularly were interested in finding answers to the following research questions:

- How to define and measure the cooperation between the human and the robot?
- What is the human's preferred motion trajectory during the collaborative task?
- What is the human's expected interaction force profile during the collaborative task?
- What robot's control strategy results in a satisfying cooperation with a human? And how to measure human's satisfaction?

We proposed to tackle these challenging research problems by following a human-inspired approach. As discussed in 1.3, by mimicking human's motion and force trajectories, we suggest that the interaction between a human and a robot would become as fluid and natural as a human-human interaction. Following this approach, we focused on studying the properties of the motion and force trajectories in human-human co-manipulation tasks. The details of our human study have been presented in Chapter 3.

Using the survey that followed the human study, we identified a set of features for the cooperation quality between two humans co-manipulating an object. We proposed to utilize these features as an abstract model for the cooperation. That is, as an answer to our first research question, these features are good candidates for quantifying the cooperation quality. In response to our second research question, we focused on the motion profile of the manipulated object and observed interesting regularities in its trajectories. In particular, we observed that it closely follows a minimum-jerk trajectory. This model paved our way towards answering the third research question.

In Chapter 6, we introduced the interaction force and the important role that it plays in fluidity and naturalness of the interaction. We presented the standard formulation of the applied forces and explained the challenges involved in computing the interaction force. We showed that the system is an under determined system of equations and, therefore, it requires additional assumptions to have a unique solution. We discussed that, while special cooperation cases such as leader/follower scenario can be modeled fairly easily, this is not the case for more general cases of cooperative manipulation. However, taking advantage of the proposed model for the object's motion (Chapter 5), we introduced a new model for the interaction force. Using the feature-set proposed in Chapter 4, we evaluated different cooperation scenarios and showed that our interaction force model outperforms the existing models in the literature.

To tackle the last research question, we studied different characteristics of interaction force. We reported our various observations regarding the interaction force properties in Chapter 8 and proposed a control policy for the robot to extend existing controllers. Then we chose a specific robot controller, an impedance controller, and proposed a more general scheme that introduces the interaction force into the control loop. We discussed how an online controller can be realized and showed that the performance of our scheme (including the estimation and prediction algorithms) is not significantly different from the performance of a human-human cooperation.

While we have presented a fairly complete solution to the problem studied in this dissertation, we made various simplifying assumptions and imposed various constraints to arrive at the solution. As a result, the proposed controller is specific for the task that was studied. In Chapter 11 we discussed a few extensions to our approach and suggestions for alleviating some of these limitations and assumptions. However, there are still some inherited limitations that need to be addressed to achieve a more general treatment for the problem. For instance, in our study, we chose a rigid body (the pot) for the manipulation task. An interesting question is that how the model would respond, if the object has some dynamics, e.g. the pot is half-full of water. Can we still utilize motion information in planning the interaction force, or we need to also include the dynamics of the object?

Another inherited limitation of our work was regarding the safety concerns. Since the manipulation task was designed with a completely safe and known object, no safety concern existed in our study. Therefore, another interesting question would be: "how the model should be modified, if there are some safety concerns about the object or the task, e.g. the pot is full of water or the object is a knife?". The preliminary results of our pilot study on this matter shows that, during handover, safety has a major role in shaping the object's motion trajectory. To be able to generalize our approach and better explore other contributing factors (including the dynamics of the object/environment and human's psychological state), a more exhaustive study with different objects and various cooperation scenarios is necessary.

Finally, our approach assumes that a perfect controller exists for the robot that can render the commanded force in real-time. Unfortunately, this is not the case for many robotic arms. While advanced manipulator arms benefit from new technologies and can achieve higher performances, the trade-off between safety (the robot can safely work in proximity of humans) and performance is still a challenge. As such, utilizing the proposed controller for cheaper robots would not result satisfying outcomes. Our preliminary results of another pilot study showed that the human partners are unable to differentiate between the standard implementation of an impedance controller and an implementation augmented with interaction force controller. We speculate that the poor performance of the controller overshadowed the difference between the controllers. While it is theoretically possible to improve the robot's performance by designing better controllers, there are practical limitations (such as saturation of motors) that put a limit on this performance improvements.

Appendices

Appendix A

RESEARCH PROTOCOL

In this appendix we present the research protocol that was our guideline for the human study. This protocol was submitted for the review to the IRB and got approved as an expedited continuing review. The associated approval notice follows in Appendix B. The approved consent document and the recruitment materials that we used in our human study are also presented in Appendix C and Appendix D, respectively.

Effective Communication with Robotic Assistants for the Elderly: Integrating Speech, Vision and Haptics

Miloš Žefran, Barbara Di Eugenio, Jezekiel Ben-Arie
College of Engineering, University of Illinois at Chicago

Mark D. Foreman
Adult Health and Gerontological Nursing, Rush University College of Nursing

Sponsor: National Science Foundation
Version: 2

February 7, 2014

1 Study Hypothesis and Specific Aims

One of the main obstacles to the widespread use of robotic assistants by the elderly is the lack of adequate interfaces: the elderly person should be able to communicate with the robot naturally, similarly to the way she would communicate with a human caregiver. The goal of this research is to develop such an interface. Communication systems that are based on speech are currently available and can be designed to understand and respond to a set of verbal instructions [4, 5]. Speech communication is practical in home or hospital surroundings and does not require any technical knowledge. But it is problematic for elderly persons since they may suffer from speech impediments of various degrees due to a variety of medical conditions [18, 20]. Furthermore, if the robot is to assist with daily activities it needs to respond to other types of user response such as gestures and touch. This motivates us to propose an adaptive multimodal user interface for robotic assistants to the elderly. It will be multimodal since the elderly should be able to communicate with the robot verbally, through bodily gestures, or through physical interaction. And it will be adaptive, since the paradigm that we want to advance within the context of assistive robotics is that the interface should adapt to the user rather than the user to the interface [7, 20].

The distinguishing characteristics of our work is that, in addition to speech and gestures, we consider communication through physical interaction between the user and the robot. By physical interaction we intend the communicative aspect of a bi-directional exchange of forces during a direct or indirect (through an object held by the robot and the user) contact. One of the main hypotheses that we advance in this research is that such an exchange can be understood as a form of dialogue between the user and the robot and processed using dialogue processing techniques. We further show that dialogue processing provides a unifying framework in which speech, gestures, and physical interaction are all seen as equal drivers of a dialogue and can be effectively interpreted.

The proposed research focuses on the area of Human-Robot interaction with an emphasis on a multimodal communication interface that is tailored to the needs of elderly persons. The transformative idea of our work is to view haptics as one of the drivers of the dialogue between the user and the robot, and to study its relation to speech and gestures through dialogue processing methods. The combination of speech, gestures and haptics has received only limited attention, but it could be critical for successful deployment of assistive robots for many elderly individuals. The proposed interface is designed with the ability to learn and adapt the communication to each user. To this end, we will use a novel, adaptive and reliable recognition methodology called RISq (Recognition by Indexing and Sequencing) which can identify signals generated by speech, gestures and haptics, and map them to an appropriate symbolic representation such as words or object identifiers. Finally, we will use a formal and modular control design methodology that guarantees that the robot responds safely and reliably to the interpretation of the user intent provided by dialogue processing.

2 Background and Significance

The world's population is aging at an ever increasing pace. There is the need to develop technologies that will support the independent functioning of older people so that they are able to remain living in the community [9], postponing the transition to living in institutional settings for as long as possible – a movement referred to as aging in place [11, 15]. This challenge is compounded by the fact that the independent functioning of these individuals is currently supported by equally old and frail spouses [19]. The potential impact of such assistive technology is immense and multi-faceted. Supporting the independent functioning (physical and cognitive) of older people so that they can safely remain living in the community directly contributes to a higher quality of life for these individuals [11, 15]. Assistive technologies have the potential to dramatically reduce the burden and worries of the intimate friends and family who are currently assisting these individuals [19]. Finally, for the larger society, the deployment of assistive technologies to older people residing in the community can potentially create massive cost savings for health care [13, 17].

From a societal point of view, the impact of robot assistive technology is immense. Supporting the independent functioning of older people so that they can safely remain living in the community is of paramount importance. The proposed project could also have significant implications for the delivery of institutionally based health care. The deployment of robots to assist nursing personnel in various care settings (e.g., hospitals and long-term care facilities), and in the home has enormous implications for improved health outcomes and quality of life for older patients while minimizing costs of care. Furthermore, the reduction of the nursing workload by such robot assistants promises to alleviate the critical shortage of nursing personnel in the USA that is only expected to worsen.

3 Methods

a. Research Design

Under our previous IRB approval (#2011-0579) we collected 20 dialogues according to the procedures described in Sec. 3.e. Five of the 20 dialogues were used to pilot the data collection, and involved 5 members of the team and one gerontological nursing student from Rush University playing the role of a helper (HEL); in the other 15 dialogues, 15 elderly people recruited from assisted living facilities participated, with two gerontological nursing students from Rush playing the role of HEL.

In the current application, we seek approval for **Phase 1**, analysis of the 20 existing dialogues; **Phase 2**, collection of additional interaction data in the investigators' laboratories to refine data processing methods; and **Phase 3**, evaluation of the resulting robotic interface. Note that Phase 2 and 3 may run at the same time.

Phase 1. The videotaped data collected so far was transcribed with the Anvil tool [12]. Some preliminary annotations for gestures and referring expressions were performed: referring expressions are pronouns - *I, you, it, they* – and demonstratives - *this, that, there* – that refer to persons and objects in the environment. We intend to further annotate this data with language episodes, physical actions, and haptics. Whereas we can rely on a wealth of coding schemes for language (e.g. [6, 8, 10]), and a number of coding schemes for actions (e.g. [14]), we will need to develop appropriate codes for haptic interactions.

Phase 2. To complement the data previously collected at Rush University, additional data will be collected in the investigators' laboratories at UIC: the Computer Vision and Robotics Laboratory (CVRL) and the Machine Vision Laboratory (MVL) in the Dept. of Electrical and Computer Eng., and the Natural Language Processing Laboratory (NLPL) in the Dept. of Computer Science. In this data collection effort, subjects will not include elderly people, but will be recruited on campus, as detailed below. These subjects will perform ADLs or tasks derived from ADLs (i.e., instead of putting a pot on the stove, they will carry it to a specific location in the lab). The data collected in those laboratories will be used to further develop and refine automated data analysis tools needed to process the data collected on the elderly subjects, and to investigate specific hypotheses arising from the more realistic dialogues, for example, *Do people speak when they exchange an object?*.

Phase 3. Ultimately, the interface will be evaluated with human subjects. Since the specifics of the evaluation can be determined only after the system has been developed, we will submit an amendment describing the evaluation at the appropriate time.

b. Eligibility Criteria

For data collection under Phase 2 and Phase 3 subjects need to be 18 years old or older.

c. Justification for inclusion of any special or vulnerable populations

Not Applicable

d. Plans for subject selection, recruitment, and documentation of informed consent

Subjects will be recruited on campus, among undergraduate and graduate UIC students, and UIC staff. An advertisement will be placed on the Announcement Board of the UIC website; an email advertisement will be sent to appropriate mailing lists; flyers will be displayed in public areas at UIC. All interested people will be asked to contact the PI or collaborators by email. When they do so, time and date for the individual session will be negotiated by email. Every attempt will be made to arrange the session at a mutually convenient time.

e. Description of procedures

Phase 2. The experiments will be conducted in one of the three Labs at UIC: the Computer Vision and Robotics Laboratory (CVRL) and the Machine Vision Laboratory (MVL) in the Dept. of Electrical and Computer Eng. department, and the Natural Language Processing Laboratory (NLPL) in the Dept. of Computer Science. In each case, the PI or one of his delegates will first explain the procedure, and obtain informed consent. Subjects will be asked to wear data gloves, and microphones. Subjects will be videotaped either with a portable camera (CVRL and NLPL) or via a multi-camera system (MVL). The portable camera to be used in CVRL and in NLPL, and the multicamera system in the MVL, are all equipped with microphones; if these microphones are sensitive enough, we may forego having subjects wear additional microphones. Likewise, if the focus of inquiry in MVL and / or in NLPL does not require haptic information, for those experiments we may forego having subjects wear the datagloves.

The exact nature of the activities to be performed will depend on the laboratory:

1. Haptics and manipulation data collection will mostly take place in CVRL. Subjects will be asked to perform activities identified during Phase 1 as warranting further study. Examples include moving a pot filled with water, either alone or with another person; handing a plate to or receiving it from another person; or supporting another person while walking.
2. Vision and gesture data collection will mostly take place in MVL. The subjects may be asked to wear a colored piece of clothing (primarily gloves) to aid in image processing. The subject will be again asked to perform various activities identified during Phase 1 such as pointing to a location or gesturing to a person to come or stop.
3. Speech and language data collection will be done mostly in NLPL. Activities of interest may include asking a helper to retrieve an object referring to the object in a variety of ways, e.g. only pointing, pointing plus a minimum of speech (e.g. using a pronoun), no gestures but a full noun phrase (the blue glass on the top shelf), etc.

At the end of the session, the person will be thanked. Participants will be compensated with a flat rate of $10 each and asked to sign a receipt.

Data will be collected with a Matlab program that was developed as part of the project. The application collects time-stamped video and audio recordings, as well as recordings from all the sensors on the data gloves. The application runs locally on a dedicated PC. A password is required to access the account under which the application can be run. Nobody except for the user of that account can access the collected data. All the user accounts, including the account with experimental data, are backed up on the laboratory server which is also password protected.

The existing 20 video and audio recordings are also stored on the laboratory server and they are subject to the same data protection policies as those for the data to be collected. The files have been assigned a random label and fixed qualifiers to identify the type of data. This label is not directly linked to the subjects identity. The files are kept in a dedicated, protected directory on `robotics.ece.uic.edu`, a server housed in the PIs laboratory. The laboratory is kept locked at all times. Whereas all the students in the PIs group have keys to the laboratory, and have password protected access to the server, only the project members have access to the specific directory on the server which contains the research data.

f. Statistical Methods

The videotaped data previously collected was transcribed with the Anvil tool [12], and so will the data still to be collected. All data will be annotated with an annotation scheme that will include provisions to code for language episodes, physical actions, gestures and haptics. Whereas we can rely on a wealth of coding schemes for language (e.g. [6, 8, 10]), and a number of coding schemes for actions (e.g. [14]) and gestures (e.g. [16]), part of our research is to develop appropriate codes for haptic interactions.

Once the data is annotated, we can run a variety of statistical methods. Part of the research is to find out which statistical and data mining methods are more appropriate to derive the information we need (data mining pertains to deriving full patterns of relationships between different features, as opposed to traditional parametric and non parametric methods from statistics which derive poorer models). The methods we will employ will include regressions of different sorts to explore correlations between features of the interactions and say, the time it took the dyad to complete a certain action; and RISq (Recognition by Indexing and Sequencing), a data mining method originally developed to recognize human activity by co-PI Ben-Arie [2, 3], and which was awarded a US patent in May 08 [1]. RISq can infer patterns from audio, visual and haptics data.

g. Safety Monitoring and Assessment

Not Applicable

h. Data management

Data will be collected with a Matlab program that was developed as part of the project. The application collects time-stamped video and audio recordings, as well as recordings from all the sensors on the data gloves. The application runs locally on a dedicated PC. A password is required to access the account under which the application can be run. Nobody except for the user of that account can access the collected data. All the user accounts, including the account with experimental data, are backed up on the laboratory server which is also password protected.

To ensure privacy, every subject will be assigned an arbitrary label, and all data analysis and discussion of results will be done with reference to that label. Video files will be stored as password protected files, on password protected computers in the PI's lab. Only project personnel will know the passwords necessary to access the video files. The files containing data from all other sensors will contain no identifying information, but they will also be password protected.

Five years after the study is completed, the consent forms will be destroyed.

4 Management Plan

For the objectives of this research, we formed an interdisciplinary team composed of experts in Robotics, Nursing, Natural Language Processing and Computer Vision & Pattern Recognition. Knowledge from these diverse areas will be fused for the development of a novel approach that employs a combination of verbal communication, bodily gestures and physical interaction patterns.

We have been working on the joint project in four laboratories: at UIC, the Computer Vision and Robotics Laboratory (CVRL) and the Machine Vision Laboratory (MVL) in the Electrical and Computer Engineering Department, and the Natural Language Processing Lab (NLP Lab) in the Computer Science Department; at Rush, Dr. Foreman's laboratory in the College of Nursing.

The groups closely interact and combine their expertise to obtain best possible results. The PI (Žefran) is responsible for overseeing the progress of the different groups and facilitate their collaboration, including regular joint meetings.

Data for Phase 2 will be collected on subjects recruited among UIC students and staff at UIC in the Computer Vision and Robotics Laboratory (CVRL) and the Machine Vision Laboratory (MVL) in the Dept. of Electrical and Computer Eng., and the Natural Language Processing Laboratory (NLPL) in the Dept. of Computer Science. These laboratories are research facilities primarily equipped with desks and computers for student use, however they provide enough space for the limited data collection needed to further develop and refine automated data analysis tools needed to process the data collected on the elderly subjects, and to investigate specific hypotheses arising from the data. The collected data has been and will be transferred for analysis to all labs. Each lab will analyze the data streams that fall within their purview. The NLP Lab is concerned with a high level annotation of the interactions, pertaining to language episodes, gestures and actions. The same video recordings will be used by MVL for visual analysis of bodily gestures. The gestures have to be translated to sequences of body parts poses that will then serve as temporal sequences of vectors that represent the poses of all the body parts that participate in the gesture (usually the hands, arms and head). The force data is being obtained from the data gloves, and later, from force sensors that will be mounted on the robots in CVRL. These signals will be digitized and then translated to a temporal sequence of vectors. The recognition of sequences of different modalities will be performed by MVL employing the RISq recognition method.

References

[1] J. Ben-Arie. Method for recognition of human motion, vector sequences and speech. US patent 7,366,645 B2, April 2008.

[2] J. Ben-Arie, D. Sivalingam, and S. Rajaram. Probabilistic labeling of human body parts. In *IASTED International Conference on Circuits, Signals and Systems*, pages 275–280, Cancun, Mexico, May 2003.

[3] J. Ben-Arie and Q. Wu. A comparison between hmm based recognition to risq-recognition by indexing and sequencing. Submitted to IEEE Trans. On Pattern Analysis and Machine Intelligence – PAMI, October 2008.

[4] R. Bischoff and V. Graefe. Dependable multimodal communication and interaction with robotic assistants. In *Proceedings of the IEEE International Workshop on Human and Robot Interactive Communication*, Berlin, Germany, Sep 2002.

[5] R. Bischoff and V. Graefe. HERMES - a versatile personal robotic assistant. *Proceedings of the IEEE*, 92(11):1759–1779, 2004.

[6] J. Carletta, A. Isard, S. Isard, J. C. Kowtko, G. Doherty-Sneddon, and A. H. Anderson. The reliability of a dialogue structure coding scheme. *Computational Linguistics*, 23(1):13–31, 1997.

[7] S. J. Czaja and C. C. Lee. Designing computer systems for older adults. In J. Jacko and A. Sears, editors, *Handbook of Human-Computer Interaction*, pages 413–427. LEA: NY, 2002.

[8] B. Di Eugenio, P. W. Jordan, and L. Pylkkanen. The COCONUT project: Dialogue annotation manual. Technical Report ISP 98-1, University of Pittsburgh, 1998.

[9] E. Dishman, J. Matthews, and J. Dunbar-Jacobs. Everyday health: technology for adaptive aging. In *Technology for adaptive aging*, pages 179–208. The National Academies Press, Washington, D.C., 2004.

[10] M. Glass, H. Raval, B. Di Eugenio, and M. Traat. The DIAG-NLP dialogues: coding manual. Technical Report UIC-CS 02-03, University of Illinois - Chicago, 2002.

[11] A. Horgas and G. Abowd. The impact of technology on living environments for older adults. In *Technology for adaptive aging*, pages 230–252. The National Academies Press, Washington, D.C., 2004.

[12] Michael Kipp. Anvil – a generic annotation tool for multimodal dialogue. In *Proceedings of Eurospeech*, pages 1367–1370, Aalborg, Denmark, 2001.

[13] M. Knapp, L. Thorgrimsen, A. Patel, A. Spector, A. Hallam, B. Woods, and M. Orrell. Cognitive stimulation therapy for people with dementia: Cost-effectiveness analysis. *British Journal of Psychiatry*, 188:574–580, 2006.

[14] B. MacWhinney. *The CHILDES project. Tools for analyzing talk: Transcription Format and Programs*. Lawrence Erlbaum, Mahwah, NJ, 2000.

[15] K. D. Marek, L. Popejoy, G. Petroski, D. Mehr, M. Rantz, and W. C. Lin. Clinical outcomes of aging in place. *Nursing Research*, 54(3):202–211, 2005.

[16] D. McNeill. *Hand and Mind: What Gestures Reveal about Thought*. University of Chicago Press, 1992.

[17] R. W. Pew. *Introduction and overview, Technology for adaptive aging*, pages 9–40. The National Academies Press, Washington, D.C., 2004.

[18] T. A. Salthouse. *Theoretical Perspectives on Cognitive Aging*. LEA: Hillsdale, NJ, 1991.

[19] K. B. Tetz, P. G. Archbold, B. J. Stewart, D. Messecar, M. C. Hornbrook, and S. A. Lucas. How frail elders evaluate their caregiver's role enactment. *Journal of Family Nursing*, 12(3):251–275, August 2006.

[20] B. Xiao, R. Lunsford, R. Coulston, M. Wesson, and S. L. Oviatt. Modeling multimodal integration patterns and performance in seniors: Toward adaptive processing of individual differences. In *International Conference on Multimodal Interfaces*, pages 265–272, Vancouver, B.C., 2003. ACM Press.

Appendix B

IRB APPROVAL NOTICE

In this appendix we present the approval notice for our research protocol (#2011-0579). Here we only include the approval notice for the latest period of this research's activities. For earlier notices, please refer to the project's PI. To read the research protocol, please refer to Appendix A.

UNIVERSITY OF ILLINOIS
AT CHICAGO

Office for the Protection of Research Subjects (OPRS)
Office of the Vice Chancellor for Research (MC 672)
203 Administrative Office Building
1737 West Polk Street
Chicago, Illinois 60612-7227

Approval Notice
Continuing Review

May 29, 2015

Milos Zefran, Ph.D.
Electrical and Computer Engineering
851 S Morgan
M/C 154
Chicago, IL 60612
Phone: (312) 996-6495

RE: **Protocol # 2011-0579**
"Effective Communication with Robotic Assistants for the Elderly: Integrating Speech, Vision and Haptics (re-submission of Protocol 2009-0541)"

Dear Dr. Zefran:

Your Continuing Review application was reviewed and approved by the Expedited review process on May 28, 2015. You may now continue your research.

Please note the following information about your approved research protocol:

Please note that this research did not have Institutional Review Board (IRB) approval beginning at 12:01 a.m. on 23 May 2015 and until IRB approval was again granted on 28 May 2015. Any research activities conducted between those dates were done without IRB approval and were not compliant with UIC's human subject protection policies, *The Belmont Report*, UIC's Assurance awarded by the Office for Human Research Protection (OHRP) at HHS, and with the federal regulations for the protection of human research subjects, 45 CFR 46.

Protocol Approval Period: May 28, 2015 - May 27, 2016
Approved Subject Enrollment #: 140 (58 subjects enrolled)
Additional Determinations for Research Involving Minors: These determinations have not been made for this study since it has not been approved for enrollment of minors.
Performance Sites: UIC, Pioneer Gardens - Chicago, IL
Sponsor: None
Research Protocol:

a) Effective Communication with Robotic Assistants for the Elderly: Integrating Speech, Vision and Haptics; Version 2; 10/20/2011

Recruitment Materials:

a) Email Recruitment Letter; Version 1; 01/30/2012

b) Flyer (The Project); Version 1; 01/31/2012
c) Flyer (Health Adults Needed for Research); Version 2; 05/22/2014

Informed Consents:

a) UIC Lab Site; Version 3; 01/31/2012
b) A waiver of documentation of consent has been granted under 45 CFR 46.117 for recruitment purposes only (minimal risk; obtaining contact information from potential subjects; written consent will be obtained at enrollment)

Your research continues to meet the criteria for expedited review as defined in 45 CFR 46.110(b)(1) under the following specific categories:

(4) Collection of data through noninvasive procedures (not involving general anesthesia or sedation) routinely employed in clinical practice, excluding procedures involving X-rays or microwaves. Where medical devices are employed, they must be cleared/approved for marketing. (Studies intended to evaluate the safety and effectiveness of the medical device are not generally eligible for expedited review, including studies of cleared medical devices for new indications.) Examples: (a) physical sensors that are applied either to the surface of the body or at a distance and do not involve input of significant amounts of energy into the subject or an invasion of the subject's privacy; (b) weighing or testing sensory acuity; (c) magnetic resonance imaging; (d) electrocardiography, electroencephalography, thermography, detection of naturally occurring radioactivity, electroretinography, ultrasound, diagnostic infrared imaging, doppler blood flow, and echocardiography; (e) moderate exercise, muscular strength testing, body composition assessment, and flexibility testing where appropriate given the age, weight, and health of the individual,
(6) Collection of data from voice, video, digital, or image recordings made for research purposes.,
(7) Research on individual or group characteristics or behavior (including but not limited to research on perception, cognition, motivation, identity, language, communication, cultural beliefs or practices and social behavior) or research employing survey, interview, oral history, focus group, program evaluation, human factors evaluation, or quality assurance methodologies.

Please note the Review History of this submission:

Receipt Date	Submission Type	Review Process	Review Date	Review Action
05/20/2015	Continuing Review	Expedited	05/28/2015	Approved

Please remember to:

→ Use your **research protocol number** (2011-0579) on any documents or correspondence with the IRB concerning your research protocol.

→ Review and comply with all requirements on the OPRS website under:
"UIC Investigator Responsibilities, Protection of Human Research Subjects"
(http://tigger.uic.edu/depts/ovcr/research/protocolreview/irb/policies/0924.pdf)

Please note that the UIC IRB has the prerogative and authority to ask further questions, seek additional information, require further modifications, or monitor the conduct of your research and the consent process.

Please be aware that if the scope of work in the grant/project changes, the protocol must be amended and approved by the UIC IRB before the initiation of the change.

We wish you the best as you conduct your research. If you have any questions or need further help, please contact OPRS at (312) 996-1711 or me at (312) 996-2014. Please send any correspondence about this protocol to OPRS at 203 AOB, M/C 672.

Sincerely,

Sandra K Costello

Sandra Costello
Assistant Director, IRB # 2
Office for the Protection of Research Subjects

Enclosures:

1. **Informed Consent Document:**
   a) UIC Lab Site; Version 3; 01/31/2012
2. **Recruiting Materials:**
   a) Email Recruitment Letter; Version 1; 01/30/2012
   b) Flyer (The Project); Version 1; 01/31/2012
   c) Flyer (Health Adults Needed for Research); Version 2; 05/22/2014

cc: Rashid Ansari, Electrical and Computer Engineering, M/C 154

Appendix C

CONSENT DOCUMENT

The approved consent document is presented here in this appendix. Every participant was briefed about the study before the experiment and signed and dated this document after he/she understood the process. A copy of the signed consent document has been provided to the participant, as well. The original signed consent documents have been stored in a secure place and is available for review upon request. Please contact PI for any further inquiries.

Leave box empty - For office use only

STARTS APPROVAL EXPIRES

MAY 22 2014 MAY 22 2015

UNIVERSITY OF ILLINOIS AT CHICAGO
INSTITUTIONAL REVIEW BOARD

University of Illinois at Chicago
Research Information and Consent for Participation in Social Behavioral Research

Effective Communication with Robotic Assistants for the Elderly: Integrating Speech, Vision and Haptics

Dr. Miloš Žefran, Principal Investigator

You are being asked to participate in a research study. Researchers are required to provide a consent form such as this one to tell you about the research, to explain that taking part is voluntary, to describe the risks and benefits of participation, and to help you to make an informed decision. You should feel free to ask the researchers any questions you may have.

Principal Investigator Name and Title: **Effective Communication with Robotic Assistants for the Elderly: Integrating Speech, Vision and Haptics**

Department and Institution: **Electrical and Computer Engineering Department, University of Illinois at Chicago**

Address and Contact Information: **851 S. Morgan St., Chicago, IL, 60607, 312-996-6495 , mzefran@uic.edu**

Sponsor: **National Science Foundation**

Why am I being asked?

You are being asked to be a subject in a research study about the way that elderly persons communicate with their caregivers while performing routine activities such as walking or preparing dinner together.

You have been asked to participate in the research because you contacted us in reply to our email or flyer, and you are 18 years old or older; hence, you are eligible to participate. Please read this form and ask any questions you may have before agreeing to be in the research.

Your participation in this research is voluntary. Your decision whether or not to participate will not affect your current or future dealings with the University of Illinois at Chicago. **If you decide to participate, you are free to withdraw at any time without affecting that relationship.**

Approximately 100 subjects may be involved in this research at UIC.

What is the purpose of this research?

The purpose of this research is to develop a way for older people to communicate with robotic assistants. Our aim is to enable the robot to understand the intent of a person talking to it, making hand gestures, or touching it either directly or through another object. The activities that the robot will be intended to help with are so called Activities of Daily Living (ADLs), such as getting out of a chair, walking, and meal preparation. To further explore these kind of interactions, we are also collecting data in a laboratory environment, where we focus on specific aspects of the interaction: for example, how one person individually, or two people together carry an object, how they identify objects via pointing gestures, and how they use spoken language when carrying out these activities.

What procedures are involved?

If you agree to be in this research, we would ask of you the following:

- For you to come to one of the following locations on the UIC East Campus: the Computer Vision and Robotics lab (CVRL, 4211 SELW); or the Machine Vision lab (MVL, 1312 SEO); or the Natural Language Processing lab (NLPL, 937 SEO).
- For you to engage in routine activities, either individually or with a partner: for example, getting up from a chair, carrying an object, pointing to objects, finding objects such as cups, pots and plates in closets, etc.
- For you to allow us to take audio- and video-recordings of you performing those activities.
- For you, to wear the wireless data glove, which record the movement a person hand makes, and the pressure that a person is applying with their fingers when touching something.

The length of the session will last no more than 1 hour.

What are the potential risks and discomforts?

To the best of our knowledge, the things you will be doing have no more risk of harm than you would experience in everyday life. There are no other risks associated with participation over and above those that arise from the daily performance of routine activities such as getting up from a chair, walking or carrying objects.

A risk of this research is a loss of privacy (revealing to others that you are taking part in this study) or confidentiality (revealing information about you to others to whom you have not given permission to see this information).

Are there benefits to taking part in the research?

There are no benefits to you personally for taking part in this research. However, this research will contribute to the development and deployment of assistive robots for the elderly. If assistive robots can be successfully deployed, they will support the independent functioning of older people. This would have huge implications for improved health outcomes and quality of life for older patients while minimizing costs of care.

What other options are there?

If you do not want to participate in the study, you are free to do so.

What about privacy and confidentiality?

The people who will know that you are a research subject are members of the research team. Otherwise information about you will only be disclosed to others with your written permission, or if necessary to protect your rights or welfare or if required by law. In addition, UIC IRB and the State of Illinois may review research records in order to monitor the conduct of the research.

If photographs, video-, or audio-recordings of you will be used for educational purposes, your identity will be protected or disguised. When the results of the research are published or discussed in conferences: if video excerpts or photographs are used, faces will be completely de-identified; when de-identified video or only audio are used, only short excerpts will be included, of length less than 2 minutes; transcribed speech (in written form) may also be used.

Any information that is obtained in connection with this study and that can be identified with you will remain confidential and will be disclosed only with your permission or as required by law. If you wish, you can review the audio- and video-recordings that we make of you and ask us to edit or erase them.

The tapes and all other parts of the record will be kept in the PI office and dedicated laboratory spaces that are locked when not in use and to which only the project members have keys.

Because collecting and analyzing dialogues is a time consuming activity, research teams on campus, or at other universities or research laboratories may ask us for access to the data. If we decide to share the data with them, we will do so only after any reference to your personal identity has been eliminated from the data. We will share only the transcribed data, not the audio or video tapes. If you object to your data possibly being shared with other research teams, you can withhold your consent for that specific usage. Withholding your consent in that regard does not prevent you from participating in this study in any way.

What are the costs for participating in this research?

There are no costs to you for participating in this research.

Will I be reimbursed for any of my expenses or paid for my participation in this research?

You will be paid a flat rate of $10 for your participation in this research. Each session will not last more than one hour, including informed consent, debriefing and payment.

Can I withdraw or be removed from the study?

You can choose whether to be in this study or not. If you volunteer to be in this study, you may withdraw at any time without consequences of any kind.

Who should I contact if I have questions?

Contact the researchers Dr. Miloš Žefran at 312-996-6495 or email address: mzefran@uic.edu

- if you have any questions about this study or your part in it,
- If you have questions, concerns or complaints about the research.

What are my rights as a research subject?

If you feel you have not been treated according to the descriptions in this form, or if you have any questions about your rights as a research subject, including questions, concerns, or complaints, you may call the Office for the Protection of Research Subjects (OPRS) at 312-996-1711 or 1-866-789-6215 (toll-free) or e-mail OPRS at uicirb@uic.edu.

What if I am a UIC student?

You may choose not to participate or to stop your participation in this research at any time. This will not affect your class standing or grades at UIC. The investigator may also end your participation in the research. If this happens, your class standing or grades will not be affected. You will not be offered or receive any special consideration if you participate in this research.

What if I am a UIC employee?

Your participation in this research is in no way a part of your university duties, and your refusal to participate will not in any way affect your employment with the university, or the benefits, privileges, or opportunities associated with your employment at UIC. You will not be offered or receive any special consideration if you participate in this research.

Remember:

Your participation in this research is voluntary. Your decision whether or not to participate will not affect your current or future relations with the University. If you decide to participate, you are free to withdraw at any time without affecting that relationship.

Signature of Subject or Legally Authorized Representative

I have read (or someone has read to me) the above information. I have been given an opportunity to ask questions and my questions have been answered to my satisfaction. I agree to participate in this research. I will be given a copy of this signed and dated form.

Signature ______________________ Date ____________

Printed Name ______________________

Signature of Person Obtaining Consent ______________________ Date (must be same as subject's) ____________

Printed Name of Person Obtaining Consent ______________________

It has been explained to me that my transcribed data, without any identifying personal information, may be shared with other research teams, at this or other universities and research laboratories. I consent to this further use of my data.

Signature ______________________ Date ____________

Printed Name ______________________

Signature of Person Obtaining Consent ______________________ Date (must be same as subject's) ____________

Printed Name of Person Obtaining Consent ______________________

Appendix D

RECRUITMENT MATERIALS

The recruitment material that was used for this study is presented in this appendix. The recruitment email was sent to the GRADLIST mailing list at UIC. All volunteers communicated with us through emails. Only three volunteers were excluded, as they were not adults. Each participant received a compensation of $10 at the end of the session and signed a receipt note. A sample of a blank receipt is included in this appendix as well.

Email Recruitment Letter

Subject: WANTED: PAID volunteers for the project "Communication with Robotic Assistants"

Help us understand how a robot should communicate with a person!

Earn extra money!

Dear students,

Three research labs (Robotics, and Machine Vision in the Electrical and Computer Engineering department; and Natural Language Processing in the Computer Science department) are developing robots that can help people, especially the elderly, perform tasks. We need to understand how two people collaborate in performing simple activities, such as carrying objects together; and how they talk about what they're doing.

We need **YOU** to perform those simple activities in our labs in order to inform the development of future assistive robots!

PAY: $10/session

TIME COMMITMENT: About 1 hour, in one single session!

WHAT: You will be asked to perform simple tasks in the labs, individually or in pairs, such as: finding objects in cabinets, taking them out and placing them in another location; carrying objects with a collaborator; talking with a collaborator about the objects to be found and carried.

WHEN: We can ACCOMMODATE your schedule.

WHERE: 4211 SELW, or 1312 SEO, or 937 SEO

To **SIGN UP**, or **ASK FOR MORE INFORMATION**: Email Maria Javaid (mjavai2@uic.edu) or Lin Chen (lchen43@uic.edu).

Thank you!

Miloš Žefran, Associate Professor (Director, Robotics Lab, ECE)
Jezekiel Ben-Arie, Professor (Director, MVL, ECE)
Barbara Di Eugenio, Associate Professor (Director, NLP, CS)

The Project

Effective Communication with Robotic Assistants

is recruiting paid volunteers to inform hardware and software development

WHAT IS THIS STUDY ABOUT?

We are developing robots that can help people, especially the elderly. To inform robot development, we need to understand how people perform simple activities; and how they communicate about what they're doing.

WHAT WOULD I DO IF I PARTICIPATE?

You will be asked to: a) perform simple tasks with a collaborator, like finding objects, carrying them; and b) talk about what you're doing. The session will take between 30' and an hour.

WHY SHOULD I DO THIS?

Help us develop the assistive robots of the future!
Get paid $10/session !

Contact: Maria at mjavai1@uic.edu or Lin at lchen43@uic.edu

UIC Departments of: Elec. & Computer Engineering
Computer Science

Healthy Adults Needed for Research

We are studying how people communicate when they perform certain collaborative activities, for example, supporting a person while walking together or making dinner. The goal of the research is to develop interfaces that will allow elderly people to communicate with assistive robots in their apartments. This research is being done by Drs. Miloš Žefran, Barbara Di Eugenio, and Jezekiel Ben-Arie from the University of Illinois at Chicago.

If you are 18 years of age you may be able to participate. You will be asked to perform certain everyday activities, possibly with another person. These activities will be videotaped and you might be asked to wear a specialized glove. The experiment will take at most 1 hour.

Each participant will be compensated $10 for their time.

How do I learn more about this study?

If you are interested in learning more about this study, contact:

Research Study (Human Collaboration) Prof. Miloš Žefran Phone: 312 9966495 Email: mzefran@uic.edu	Research Study (Human Collaboration) Prof. Miloš Žefran Phone: 312 9966495 Email: mzefran@uic.edu	Research Study (Human Collaboration) Prof. Miloš Žefran Phone: 312 9966495 Email: mzefran@uic.edu	Research Study (Human Collaboration) Prof. Miloš Žefran Phone: 312 9966495 Email: mzefran@uic.edu	Research Study (Human Collaboration) Prof. Miloš Žefran Phone: 312 9966495 Email: mzefran@uic.edu	Research Study (Human Collaboration) Prof. Miloš Žefran Phone: 312 9966495 Email: mzefran@uic.edu

Cash Receipt

University of Illinois
at Chicago (UIC)
Robotics Lab

Paid to ………………………………………….. the amount of $ ………

For volunteering for the project “Effective Communication with Robotic Assistants for the Elderly: Integrating Speech Vision and Haptics”

Paid by	Received by	Date

Cash Receipt

University of Illinois
at Chicago (UIC)
Robotics Lab

Paid to ………………………………………….. the amount of $ ………

For volunteering for the project “Effective Communication with Robotic Assistants for the Elderly: Integrating Speech Vision and Haptics”

Paid by	Received by	Date

Cash Receipt

University of Illinois
at Chicago (UIC)
Robotics Lab

Paid to ………………………………………….. the amount of $ ………

For volunteering for the project “Effective Communication with Robotic Assistants for the Elderly: Integrating Speech Vision and Haptics”

Paid by	Received by	Date

Cash Receipt

University of Illinois
at Chicago (UIC)
Robotics Lab

Paid to ………………………………………….. the amount of $ ………

For volunteering for the project “Effective Communication with Robotic Assistants for the Elderly: Integrating Speech Vision and Haptics”

Paid by	Received by	Date

Cash Receipt

University of Illinois
at Chicago (UIC)
Robotics Lab

Paid to ………………………………………….. the amount of $ ………

For volunteering for the project “Effective Communication with Robotic Assistants for the Elderly: Integrating Speech Vision and Haptics”

Paid by	Received by	Date

Cash Receipt

University of Illinois
at Chicago (UIC)
Robotics Lab

Paid to ………………………………………….. the amount of $ ………

For volunteering for the project “Effective Communication with Robotic Assistants for the Elderly: Integrating Speech Vision and Haptics”

Paid by	Received by	Date

Appendix E

THE QUESTIONNAIRE

The questionnaire included seven question on how participants assess the quality of their interaction. The questions are:

1. How fast was the whole manipulation task?
2. How do you characterize your relative speeds?
3. How do you feel about the nature of your partner's effort?
4. How fair do you feel the collaboration was?
5. How do you characterize the cooperative nature of this collaborative task?
6. How natural do you feel the motion trajectory was?
7. How much attention (mental workload) did the task demand, compared to doing the manipulation on your own?

Possible answers for each question were arranged in a Visual Analogue Scale (VAS) format. The questionnaire and the personal information form is attached in this appendix. Note that for personal information, no measurement were taken and all information is self-declared and unverified.

Questionnaire:

Name: ………………. Role: ……………
Dominant hand? ……… Color: ….……….
Time: ……………

Please read the following questions and put an X mark on the bar, where best fits to your answer.
Please first read all answers carefully and then mark your answer.

1- How fast was the whole manipulation task? The whole collaboration experience was ...

too slow; I would do it faster myself	slower than I prefer; but not annoyingly	very good; it matched my natural speed	faster than I prefer; but not annoyingly	too fast; I would prefer to do it slower myself

2- How do you characterize your relative speeds? My partner was ...

too slow; I had to push him/her to go faster	slower than me; but not annoyingly	pleasant; in the same speed range as me	faster than me; but not annoyingly	too fast; I had to slow him/her down

3- How do you feel about the nature of your partner's effort? I felt my partner was ...

resisting my actions during the whole experience	forcing his/her actions over mine during the task	exerting some pushes/pulls, but they were not annoying	quite cooperative; no pushes/pulls

Robotics Lab, University of Illinois at Chicago (UIC)

4- How fair do you feel the collaboration was? I feel ...

he/she applied most of the effort; I had a free ride	we contributed equally in performing the task	I did most of the work and he/she enjoyed a free ride

5- How do you characterize the cooperative nature of this collaborative task? I felt ....

I was leading the task the whole time	we were switching the roles, but I was leading most of the time	we both actively cooperated	we were switching the roles, but I was following most of the time	I was following him/her the whole time

6- How natural do you feel the motion trajectory was? I feel ....

it was even smoother than I would do it alone	it was as smooth as if I did it alone	there were some unusual pauses & accelerations, but overall fine	it was totally abnormal way of doing the task, I would never do it like this

7- How much attention (mental workload) did the task demand, compared to doing the manipulation on your own? I feel the task needed ...

no attention; I just moved naturally	little attention to synchronizing our motions	a lot of mental involvement due to the need to synchronize our actions

Name: …………………………. Email: ………………………….

Do you like to participate in the follow-up experiment? ……………………….

Gender: …………………………. Ethnicity: ………………………….

Height: …………………………. Arm length: ………………………….

Age: ……………………………. Frame: ……………………………

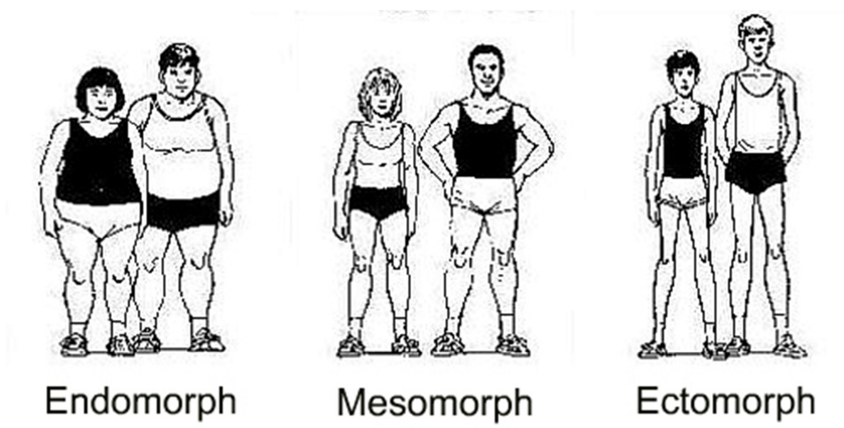

Appendix F

COPYRIGHT PERMISSIONS

In this appendix, we present the copyright permissions for the articles, whose contents were used in this thesis. The list of the articles include Humanoids'14 (Noohi and Žefran, 2014), WHC'15 (Noohi et al., 2015) and RO-MAN'16 (Noohi and Žefran, 2016) conference papers following by an article in IEEE Transactions on Robotics (Noohi et al., 2016) and a book chapter in Springer (Noohi and Žefran, 2017). The permissions follow in the same order.

Copyright Clearance Center RightsLink®

Home | Create Account | Help

IEEE
Requesting permission to reuse content from an IEEE publication

Title: Quantitative measures of cooperation for a dyadic physical interaction task

Conference Proceedings: Humanoid Robots (Humanoids), 2014 14th IEEE-RAS International Conference on

Author: Ehsan Noohi

Publisher: IEEE

Date: Nov. 2014

LOGIN

If you're a copyright.com user, you can login to RightsLink using your copyright.com credentials. Already **a RightsLink user** or want to learn more?

Thesis / Dissertation Reuse

The IEEE does not require individuals working on a thesis to obtain a formal reuse license, however, you may print out this statement to be used as a permission grant:

Requirements to be followed when using any portion (e.g., figure, graph, table, or textual material) of an IEEE copyrighted paper in a thesis:

1) In the case of textual material (e.g., using short quotes or referring to the work within these papers) users must give full credit to the original source (author, paper, publication) followed by the IEEE copyright line � 2011 IEEE.
2) In the case of illustrations or tabular material, we require that the copyright line � [Year of original publication] IEEE appear prominently with each reprinted figure and/or table.
3) If a substantial portion of the original paper is to be used, and if you are not the senior author, also obtain the senior author�s approval.

Requirements to be followed when using an entire IEEE copyrighted paper in a thesis:

1) The following IEEE copyright/ credit notice should be placed prominently in the references: � [year of original publication] IEEE. Reprinted, with permission, from [author names, paper title, IEEE publication title, and month/year of publication]
2) Only the accepted version of an IEEE copyrighted paper can be used when posting the paper or your thesis on-line.
3) In placing the thesis on the author's university website, please display the following message in a prominent place on the website: In reference to IEEE copyrighted material which is used with permission in this thesis, the IEEE does not endorse any of [university/educational entity's name goes here]'s products or services. Internal or personal use of this material is permitted. If interested in reprinting/republishing IEEE copyrighted material for advertising or promotional purposes or for creating new collective works for resale or redistribution, please go to http://www.ieee.org/publications_standards/publications/rights/rights_link.html to learn how to obtain a License from RightsLink.

If applicable, University Microfilms and/or ProQuest Library, or the Archives of Canada may supply single copies of the dissertation.

BACK ��� CLOSE WINDOW

Copyright Clearance Center RightsLink®

Home Create Account Help

IEEE Requesting permission to reuse content from an IEEE publication

Title: Computational model for dyadic and bimanual reaching movements

Conference Proceedings: World Haptics Conference (WHC), 2015 IEEE

Author: Ehsan Noohi

Publisher: IEEE

Date: June 2015

LOGIN

If you're a copyright.com user, you can login to RightsLink using your copyright.com credentials. Already **a RightsLink user** or want to learn more?

Thesis / Dissertation Reuse

The IEEE does not require individuals working on a thesis to obtain a formal reuse license, however, you may print out this statement to be used as a permission grant:

Requirements to be followed when using any portion (e.g., figure, graph, table, or textual material) of an IEEE copyrighted paper in a thesis:

1) In the case of textual material (e.g., using short quotes or referring to the work within these papers) users must give full credit to the original source (author, paper, publication) followed by the IEEE copyright line � 2011 IEEE.
2) In the case of illustrations or tabular material, we require that the copyright line � [Year of original publication] IEEE appear prominently with each reprinted figure and/or table.
3) If a substantial portion of the original paper is to be used, and if you are not the senior author, also obtain the senior author�s approval.

Requirements to be followed when using an entire IEEE copyrighted paper in a thesis:

1) The following IEEE copyright/ credit notice should be placed prominently in the references: � [year of original publication] IEEE. Reprinted, with permission, from [author names, paper title, IEEE publication title, and month/year of publication]
2) Only the accepted version of an IEEE copyrighted paper can be used when posting the paper or your thesis on-line.
3) In placing the thesis on the author's university website, please display the following message in a prominent place on the website: In reference to IEEE copyrighted material which is used with permission in this thesis, the IEEE does not endorse any of [university/educational entity's name goes here]'s products or services. Internal or personal use of this material is permitted. If interested in reprinting/republishing IEEE copyrighted material for advertising or promotional purposes or for creating new collective works for resale or redistribution, please go to http://www.ieee.org/publications_standards/publications/rights/rights_link.html to learn how to obtain a License from RightsLink.

If applicable, University Microfilms and/or ProQuest Library, or the Archives of Canada may supply single copies of the dissertation.

BACK ��� CLOSE WINDOW

Title: Modeling the interaction force during a haptically-coupled cooperative manipulation

Conference Proceedings: Robot and Human Interactive Communication (RO-MAN), 2016 25th IEEE International Symposium on

Author: Ehsan Noohi

Publisher: IEEE

Date: Aug. 2016

Thesis / Dissertation Reuse

The IEEE does not require individuals working on a thesis to obtain a formal reuse license, however, you may print out this statement to be used as a permission grant:

Requirements to be followed when using any portion (e.g., figure, graph, table, or textual material) of an IEEE copyrighted paper in a thesis:

1) In the case of textual material (e.g., using short quotes or referring to the work within these papers) users must give full credit to the original source (author, paper, publication) followed by the IEEE copyright line � 2011 IEEE.
2) In the case of illustrations or tabular material, we require that the copyright line � [Year of original publication] IEEE appear prominently with each reprinted figure and/or table.
3) If a substantial portion of the original paper is to be used, and if you are not the senior author, also obtain the senior author�s approval.

Requirements to be followed when using an entire IEEE copyrighted paper in a thesis:

1) The following IEEE copyright/ credit notice should be placed prominently in the references: � [year of original publication] IEEE. Reprinted, with permission, from [author names, paper title, IEEE publication title, and month/year of publication]
2) Only the accepted version of an IEEE copyrighted paper can be used when posting the paper or your thesis on-line.
3) In placing the thesis on the author's university website, please display the following message in a prominent place on the website: In reference to IEEE copyrighted material which is used with permission in this thesis, the IEEE does not endorse any of [university/educational entity's name goes here]'s products or services. Internal or personal use of this material is permitted. If interested in reprinting/republishing IEEE copyrighted material for advertising or promotional purposes or for creating new collective works for resale or redistribution, please go to http://www.ieee.org/publications_standards/publications/rights/rights_link.html to learn how to obtain a License from RightsLink.

If applicable, University Microfilms and/or ProQuest Library, or the Archives of Canada may supply single copies of the dissertation.

Copyright Clearance Center RightsLink®

Home | Create Account | Help

IEEE

Requesting permission to reuse content from an IEEE publication

Title: A Model for Human–Human Collaborative Object Manipulation and Its Application to Human–Robot Interaction

Author: Ehsan Noohi

Publication: Robotics, IEEE Transactions on

Publisher: IEEE

Date: Aug. 2016

LOGIN

If you're a copyright.com user, you can login to RightsLink using your copyright.com credentials. Already **a RightsLink user** or want to learn more?

Thesis / Dissertation Reuse

The IEEE does not require individuals working on a thesis to obtain a formal reuse license, however, you may print out this statement to be used as a permission grant:

Requirements to be followed when using any portion (e.g., figure, graph, table, or textual material) of an IEEE copyrighted paper in a thesis:

1) In the case of textual material (e.g., using short quotes or referring to the work within these papers) users must give full credit to the original source (author, paper, publication) followed by the IEEE copyright line � 2011 IEEE.
2) In the case of illustrations or tabular material, we require that the copyright line � [Year of original publication] IEEE appear prominently with each reprinted figure and/or table.
3) If a substantial portion of the original paper is to be used, and if you are not the senior author, also obtain the senior author�s approval.

Requirements to be followed when using an entire IEEE copyrighted paper in a thesis:

1) The following IEEE copyright/ credit notice should be placed prominently in the references: � [year of original publication] IEEE. Reprinted, with permission, from [author names, paper title, IEEE publication title, and month/year of publication]
2) Only the accepted version of an IEEE copyrighted paper can be used when posting the paper or your thesis on-line.
3) In placing the thesis on the author's university website, please display the following message in a prominent place on the website: In reference to IEEE copyrighted material which is used with permission in this thesis, the IEEE does not endorse any of [university/educational entity's name goes here]'s products or services. Internal or personal use of this material is permitted. If interested in reprinting/republishing IEEE copyrighted material for advertising or promotional purposes or for creating new collective works for resale or redistribution, please go to http://www.ieee.org/publications_standards/publications/rights/rights_link.html to learn how to obtain a License from RightsLink.

If applicable, University Microfilms and/or ProQuest Library, or the Archives of Canada may supply single copies of the dissertation.

BACK ��� CLOSE WINDOW

SPRINGER LICENSE
TERMS AND CONDITIONS

Feb 07, 2017

This Agreement between Ehsan Noohi bezanjani ("You") and Springer ("Springer") consists of your license details and the terms and conditions provided by Springer and Copyright Clearance Center.

License Number	4043850671334
License date	Feb 07, 2017
Licensed Content Publisher	Springer
Licensed Content Publication	Springer eBook
Licensed Content Title	Estimating Human Intention During a Human–Robot Cooperative Task Based on the Internal ForceInternal force Model
Licensed Content Author	Ehsan Noohi
Licensed Content Date	Jan 1, 2017
Type of Use	Thesis/Dissertation
Portion	Full text
Number of copies	1
Author of this Springer article	Yes and you are the sole author of the new work
Order reference number	
Title of your thesis / dissertation	Control of Physical Human-Robot Interaction: Mimicking Human Assistance
Expected completion date	Feb 2017
Estimated size(pages)	200
Requestor Location	Ehsan Noohi bezanjani [redacted] CHICAGO, IL [redacted] United States Attn: Ehsan Noohi bezanjani
Billing Type	Invoice
Billing Address	Ehsan Noohi bezanjani [redacted] Chicago, IL [redacted] United States Attn: Ehsan Noohi bezanjani
Total	0.00 USD
Terms and Conditions	

Introduction
The publisher for this copyrighted material is Springer. By clicking "accept" in connection with completing this licensing transaction, you agree that the following terms and conditions apply to this transaction (along with the Billing and Payment terms and conditions

established by Copyright Clearance Center, Inc. ("CCC"), at the time that you opened your Rightslink account and that are available at any time at http://myaccount.copyright.com).
Limited License
With reference to your request to reuse material on which Springer controls the copyright, permission is granted for the use indicated in your enquiry under the following conditions:
- Licenses are for one-time use only with a maximum distribution equal to the number stated in your request.
- Springer material represents original material which does not carry references to other sources. If the material in question appears with a credit to another source, this permission is not valid and authorization has to be obtained from the original copyright holder.
- This permission
• is non-exclusive
• is only valid if no personal rights, trademarks, or competitive products are infringed.
• explicitly excludes the right for derivatives.
- Springer does not supply original artwork or content.
- According to the format which you have selected, the following conditions apply accordingly:
• **Print and Electronic:** This License include use in electronic form provided it is password protected, on intranet, or CD-Rom/DVD or E-book/E-journal. It may not be republished in electronic open access.
• **Print:** This License excludes use in electronic form.
• **Electronic:** This License only pertains to use in electronic form provided it is password protected, on intranet, or CD-Rom/DVD or E-book/E-journal. It may not be republished in electronic open access.
For any electronic use not mentioned, please contact Springer at permissions.springer@spi-global.com.
- Although Springer controls the copyright to the material and is entitled to negotiate on rights, this license is only valid subject to courtesy information to the author (address is given in the article/chapter).
- If you are an STM Signatory or your work will be published by an STM Signatory and you are requesting to reuse figures/tables/illustrations or single text extracts, permission is granted according to STM Permissions Guidelines: http://www.stm-assoc.org/permissions-guidelines/
For any electronic use not mentioned in the Guidelines, please contact Springer at permissions.springer@spi-global.com. If you request to reuse more content than stipulated in the STM Permissions Guidelines, you will be charged a permission fee for the excess content.
Permission is valid upon payment of the fee as indicated in the licensing process. If permission is granted free of charge on this occasion, that does not prejudice any rights we might have to charge for reproduction of our copyrighted material in the future.
-If your request is for reuse in a Thesis, permission is granted free of charge under the following conditions:
This license is valid for one-time use only for the purpose of defending your thesis and with a maximum of 100 extra copies in paper. If the thesis is going to be published, permission needs to be reobtained.
- includes use in an electronic form, provided it is an author-created version of the thesis on his/her own website and his/her university's repository, including UMI (according to the definition on the Sherpa website: http://www.sherpa.ac.uk/romeo/);
- is subject to courtesy information to the co-author or corresponding author.
Geographic Rights: Scope
Licenses may be exercised anywhere in the world.
Altering/Modifying Material: Not Permitted
Figures, tables, and illustrations may be altered minimally to serve your work. You may not

alter or modify text in any manner. Abbreviations, additions, deletions and/or any other alterations shall be made only with prior written authorization of the author(s).

Reservation of Rights

Springer reserves all rights not specifically granted in the combination of (i) the license details provided by you and accepted in the course of this licensing transaction and (ii) these terms and conditions and (iii) CCC's Billing and Payment terms and conditions.

License Contingent on Payment

While you may exercise the rights licensed immediately upon issuance of the license at the end of the licensing process for the transaction, provided that you have disclosed complete and accurate details of your proposed use, no license is finally effective unless and until full payment is received from you (either by Springer or by CCC) as provided in CCC's Billing and Payment terms and conditions. If full payment is not received by the date due, then any license preliminarily granted shall be deemed automatically revoked and shall be void as if never granted. Further, in the event that you breach any of these terms and conditions or any of CCC's Billing and Payment terms and conditions, the license is automatically revoked and shall be void as if never granted. Use of materials as described in a revoked license, as well as any use of the materials beyond the scope of an unrevoked license, may constitute copyright infringement and Springer reserves the right to take any and all action to protect its copyright in the materials.

Copyright Notice: Disclaimer

You must include the following copyright and permission notice in connection with any reproduction of the licensed material:

"Springer book/journal title, chapter/article title, volume, year of publication, page, name(s) of author(s), (original copyright notice as given in the publication in which the material was originally published) "With permission of Springer"

In case of use of a graph or illustration, the caption of the graph or illustration must be included, as it is indicated in the original publication.

Warranties: None

Springer makes no representations or warranties with respect to the licensed material and adopts on its own behalf the limitations and disclaimers established by CCC on its behalf in its Billing and Payment terms and conditions for this licensing transaction.

Indemnity

You hereby indemnify and agree to hold harmless Springer and CCC, and their respective officers, directors, employees and agents, from and against any and all claims arising out of your use of the licensed material other than as specifically authorized pursuant to this license.

No Transfer of License

This license is personal to you and may not be sublicensed, assigned, or transferred by you without Springer's written permission.

No Amendment Except in Writing

This license may not be amended except in a writing signed by both parties (or, in the case of Springer, by CCC on Springer's behalf).

Objection to Contrary Terms

Springer hereby objects to any terms contained in any purchase order, acknowledgment, check endorsement or other writing prepared by you, which terms are inconsistent with these terms and conditions or CCC's Billing and Payment terms and conditions. These terms and conditions, together with CCC's Billing and Payment terms and conditions (which are incorporated herein), comprise the entire agreement between you and Springer (and CCC) concerning this licensing transaction. In the event of any conflict between your obligations established by these terms and conditions and those established by CCC's Billing and Payment terms and conditions, these terms and conditions shall control.

Jurisdiction

All disputes that may arise in connection with this present License, or the breach thereof, shall be settled exclusively by arbitration, to be held in the Federal Republic of Germany, in accordance with German law.

Other conditions:

V 12AUG2015

Gmail

Ehsan Noohi <[redacted]@gmail.com>

Case #00258810 - Dissertation reuse permission question [ref:_00D30oeGz._500a01HNYoN:ref]

Springer, Permissions <permissions.springer@spi-global.com>
To: Ehsan Noohi <enoohi2@uic.edu>

Wed, Feb 8, 2017 at 2:00 AM

Dear Dr. Noohi,

Thank you very much for your email.

Yes, you are allowed to use the author-created version of the material in your university's repository.

Sincerely,

Springer

Rights and Permissions

Springer Science+Business Media

Tiergartenstr. 17

69121 Heidelberg

Germany

From: Ehsan Noohi [mailto:enoohi2@uic.edu]
Sent: Wednesday, February 08, 2017 7:44 AM
To: Springer, Permissions
Cc: customercare@copyright.com
Subject: Re: Case #00258810 - Dissertation reuse permission question [ref:_00D30oeGz._500a01HNYoN:ref]

Dear Springer,

While I was waiting for your response, I read the licence terms and conditions for "Thesis/Dissertation reuse". It says:

"-If your request is for reuse in a Thesis, permission is granted free of charge under the following conditions:

This license is valid for one-time use only for the purpose of defending your thesis and with a maximum of 100 extra copies in paper. If the thesis is going to be published, permission needs to be reobtained.
- includes use in an electronic form, provided it is an author-created version of the thesis on his/her own website and his/her **university's repository**, including UMI (according to the definition on the Sherpa website: http://www.sherpa.ac.uk/romeo/);

- is subject to courtesy information to the co-author or corresponding author.".

So, if I understand it correctly, I am allowed to reuse the material in my thesis and submit the thesis to school for their records. Is that true? Should I take any extra actions? Please advise since I need to submit my thesis to school immediately.

I've attached the permission I obtained through the RightsLink here to this email as well.

Thank you very much,

-Ehsan

On Mon, Feb 6, 2017 at 1:01 PM, customercare@copyright.com <customercare@copyright.com> wrote:

Dear Springer:

Ehsan Noohi is your Springer author and he would like to make sure it is okay to use his material for a dissertation and to have it posted on the University of Illinois at Chicago website where they post dissertations. They are able to make this password protected or it may be available to open to the public.
https://indigo.uic.edu/

Could he have permission to post on this site. His email is enoohi2@uic.edu

Thank you.

Kind regards,

Jeanne

Jeanne Brewster
Customer Account Specialist
Copyright Clearance Center
222 Rosewood Drive

Danvers, MA 01923
www.copyright.com
+1.855.239.3415

Facebook - Twitter - LinkedIn

ref:_00D30oeGz._500a01HNYoN:ref

--------------- Original Message ---------------

From: Ehsan Noohi [enoohi2@uic.edu]
Sent: 2/4/2017 5:24 PM
To: customercare@copyright.com
Subject: Dissertation reuse permission question

Dear Sir/Madam,

I am an author of a book chapter (Ch. 5) in the following Springer ebook:

E-Book:

http://link.springer.com/book/10.1007/978-3-319-40533-9

Chapter:

http://link.springer.com/chapter/10.1007/978-3-319-40533-9_5

I need to reuse my chapter material in my PhD dissertation. While obtaining the reuse permission I was forwarded to the RightsLink website. When I chose "thesis/dissertation" in your website, it prompted:

The material can only be used for the purpose of defending your thesis limited to university-use only. If the thesis is going to be published, permission needs to be re-obtained (selecting "book/textbook" as the type of use).

My university (University of Illinois at Chicago) posts all dissertations on the library website online (which is available to anyone). Is this practice considered as "publishing" the thesis or it is assumed as "university-use"?

What if the school restricts access to the dissertation only to the members of the University of Illinois community?

Can I choose "thesis/dissertation" option to obtain appropriate permissions? Should I use "book/textbook" option instead (considering it is not paper book or CDROM, it is on a public website)?

While the reuse for both options are free, I'm not sure if I'm choosing proper service.

Thanks for your time,

Sincerely,

--

Ehsan Noohi, PhD

Robotics Lab, University of Illinois at Chicago,

Robotics Lab, Rehabilitation Institute of Chicago,

web: http://enoohi2.people.uic.edu/

CV: http://enoohi2.people.uic.edu/CV.pdf

ref:_00D30oeGz._500a01HNYoN:ref

--

Ehsan Noohi, PhD

Robotics Lab, University of Illinois at Chicago,

Robotics Lab, Rehabilitation Institute of Chicago,

web: http://enoohi2.people.uic.edu/

CV: http://enoohi2.people.uic.edu/CV.pdf

Appendix G

AUTHOR'S BIOGRAPHY

Ehsan Noohi graduated from University of Tehran, Iran, and received his BSc degree in Electrical Engineering in 1999. His senior project was supervised by Prof. Mahmoud Kamarei and resulted in an application for real-time voice compression. He then started his graduate studies at K.N.Toosi University of Technology, Iran. He received his MSc degree in Control Engineering in 2002. His thesis project was centered on a novel controller for permanent magnet synchronous (PMS) motors. Under the supervision of his adviser, Prof. Hamid D Taghirad, he proposed a sensorless vector control method for PMS motors (Taghirad et al., 2002).

Later he continued his graduate studies and joined Robotics and AI Laboratory at University of Tehran, Iran. He got involved in various projects in the lab, particularly, modeling and control of a wheel-based pole-climbing robot (Mahdavi et al., 2006; Mahdavi et al., 2007; Noohi et al., 2010). Under the supervision of his adviser, Prof. Majid Nili Ahmadabadi, he introduced a novel robotic grasping mechanism (Noohi et al., 2008) and proposed a few path planning techniques for the proposed mechanism that guaranteed the grasp stability (Noori et al., 2009; Parastegari et al., 2012; Noohi et al., 2011). Later, he built the mechanism and implemented a general motion planning technique that enabled the robot to manipulate irregular objects stably and perform the tasks that was impractical without the proposed mechanism (Noohi et al., 2015). He successfully defended his dissertation and received his PhD degree in Electrical Engineering from University of Tehran, Iran, in 2010.

Appendix G (Continued)

Later on, he moved to the United States of America and joined the Robotics Lab at the University of Illinois at Chicago. He got involved in various projects in this lab, including: estimating interaction force during laparoscopic surgery (Noohi et al., 2014), control of a robotic gripper during the handover task (Parastegari et al., 2016), study of human's force distribution during everyday grasps (Abbasi et al., 2016), the premitives for human manipulative actions (Noohi et al., 2017) and scheduling memory requests to increase fairness in multi-thread processors (Fang et al., 2012). However, the center theme of his research activities at UIC was modeling and control of human-robot physical interactions, during cooperative manipulation. This dissertation is a report on the majority of the projects he was leading during his PhD at UIC under this topic. In 2015, he joined the Robotics Lab at the Rehabilitation Institute of Chicago (RIC) as a visiting researcher. With the support of the lab director, Prof. James L. Patton, the collaboration between the two labs at UIC and RIC resulted in an article, published in IEEE Transactions on Robotics (Noohi et al., 2016).

CITED LITERATURE

[Abbasi et al. , 2016] Abbasi, B., Noohi, E., Parastegari, S., and Žefran, M.: Grasp taxonomy based on force distribution. In Robot and Human Interactive Communication (RO-MAN), 2016 25th IEEE International Symposium on, pages 1098–1103, Aug 2016.

[Abdel-Malek and Yang, 2005] Abdel-Malek, K. and Yang, J.: Human Performance Measures: Mathematics. Technical report, Department of Mechanical Engineering The University of Iowa, Technical report, 2005.

[American National Standard, 2000] American National Standard: Guide to Human Performance Measurements. American Institute of Aeronautics and Astronautics, 2000.

[Anderson and Pandy, 2001] Anderson, F. C. and Pandy, M. G.: Dynamic optimization of human walking. Journal of biomechanical engineering, 123(5):381–390, 2001.

[ATI, 2014] ATI: ATI Industrial Automation, F/T Sensor: Gamma, force/torque sensor. `http://www.ati-ia.com/products/ft/ft_models.aspx?id=Gamma`, 2014.

[Barrett, 2015] Barrett: The wam arm. `http://www.barrett.com/products-arm.htm`, 2015.

[Basdogan et al. , 2000] Basdogan, C., Ho, C.-H., Srinivasan, M. A., and Slater, M.: An experimental study on the role of touch in shared virtual environments. ACM Transactions on Computer-Human Interaction (TOCHI), 7(4):443–460, 2000.

[Bicchi and Prattichizzo, 2000] Bicchi, A. and Prattichizzo, D.: Manipulability of cooperating robots with unactuated joints and closed-chain mechanisms. IEEE Transactions on Robotics and Automation, 16(4):336–345, 2000.

[Bussy et al. , 2012] Bussy, A., Kheddar, A., Crosnier, A., and Keith, F.: Human-humanoid haptic joint object transportation case study. In Intelligent Robots and Systems (IROS), 2012 IEEE/RSJ International Conference on, pages 3633–3638, Oct 2012.

[Chen et al. , 2015] Chen, L., Javaid, M., Di Eugenio, B., and Žefran, M.: The roles and recognition of haptic-ostensive actions in collaborative multimodal human–human dialogues. Computer Speech & Language, 34:201–231, 2015.

[Crevecoeur et al. , 2009] Crevecoeur, F., Thonnard, J.-L., and Lefèvre, P.: Optimal integration of gravity in trajectory planning of vertical pointing movements. Journal of Neurophysiology, 102(2):786–796, 2009.

[Diedrichsen, 2007] Diedrichsen, J.: Optimal task-dependent changes of bimanual feedback control and adaptation. Current Biology, 17(19):1675–1679, 2007.

[Donner et al. , 2013] Donner, P., Mortl, A., Hirche, S., and Buss, M.: Human-robot cooperative object swinging. In Robotics and Automation (ICRA), 2013 IEEE International Conference on, pages 4343–4349. IEEE, 2013.

[Dumora et al. , 2013] Dumora, J., Geffard, F., Bidard, C., and Fraisse, P.: Towards a robotic partner for collaborative manipulation. In HRI Workshop on Collaborative Manipulation, 2013.

[Evrard and Kheddar, 2009] Evrard, P. and Kheddar, A.: Homotopy switching model for dyad haptic interaction in physical collaborative tasks. In World Haptics, pages 45–50, March 2009.

[Fang et al. , 2012] Fang, K., Iliev, N., Noohi, E., Zhang, S., and Zhu, Z.: Thread-fair memory request reordering. resource, 5(8):2, 2012.

[Faul et al. , 2009] Faul, F., Erdfelder, E., Buchner, A., and Lang, A.-G.: Statistical power analyses using g*power 3.1: Tests for correlation and regression analyses. Behavior Research Methods, 41:1149–1160, 2009.

[Feth et al. , 2009] Feth, D., Groten, R., Peer, A., Hirche, S., and Buss, M.: Performance related energy exchange in haptic human-human interaction in a shared virtual object manipulation task. World Haptics 2009 - Third Joint EuroHaptics conference and Symposium on Haptic Interfaces for Virtual Environment and Teleoperator Systems, pages 338–343, 2009.

[Finn et al. , 2016] Finn, C., Goodfellow, I., and Levine, S.: Unsupervised learning for physical interaction through video prediction. arXiv preprint arXiv:1605.07157, 2016.

[Fisher, 1915] Fisher, R. A.: Frequency distribution of the values of the correlation coefficient in samples from an indefinitely large population. Biometrika, pages 507–521, 1915.

[Fitts, 1954] Fitts, P. M.: The information capacity of the human motor system in controlling the amplitude of movement. Journal of experimental psychology, 47:381–391, 1954.

[Flash and Gurevich, 1997] Flash, T. and Gurevich, I.: Models of motor adaptation and impedance control in human arm movements. Advances in Psychology, 119:423–481, 1997.

[Flash and Hogan, 1985] Flash, T. and Hogan, N.: The coordination of arm movements: An experimentally confirmed mathematical model. Journal of neuroscience, 5(7):1688–1703, 1985.

[Ganesh et al. , 2014] Ganesh, G., Takagi, A., Osu, R., Yoshioka, T., Kawato, M., and Burdet, E.: Two is better than one: physical interactions improve motor performance in humans. Scientific reports, 4:3824, 2014.

[Garvin et al. , 1997] Garvin, G., Žefran, M., Henis, E., and Kumar, V.: Two-arm trajectory planning in a manipulation task. Biological Cybernetics, 76(1):53–62, 1997.

[Gere and Goodno, 2012] Gere, J. and Goodno, B.: Mechanics of materials. Nelson Education, 2012.

[Groten et al. , 2009] Groten, R., Feth, D., Goshy, H., Peer, A., Kenny, D., and Buss, M.: Experimental analysis of dominance in haptic collaboration. In Robot and Human Interactive Communication, 2009. RO-MAN 2009. The 18th IEEE International Symposium on, pages 723–729, 2009.

[Groten et al. , 2013] Groten, R., Feth, D., Klatzky, R. L., and Peer, A.: The role of haptic feedback for the integration of intentions in shared task execution. Haptics, IEEE Transactions on, 6(1):94–105, 2013.

[Groten et al. , 2009] Groten, R., Feth, D., Peer, A., Buss, M., and Klatzky, R.: Efficiency analysis in a collaborative task with reciprocal haptic feedback. 2009 IEEE/RSJ International Conference on Intelligent Robots and Systems, pages 461–466, 2009.

[Guiard, 1987] Guiard, Y.: Asymmetric division of labor in human skilled bimanual action: The kinematic chain as a model. Journal of motor behavior, 19(4):486–517, 1987.

[Harris and Wolpert, 1998] Harris, C. M. and Wolpert, D. M.: Signal-dependent noise determines motor planning. Nature, 394:780–784, 1998.

[Hughes et al. , 2004] Hughes, V. A., Roubenoff, R., Wood, M., Frontera, W. R., Evans, W. J., and Singh, M. A. F.: Anthropometric assessment of 10-y changes in body composition in the elderly. The American journal of clinical nutrition, 80(2):475–482, 2004.

[Hwang et al. , 2003] Hwang, E. J., Donchin, O., Smith, M. A., and Shadmehr, R.: A gain-field encoding of limb position and velocity in the internal model of arm dynamics. PLoS Biology, 1(2):209–220, 2003.

[Jankovic, 2008] Jankovic, J.: Parkinsons disease: clinical features and diagnosis. Journal of Neurology, Neurosurgery & Psychiatry, 79(4):368–376, 2008.

[Javaid et al. , 2014] Javaid, M., Zefran, M., and Di Eugenio, B.: Communication through physical interaction: A study of human collaborative manipulation of a planar object. In 2014 RO-MAN: The 23rd IEEE International Symposium on Robot and Human Interactive Communication, pages 838–843, August 2014.

[Jeannerod, 1988] Jeannerod, M.: The neural and behavioural organization of goal-directed movements.. Clarendon Press/Oxford University Press, 1988.

[Kawato, 1999] Kawato, M.: Internal models for motor control and trajectory planning. Current Opinion in Neurobiology, 9(6):718–727, 1999.

[Lacquaniti et al. , 1983] Lacquaniti, F., Terzuolo, C., and Viviani, P.: The law relating the kinematic and figural aspects of drawing movements. Acta Psychologica, 54:115130, 1983.

[Lee et al. , 2014] Lee, D.-H., Kim, U., and Choi, H. R.: Development of multi-axial force sensing system for haptic feedback enabled minimally invasive robotic surgery. 2014 IEEE/RSJ International Conference on Intelligent Robots and Systems, pages 4309–4314, 2014.

[Levine et al. , 2016] Levine, S., Pastor, P., Krizhevsky, A., and Quillen, D.: Learning hand-eye coordination for robotic grasping with deep learning and large-scale data collection. arXiv preprint arXiv:1603.02199, 2016.

[Madhavan et al. , 2009] Madhavan, R., Tunstel, E., and Messina, E.: Performance Evaluation and Benchmarking of Intelligent Systems. Boston, MA, Springer US, 2009.

[Mahdavi et al. , 2006] Mahdavi, S., Noohi, E., and Ahmadabadi, M. N.: Path planning of the nonholonomic pole climbing robot ut-pcr. In 2006 IEEE International Conference on Robotics and Biomimetics, pages 1517–1522, 2006.

[Mahdavi et al. , 2007] Mahdavi, S., Noohi, E., and Ahmadabadi, M. N.: Basic movements of a nonholonomic wheel-based pole climbing robot. In 2007 IEEE/ASME international conference on advanced intelligent mechatronics, pages 1–6, 2007.

[Medina et al. , 2011] Medina, J. R., Lawitzky, M., Mortl, A., Lee, D., and Hirche, S.: An experience-driven robotic assistant acquiring human knowledge to improve haptic cooperation. In Intelligent Robots and Systems (IROS), 2011 IEEE/RSJ International Conference on, pages 2416–2422. IEEE, 2011.

[Medina et al. , 2012] Medina, J. R., Lee, D., and Hirche, S.: Risk-sensitive optimal feedback control for haptic assistance. In Robotics and Automation (ICRA), 2012 IEEE International Conference on, pages 1025–1031. IEEE, 2012.

[Melendez-Calderon et al. , 2015] Melendez-Calderon, A., Fisher, M., Tan, M., Burdet, E., and Patton, J. L.: Acquisition of motor skills in isometric conditions through synesthetic illusions of movement. In IEEE World Haptics Conference (WHC), pages 428–433, 2015.

[Merlet, 2006] Merlet, J. P.: Jacobian, Manipulability, Condition Number, and Accuracy of Parallel Robots. Journal of Mechanical Design, 128(1):199, 2006.

[Milner and Ijaz, 1990] Milner, T. and Ijaz, M.: The effect of accuracy constraints on three-dimensional movement kinematics. Neuroscience, 35(2):365 – 374, 1990.

[Mörtl et al. , 2012] Mörtl, A., Lawitzky, M., Kucukyilmaz, A., Sezgin, M., Basdogan, C., and Hirche, S.: The role of roles: Physical cooperation between humans and robots. The International Journal of Robotics Research, 31(13):1656–1674, 2012.

[Nakano et al. , 1999] Nakano, E., Imamizu, H., Osu, R., Uno, Y., Gomi, H., Yoshioka, T., and Kawato, M.: Quantitative examinations of internal representations for arm trajectory planning: Minimum commanded torque change model. Journal of Neurophysiology, 81(5):2140–2155, 1999.

[NI, 2014] NI: National Instruments, NI PCI-6034E (Legacy) data aquisition board. http://sine.ni.com/nips/cds/view/p/lang/en/nid/11916, 2014.

[Noohi et al. , 2015] Noohi, E., Moradi, H., Parastegari, S., and Ahmadabadi, M. N.: Object manipulation using unlimited rolling contacts: 2-d kinematic modeling and motion planning. IEEE Transactions on Robotics, 31(3):790–797, June 2015.

[Noohi et al. , 2017] Noohi, E., Abbasi, B., Parastegari, S., and Žefran, M.: Motion primitives for human manipulation actions and their role in multimodal human-robot communication. In Technical Report, 2017.

[Noohi et al. , 2010] Noohi, E., Mahdavi, S. S., Baghani, A., and Ahmadabadi, M. N.: Wheel-based climbing robot: Modeling and control. Advanced Robotics, 24(8-9):1313–1343, 2010.

[Noohi et al. , 2008] Noohi, E., Moradi, H., and Nili Ahmadabadi, M.: Manipulation using wheeled tips: benefits and challenges. In 39th International Symposium on Robotics (ISR'08), pages 442–447, 2008.

[Noohi et al. , 2011] Noohi, E., Moradi, H., Noori, N., and Ahmadabadi, M. N.: Manipulation of polygonal objects with two wheeled-tip fingers: Planning in the presence of contact position error. Robotics and Autonomous Systems, 59(1):44–55, 2011.

[Noohi et al. , 2014] Noohi, E., Parastegari, S., and Žefran, M.: Using monocular images to estimate interaction forces during minimally invasive surgery. 2014 IEEE/RSJ International Conference on Intelligent Robots and Systems, pages 4297–4302, 2014.

[Noohi et al. , 2015] Noohi, E., Parastegari, S., and Žefran, M.: Computational model for dyadic and bimanual reaching movement. In IEEE World Haptics Conference (WHC), pages 260–265, 2015.

[Noohi and Žefran, 2014] Noohi, E. and Žefran, M.: Quantitative measures of cooperation for a dyadic physical interaction task. In Humanoid Robots (Humanoids), 2014 14th IEEE-RAS International Conference on, pages 469–474. IEEE, 2014.

[Noohi and Žefran, 2016] Noohi, E. and Žefran, M.: Modeling the interaction force during a haptically-coupled cooperative manipulation. In Robot and Human Interactive Communication (RO-MAN), 2016 25th IEEE International Symposium on, pages 119–124, Aug 2016.

[Noohi and Žefran, 2017] Noohi, E. and Žefran, M.: Trends in Control and Decision-Making for Human-Robot Collaboration Systems, chapter Estimating Human Intention during a Human-Robot Cooperative Task Based on the Internal Force Model. Springer International Publishing, 2017.

[Noohi et al. , 2016] Noohi, E., Žefran, M., and Patton, J. L.: A model for human-human collaborative object manipulation and its application to human-robot interaction. IEEE Transactions on Robotics, 32(4):880–896, Aug 2016.

[Noohi and Žefran, 2017] Noohi, E. and Žefran, M.: Estimating human intention during a human–robot cooperative task based on the internal forceinternal force model. In Trends in Control and Decision-Making for Human–Robot Collaboration Systems, pages 83–109. Springer, 2017.

[Noori et al. , 2009] Noori, N., Noohi, E., Moradi, H., Bakhtiary, A., and Ahmadabadi, M. N.: A probabilistic roadmap based planning algorithm for wheeled-tip robots manipulating polygonal objects. In 2009 IEEE/ASME International Conference on Advanced Intelligent Mechatronics, pages 1040–1046, 2009.

[Parastegari et al. , 2012] Parastegari, S., Ahmadabadi, M. N., Noohi, E., and Moradi, H.: Wheeled-tip object manipulation: Modeling and motion planning of throwing an object. In Robotics and Biomimetics (ROBIO), 2012 IEEE International Conference on, pages 1800–1805, Dec 2012.

[Parastegari et al. , 2016] Parastegari, S., Noohi, E., Abbasi, B., and Žefran, M.: A fail-safe object handover controller. In 2016 IEEE International Conference on Robotics and Automation (ICRA), pages 2003–2008, May 2016.

[Rahman et al. , 2000] Rahman, M., Ikeura, R., and Mizutani, K.: Control characteristics of two humans in cooperative task and its application to robot control. In Industrial Electronics Society, 2000. IECON 2000. 26th Annual Confjerence of the IEEE, volume 3, pages 1773–1778, 2000.

[Reed et al. , 2006] Reed, K., Peshkin, M., Hartmann, M. J., Grabowecky, M., Patton, J., and Vishton, P. M.: Haptically linked dyads: are two motor-control systems better than one? Psychological science, 17(5):365–6, 2006.

[Reed et al. , 2005] Reed, K. B., Peshkin, M., Hartmann, M. J., Colgate, J. E., and Patton, J.: Kinesthetic interaction. In Rehabilitation Robotics, 2005. ICORR 2005. 9th International Conference on, pages 569–574. IEEE, 2005.

[Reinkensmeyer et al. , 1992] Reinkensmeyer, D. J., Lum, P. S., and Lehman, S. L.: Human control of a simple two-hand grasp. Biological cybernetics, 67(6):553–564, 1992.

[Sabes et al. , 1998] Sabes, P. N., Jordan, M. I., and Wolpert, D. M.: The role of inertial sensitivity in motor planning. The Journal of Neuroscience, 18(15):5948–5957, 1998.

[Sawers and Ting, 2014] Sawers, A. and Ting, L. H.: Perspectives on human-human sensorimotor interactions for the design of rehabilitation robots. Journal of neuroengineering and rehabilitation, 11(1):142, 2014.

[Schafer, 2011] Schafer, R.: What is a Savitzky-Golay filter? [lecture notes]. Signal Processing Magazine, IEEE, 28(4):111–117, July 2011.

[Shadmehr and Mussa-Ivaldi, 1994] Shadmehr, R. and Mussa-Ivaldi, F. A.: Adaptive representation of dynamics during learning of a motor task. Journal of Neuroscience, 14(5):3208–3224, 1994.

[Shadmehr and Wise, 2005] Shadmehr, R. and Wise, S. P.: The Computational Neurobiology of Reaching and Pointing: A foundation for motor learning. Cambridge, MA, MIT Press, 2005.

[Shahriman et al. , 2009] Shahriman, A., Ikeura, R., Faizal, S., Yano, T., Mizutani, K., and Sawai, H.: A study of human sense effects and characteristic during human-human cooperative task. In Human System Interactions, pages 679–684, 2009.

[Singer and Akin, 2011] Singer, S. and Akin, D.: A Survey of Quantitative Team Performance Metrics for Human-Robot Collaboration. International Conference on Environmental Systems, pages 1–19, July 2011.

[Sparkfun, 2014] Sparkfun: 9 Degrees of Freedom - Sensor Stick, (accelerometer, gyroscope and magnetometer). `https://www.sparkfun.com/products/10724`, 2014.

[Steinfeld et al. , 2006] Steinfeld, A., Fong, T., Kaber, D., Lewis, M., Scholtz, J., Schultz, A., and Goodrich, M.: Common metrics for human-robot interaction. Proceedings of the 1st ACM SIGCHI/SIGART Conference on Human-robot Interaction, pages 33—-40, 2006.

[Szulc et al. , 2005] Szulc, P., Beck, T. J., Marchand, F., and Delmas, P. D.: Low skeletal muscle mass is associated with poor structural parameters of bone and impaired balance in elderly menthe minos study. Journal of Bone and Mineral Research, 20(5):721–729, 2005.

[Taghirad et al. , 2002] Taghirad, H., Abedi, N., and Noohi, E.: A new sensorless vector control method for permanent magnet synchronous motor without velocity estimator. In Control and Automation, 2002. ICCA. Final Program and Book of Abstracts. The 2002 International Conference on, pages 242–246, 2002.

[Arduino Mega, 2014] Arduino Mega: `http://arduino.cc/en/Main/arduinoBoardMega`, 2014.

[Todorov, 2004] Todorov, E.: Optimality principles in sensorimotor control (review). Nature neuroscience, 7(9):907–915, 2004.

[Tresilian and Stelmach, 1997] Tresilian, J. and Stelmach, G.: Common organization for unimanual and bimanual reach-to-grasp tasks. Experimental brain research, 115(2):283–299, 1997.

[Uchiyama and Dauchez, 1988] Uchiyama, M. and Dauchez, P.: A symmetric hybrid position/force control scheme for the coordination of two robots. In Robotics and Automation, 1988. Proceedings., 1988 IEEE International Conference on, pages 350–356. IEEE, 1988.

[Uno et al. , 1989] Uno, Y., Kawato, M., and Suzuki, R.: Formation and control of optimal trajectory in human multijoint arm movement. minimum torque-change model. Biological Cybernetics, 61:89–101, 1989.

[van der Wel et al. , 2011] van der Wel, R. P., Knoblich, G., and Sebanz, N.: Let the force be with us: dyads exploit haptic coupling for coordination. Journal of Experimental Psychology: Human Perception and Performance, 37(5):1420–31, 2011.

[Žefran et al. , 1994] Žefran, M., Kumar, V., and Yun, X.: Optimal trajectories and force distribution for cooperating arms. In Robotics and Automation, 1994. Proceedings., 1994 IEEE International Conference on, volume 1, pages 874–879, 1994.

[Waller and Whitall, 2008] Waller, S. M. and Whitall, J.: Bilateral arm training: why and who benefits? NeuroRehabilitation, 23:2941, 2008.

[Williams and Khatib, 1993] Williams, D. and Khatib, O.: The virtual linkage: A model for internal forces in multi-grasp manipulation. In Robotics and Automation, 1993. Proceedings., 1993 IEEE International Conference on, pages 1025–1030. IEEE, 1993.

[Yoshikawa, 1985] Yoshikawa, T.: Manipulability and redundancy control of robotic mechanisms. In Robotics and Automation. Proceedings. 1985 IEEE International Conference on, volume 2, pages 1004–1009, Mar 1985.

VITA

Ehsan Noohi

Education

- Ph.D. Electrical and Computer Engineering, University of Illinois at Chicago 2011 – 2017

  Dissertation: *Control of pHRI: Mimicking Human Assistance*.
- Ph.D. Electrical Engineering (Robotics), University of Tehran 2004 – 2010

  Dissertation: *Kinematic Analysis of Wheeled-tip Manipulators*.
- M.S. Electrical Engineering (Control), K.N.Toosi University of Technology 1999 – 2002

  Thesis: *Sensorless Vector Control of PMS Motors*.
- B.S. Electrical Engineering (Electronics), University of Tehran 1995 – 1999

  Thesis: *Voice Compression Software for WEB Applications*

Publications

- **Book Chapter:**

  B1. **E. Noohi** and M. Žefran, "Estimating Human Intention during a Human-Robot Cooperative Task Based on the Internal Force Model", (*appearing in*) Trends in Control and Decision-Making for Human-Robot Collaboration Systems, Yue Wang and Fumin Zhang (Eds.), Springer, Berlin Heidelberg, 2017.

- **Refereed Journal Papers:**

  J4. **E. Noohi**, M. Žefran and J. L. Patton , "A Model for Human-Human Collaborative Object Manipulation and Its Application to Human-Robot Interaction". IEEE Transaction on Robotics (Special Issue on Movement Science for Humans and Humanoids), Vol. 32, Issue 4, August 2016, pp. 880-896.

  J3. **E. Noohi**, H. Moradi, S. Parastegari and M. Nili Ahmadabadi, "Object Manipulation Using Unlimited Rolling Contacts: 2D Kinematic Modeling and Motion Planning". IEEE Transaction on Robotics, Vol. 31, Issue 3, April 2015, pp. 790-797.

  J2. **E. Noohi**, H. Moradi, N. Noori and M. Nili Ahmadabadi, "Manipulation of Polygonal Objects with Two Wheeled-tip Fingers: Planning in Presence of Contact Position Error". Elsevier, Robotics and Autonomous Systems, Vol. 59, Issue 1, January 2011, pp. 44-55.

  J1. **E. Noohi**, S. Mahdavi, A. Baghani and M. Nili Ahmadabadi, "Wheel-Based Climbing Robot: Modeling and Control". Advanced Robotics, Vol. 24, No. 8-9, May 2010, pp. 1313-1343.

- **Refereed Conference Papers:**

  C13. **E. Noohi** and M. Žefran, "Modeling the Interaction Force During a Haptically-Coupled Cooperative Manipulation", 25th IEEE International Symposium on Robot and Human Interactive Communication (RO-MAN), pages 119–124, Columbia University, NY, USA, August 26-31, 2016.

  C12. B. Abbasi, **E. Noohi**, S. Parastegari and M. Žefran, "Grasp Taxonomy Based on Force Distribution", 25th IEEE International Symposium on Robot and Human Interactive Communication (RO-MAN), pages 1098–1103, Columbia University, NY, USA, August 26-31, 2016.

  C11. S. Parastegari, **E. Noohi**, B. Abbasi and M. Žefran, "A Fail-safe Object Handover Controller", IEEE International Conference on Robotics and Automation (ICRA'16), pages 2003–2008, Stockholm, Sweden, May 16-21, 2016.

  C10. **E. Noohi**, S. Parastegari, and M. Žefran, "Computational Model for Dyadic and Bimanual Reaching Movements", IEEE World Haptic Conference (WHC'15), pages 260–265, Northwestern University, Evanston, IL, June 22-25, 2015.

  C9. **E. Noohi** and M. Žefran, "Quantitative Measures of Cooperation for a Dyadic Physical Interaction Task," in International Conference on Humanoid Robots (Humanoids'14), pages 469–474, Madrid, Spain, Nov. 18-20, 2014.

  C8. **E. Noohi**, S. Parastegari, and M. Žefran, "Using Monocular Images to Estimate Interaction Forces During Minimally Invasive Surgery", 2014 IEEE/RSJ International Conference on Intelligent Robots and Systems (IROS'14), pages 4297–4302, Chicago, IL, Sept. 14-18, 2014.

  C7. S. Parastegari, M. Nili Ahmadabadi, **E. Noohi** and H. Moradi, "Wheeled-tip Object Manipulation: Modeling and Motion Planning of Throwing an Object", In Proceedings of IEEE International Conference on Robotics and Biomimetics (ROBIO'12), pages 1800-1805, Dec. 11-14 2012.

  C6. K. Fang, N. Iliev, **E. Noohi**, S. Zhang, and Z. Zhu, "Thread-Fair Memory Request Reordering", 3rd JILP Workshop on Computer Architecture Competitions (JWAC-3): Memory Scheduling Championship (MSC), Portland, OR, USA, June 9-13, 2012.

  C5. N. Noori, **E. Noohi**, H. Moradi, A.H. Bakhtiary, and M. Nili Ahmadabadi. "A Probabilistic Roadmap Based Planning Algorithm for Wheeled-tip Robots Manipulating Polygonal Objects". In Proceedings of ASME/IEEE International Conference on Advanced Intelligent Mechatronics (AIM'09), pages 1040–1046, Singapore, July 14-17, 2009.

  C4. **E. Noohi**, H. Moradi, and M. Nili Ahmadabadi. "Manipulation Using Wheeled Tips: Benefits and Challenges". In Proceedings of 39th International Symposium on Robotics (ISR'08), pages 442–447, Seoul, South Korea, October 15-17, 2008.

  C3. S. Mahdavi, **E. Noohi** and M. Nili Ahmadabadi, "Basic Movement of a Nonholonomic Wheel-based Pole Climbing Robot". In Proceedings of IEEE/ASME International Conference on Advanced Intelligent Mechatronics (AIM'07), ETH Zurich, Switzerland, Sept 4–7 2007.

C2. S. Mahdavi, **E. Noohi**, and M. Nili Ahmadabadi, "Path Planning of the Nonholonomic Pole Climbing Robot UT-PCR". In Proceedings of IEEE International Conference on Robotics and Biomimetics (ROBIO'06), pages 1517-1522, Kunming, China, Dec. 17-20 2006.

C1. H. D. Taghirad, N. Abedi, **E. Noohi**, "A New Sensorless Vector Control Method for Permanent Magnet Synchronous Motors without Velocity Estimator". In Proceedings of 7th International Workshop on Advanced Motion Control(AMC'02), pages 242-247, Maribor, Slovenia, July 3-5 2002

- **Workshop Papers:**

W4. **E. Noohi**, H. Moradi, S. Parastegari and M. Nili Ahmadabadi, "A Planar (2D) Wheeled-tip Robotic Hand: Dexterous Object Manipulation with Unlimited Rolling Contacts", Workshop on Robotic Hands, Grasping, and Manipulation @ IEEE International Conference on Robotics and Automation (ICRA'15), Seattle, Washington, USA, May 26th - 30th, 2015.

W3. **E. Noohi** and M. Žefran, "Human-Robot Cooperation Strategy based on the Interaction Model of a Human-Human Collaborative Object Manipulation", Workshop on Rehabilitation Robotics and Human-Robot Interaction @ IEEE International Conference on Robotics and Automation (ICRA'15), Seattle, Washington, USA, May 26th - 30th, 2015.

W2. **E. Noohi** and M. Žefran, "Biomechanical Predictive Model for Bimanual and Dyadic Object Manipulation: A Cooperation Strategy for Two Hands", Workshop on Haptics for Neuroscience and Neuroimaging @ IEEE International Conference on Robotics and Automation (ICRA'15), Seattle, Washington, USA, May 26th - 30th, 2015.

W1. **E. Noohi** and M. Žefran, "Modeling Human Arm Motion and the Internal Force during a Human-Human Dyadic Reaching Movement", Workshop on Human Movement Understanding and Neuromechanics @ IEEE International Conference on Robotics and Automation (ICRA'15), Seattle, Washington, USA, May 26th - 30th, 2015.

- **Posters:**

P3. **E. Noohi**, B. Abbasi, S. Parastegari and M. Žefran, "Motion Primitives for Human Manipulation Actions and their Role in Multimodal Human-Robot Communication", (25th IEEE International Symposium on Robot and Human Interactive Communication (RO-MAN), Columbia University, NY, USA, August 26-31, 2016.

P2. **E. Noohi** and M. Žefran, "A Control Policy for Human-Robot Cooperation based on Internal Force Model", IEEE International Conference on Robotics and Automation (ICRA'15), Seattle, Washington, USA, May 26th - 30th, 2015.

P1. **E. Noohi** and M. Žefran, "Human-Robot Cooperation Strategy based on the Interaction Model of a Human-Human Collaborative Object Manipulation", The 4th Midwest

Workshop on Control and Game Theory (WCGT 2015), Iowa State University, April 26, 2015.

- **Doctoral Consortium:**

  D1. **E. Noohi**, "Kinematic analysis of Object Manipulation using Wheeled- tip Manipulators", IEEE International Conference on Networking, Sensing and Control (ICNSC 2010), Chicago, IL, USA, April 11 - 13, 2010.

Awards

- ECE Department Nominee for Dean's Scholar Award, University of Illinois at Chicago 2016
- Provost's Award for Graduate Research, University of Illinois at Chicago 2015
- The Graduate Student Presenter Award, University of Illinois at Chicago 2015
- The Graduate Student Council Travel Award, University of Illinois at Chicago 2015
- "Energy Track" Award in "Memory Scheduling Championship (MSC)" 2012
  In the 3rd JILP Workshop on Computer Architecture Competitions (JWAC-3)
  University of Utah, Salt Lake City, Utah
- Graded "A" for dissertation and all courses in previous PhD and therefore in GPA. 2010
  University of Tehran, Tehran, Iran.
- Ranked 1st of graduated Master students based on overall GPA. 2002
  K.N.Toosi University of Technology, Tehran, Iran.
- Ranked top 10% of graduated seniors of Electrical and Computer Engineering. 1999
  University of Tehran, Tehran, Iran.
- Ranked 17 among 400,000 applicants in B.Sc. National Universities Entrance Exam, Iran. 1995

Presentations

- **Invited Talks**

  Motor Learning & Biorobotics meetings at Rehabilitation Institute of Chicago (RIC) Dec. 2014

- **Conference Presentations**

  IEEE World Haptic Conference (WHC'15) June 2015

  IEEE International Conference on Robotics and Automation (ICRA'15) May 2015

  IEEE/RSJ International Conf. on Intelligent Robots and Systems (IROS'14) Sept. 2014

  ASME/IEEE International Conf. on Advanced Intelligent Mechatronics (AIM'09) July 2009

  39th International Symposium on Robotics (ISR'08) Oct. 2008

  International Workshop on Advanced Motion Control (AMC'02) July 2002

- **Poster Presentations**

  IEEE International Conference on Robotics and Automation (ICRA'15) May 2015

  The 4th Midwest Workshop on Control and Game Theory (WCGT 2015) April 2015

Memberships

- Golden Key International Honor Society — Lifetime Member
- IEEE Robotics and Automation Society — Student Member
- American Federation of Teachers (AFT) — Higher Education Member

Professional Service

- **Journal Article Referee**

  IEEE Transactions on Automation Science and Engineering

  Robotics and Autonomous Systems (Elsevier Journal)

  Robotica (Cambridge Journals)

- **Conference Paper Referee**

  RSI International Conference on Robotics and Mechatronics (ICROM) 2015, 2016

  IEEE Haptics Symposium (HAPTICS) 2015

  IEEE International Workshop on Advanced Robotics and its Social Impacts (ARSO) 2015

  IEEE World Haptics Conference (WHC) 2015

  IEEE/RSJ International Conference on Intelligent Robots and Systems (IROS) 2014

  IEEE Conference on Decision and Control (CDC) 2014, 2015

  American Control Conference (ACC) 2012, 2014

- **Graduate Employee's Organization (GEO) Steward**

  ECE representative in GEO at the University of Illinois at Chicago 2011-2013

- **Student Volunteer**

  The American Control Conference (ACC) July 2015

Work Experience

- **Visiting Researcher**, Robotics Lab, Rehabilitation Institute of Chicago (RIC) 2015 – 2016
- **Research Assistant**, Robotics Lab, University of Illinois at Chicago (UIC) 2011 – 2016
- **Summer Intern**, System Analyst, Intuitive Surgical Inc., Sunnyvale, CA Summer 2016
- **Mentor for Undergraduate Students**

  Joshua Shubert — Design and development of a data glove Fall 2015

  Zeus-Deo Ceniza — Implementation of an autonomous mobile robot in ROS Summer 2014

- **Adjunct Lecturer**

  Computer Organization II (ECE366)
  Electrical and Computer Engineering Dept., UIC — Spring 2015

  Discrete and Continuous Signals and Systems (ECE310)
  Electrical and Computer Engineering Dept., UIC — Summer 2014

  Computer Organization II (ECE366)
  Electrical and Computer Engineering Dept., University of Illinois at Chicago — Fall 2013

- **Teaching Assistant**

  Electrical and Computer Engineering Dept., University of Illinois at Chicago — 2011 – 2016